

國立臺灣大學生命科學院基因體與系統生物學學位學程

博士論文

Genome and Systems Biology Degree Program

College of Life Science

National Taiwan University

Ph.D. Thesis



探討突觸囊泡專屬蛋白 Synapsin Ia 如何調控緻密核

心囊泡的釋放

**Exploring how the synaptic vesicle-specific protein  
Synapsin Ia regulates the release of dense-core  
vesicles**

楊蕙如

Hui-Ju Yang

指導教授：王致恬 博士

Advisor: Chih-Tien Wang, Ph.D.

中華民國 108 年 7 月

July, 2019



## 致謝



感謝在就讀博士班這些年幫助著我、鼓勵著我、關心著我並陪伴著我的你們，因為有了你們的支持，我才能順利完成我的博士論文。

首先，我要將最高、最誠摯的感謝，獻給我的指導老師—王致恬老師，老師總是毫不藏私地、並耐心地、有條理地教導我每件事。在老師一步一步的指導下，我了解電生理實驗系統的是如何從零開始建立，並在老師的帶領下學會如何焊接以及製作許多精密的電生理實驗專屬的特別器材，有了老師的指導，我才能順利完成論文中的許多實驗成果。為了培養一個獨立的研究者，老師細心地教導我如何撰寫並執行研究計畫，還耐心地訓練我的口頭報告技巧，因此，我才能夠將研究成果很好地呈現與發表，這些全部都要歸功於老師的指導與建議。在我面臨巨大的挫折與困難的時候，老師總是我的明燈，在我迷惘、失去未來方向的時候，指引我明確的道路，我才能勇敢地繼續向前邁進。

感謝我的論文指導委員—陳倩瑜老師、溫進德老師、徐立中老師以及盧主欽老師，感謝陳倩瑜老師在我博一 rotation 時期的指導，因為有老師的指導與幫助，我才能學會蛋白質交互作用的預測技術，並進一步找到論文中最關鍵的蛋白質。感謝溫進德老師擔任我博士論文口試的主席，給予我很多非常有用的寶貴建議，我才能順利完成博士論文口試與論文。感謝徐立中老師能夠讓我到老師的實驗室學習新的實驗技術，因為有了老師的幫助，我才能順利地學會並

應用這些技術。感謝盧主欽老師在免疫沉澱實驗的指導，一開始進行實驗時面臨極大的困境，因為有了老師的指導與幫助，最後才能順利完成實驗。感謝所有的口委老師們在百忙之中，撥空閱讀我的論文並參與我的博士論文口試，給予我許多寶貴的建議與指導，使我的論文更加完整。

感謝實驗室的學長姐以及學弟妹們，在博士班的旅程中一直是我的好夥伴，並在這一路上給予我支持與幫助。感謝愉恬學姊教導我學習細胞培養以及電生理的實驗，在我對於實驗有所困惑時，都能盡心給予我幫助。感謝妮晏和毓紘，總是擔任我的好幫手，在我實驗繁忙之際，給予即刻的救援。感謝品君總是幫實驗室訂購實驗器材，讓我能無後顧之憂做實驗。感謝聖平、彥儒、子霖、琳欣、千庭、信祐、怡玳、爾中、清媛、玟琦、亭諭、士元、一婷、政璋以及韶巖在各個方面的幫助與支持，因為實驗室有你們的總是有著和樂融融的氣氛，所以我才能很愉快地做實驗。感謝陳倩瑜老師實驗室的東祈，在蛋白質交互作用預測實驗上的幫助，還有玟如學姊和 fish 學長在研究上的建議。感謝徐立中老師實驗室的詠琪和志璋學長在實驗技術上的教學與幫助。

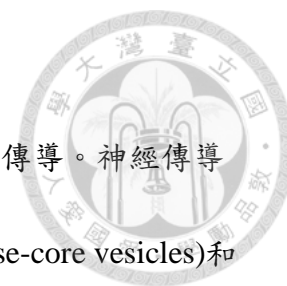
感謝台大生科院科技共同空間提供實驗儀器設備以及實驗技術的建議與討論，感謝校方、院方、國衛院以及科技部的經費支持，使我能夠順利完成我的博士論文研究。



最後，感謝我的家人，在這一路上一直是我的心靈支柱，我才能夠度過重重難關與低潮，非常感謝在低潮的時候給我鼓勵的你們，也非常感謝喜悅的時候和我一起分享的你們，因為有了你們的陪伴與幫助，我才能順利完成博士論文，順利取得學位。



## 中文摘要

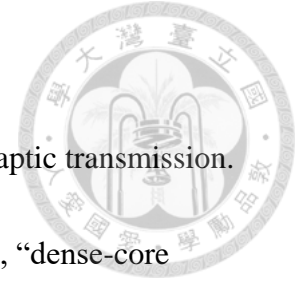


神經傳導物質的釋放與接受驅動神經系統中的化學性突觸傳導。神經傳導物質主要被包圍在兩種截然不同的囊泡中—緻密核心囊泡(dense-core vesicles)和突觸囊泡(synaptic vesicles)，雖然此兩種囊泡的釋放都是藉由相同的機制—鈣離子調控胞吐作用；然而，Synapsin (Syn) Ia 卻為唯一一種只特定存在於突觸囊泡的專屬蛋白，其藉由自身的磷酸化對調控突觸囊泡的補給至為重要。在適當的刺激下，Syn Ia 會被磷酸化，進而將突觸囊泡帶至釋放位置，因此，Syn Ia 的磷酸化會促進突觸囊泡的釋放。儘管已在含有緻密核心囊泡的突觸末端中發現大量的 Syn Ia，但目前仍完全未知的是 Syn Ia 是否也會(或如何)去影響緻密核心囊泡的胞吐作用。因此，為了在單一囊泡的層級釐清 Syn Ia 如何調控緻密核心囊泡的釋放，我們利用單一囊泡安培測定法(single-vesicle amperometry)直接偵測在 transfected PC12 細胞中，正腎上腺素從緻密核心囊泡的釋放。研究結果顯示，Syn Ia 可以藉由其磷酸化調控緻密核心囊泡胞吐作用的動態變化；除此之外，Syn Ia 還可以調節融合孔(緻密核心囊泡融合時的中間體)的動態，藉此影響緻密核心囊泡融合孔開啟狀態時的穩定性。由於已知 Syn I 不存在於緻密核心囊泡，推測 Syn Ia 應該是藉由和某特定蛋白結合，進而調控緻密核心囊泡的胞吐作用動態。為了進一步找出這個特別的蛋白，我們結合生物資訊、免疫共沉澱以及蛋白質交互作用檢測技術，證明 Syn I 能夠和 Synaptophysin (Syp)在細

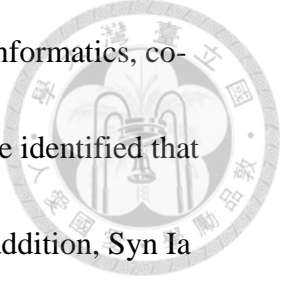
胞內進行交互作用；除此之外，在同一個細胞中，Syn I 能夠和 Syp 直接性且原位的交互作用。最後，我們發現 Syn I 和 Syp 的交互作用不是因為蛋白質表現量的改變而影響，而是倚賴 Syn Ia 的磷酸化。因此，這些結果除了揭開了突觸囊泡專屬蛋白 Syn Ia 如何去調控緻密核心囊泡胞吐作用的動態，還提供了關於 Syn Ia 在緻密核心囊泡和突觸囊泡共釋放機制上的角色；這些結果引導出一個新觀念的突破，並賦予神經傳導物質釋放的多樣性。

關鍵字: Synapsin Ia; 胞吐作用; 緻密核心囊泡; 融合孔動態; Synaptophysin

## Abstract



Neurotransmitters release and reception mediate chemical synaptic transmission. Neurotransmitters are packaged into two distinct classes of vesicles, “dense-core vesicles” (DCVs) and “synaptic vesicles” (SVs). The secretion from both DCVs and SVs share the common exocytotic machinery, i.e.,  $\text{Ca}^{2+}$  regulated exocytosis. Instead, Synapsin (Syn) Ia is a SV-specific SV protein, essential for recruiting SVs by phosphorylation. Upon the appropriate stimulus, Syn Ia undergoes phosphorylation, thus recruiting SVs to release sites. Therefore, the phosphorylation of Syn Ia up-regulates the release of SVs. Although Syn Ia is also abundant in the axon terminals containing DCVs, whether (or how) Syn Ia regulates the DCV release remains completely unknown. To determine the Syn Ia’s regulation of DCV exocytosis at the single-vesicle level, we directly measured the NE release from DCVs by performing single-vesicle amperometry in transfected PC12 cells following molecular perturbation. We showed that Syn Ia can regulate the dynamics of DCV exocytosis in a phosphorylation-dependent manner. In addition, Syn Ia can modulate the kinetics of fusion pores, the intermediates during DCV fusion, suggesting that Syn Ia regulates the stabilization of opening DCV fusion pores. Since Syn I rarely localized to DCVs, Syn Ia may interact certain protein to regulate DCV exocytosis. To further predict and



identify the candidate Syn Ia-interacting proteins, we combined bioinformatics, co-immunoprecipitation, and proximity ligation assay. As the results, we identified that the *in vivo* interaction between Syn Ia and Synaptophysin (Syp). In addition, Syn Ia may directly interact with Syp *in situ* in the same cell. Finally, we showed that the *in vivo* interaction between Syn Ia and Syp was not attributed to the change in expression levels, but dependent on the phosphorylation of Syn Ia. In conclusion, our results not only unveil how the SV-specific protein Syn Ia regulates the dynamics of DCV exocytosis, but also provide a new conceptual advance regarding the co-release mechanism of DCVs and SVs, conferring the versatility of neurotransmitter release.

Keywords: Synapsin Ia; Exocytosis; Dense-core vesicles; Fusion pore kinetics; Synaptophysin

## Abbreviations



ACh: Acetylcholine

Ap3d1: Adaptor-related protein complex 3 subunit delta 1

ATMK: Ataxia telangiectasia mutated kinases

BDNF: Brain-derived neurotrophic factor

C: close state

Calcium:  $\text{Ca}^{2+}$

CaMK I:  $\text{Ca}^{2+}$ / calmodulin-dependent protein kinase I

CaMK II:  $\text{Ca}^{2+}$ / calmodulin-dependent protein kinase II

CaMK IIa:  $\text{Ca}^{2+}$ / calmodulin-dependent protein kinase II alpha

CaMK IIg:  $\text{Ca}^{2+}$ / calmodulin-dependent protein kinase II gamma

CaMK IV:  $\text{Ca}^{2+}$ / calmodulin-dependent protein kinase IV

CAPON: Carboxyl-terminal PDZ ligand of neuronal nitric oxide synthase protein;

NOS1ap

Cdk1/5: P olo-like kinase Cdk 1/5

cdks: Cyclin-dependent protein kinases

CFE: Carbon fiber electrode

ChB: Chromogranin B

CMV: Cytomegalovirus

CNS: Central nervous system

Co-IP: Co-immunoprecipitation

Crk: Adapter molecule crk

Ct: cycle threshold

Ctrl: pCMV-IRES2-EGFP

D: Dilation state

DA: Dopamine

DAPI: 4',6- diamidino-2-phenylindole

DCV: Dense-core vesicle

DEPC: Diethyl pyrocarbonate

Dgki: Diacylglycerol kinase

Dgkz: Diacylglycerol kinase zeta

ECL: Enhanced chemiluminescence

EDTA: Ethylenediaminetetraacetic acid disodium salt dehydrate

EGFP: Enhanced green fluorescent protein

EM: Electron microscopy

Erc 1: ELKS/Rab6-interacting/CAST family member 1



Erk: Extracellular signal-regulated kinase

FF: Full fusion

GABA:  $\gamma$ -aminobutyric acid

IB: Immunoblotting

IF: Immunofluorescence

IP: Immunoprecipitated

IRES: Internal ribosome entry site

Hank's solution: Hank's balanced salts modified

HNS: Hypothalamic-neurohypophysial system

kb: Kilo-base pair

$k_c$ : The rate constants of fusion pore closure and dilation ( $k_d$ )

$k_c$ : The rate constants of fusion pore dilation

Kcnma1: Calcium-activated potassium channel subunit alpha-1

KR: Kiss and run

LB: Luria broth

Lrrk2: Leucine-rich repeat kinase 2

LTP: long term potentiation

MAPK: Mitogen-activated protein kinase





Marcks: Myristoylated alanine-rich C-kinase substrate

MSA: multiple sequence alignment

NE: Norepinephrine

NMDA 3B: *N*-methyl-D-aspartate receptor subunit 3B

NMDAR: NMDAR receptors

NO: nitric oxide

NOS1ap: Nitric oxide synthase 1 adaptor protein

nNOS: neuronal NO synthase

O: Open state

OT: Oxytocin

PAK: p21-activated kinase

PBS: Phosphate buffer solution

PFA: Paraformaldehyde

PKA: Protein kinase A

PKC: Protein kinase C

PLA: Proximity Ligation Assay

PSF: Prespike foot or prespike feet

PP: Posterior pituitary



PPI: Protein-Protein Interaction

Prickle 1: Prickle-like protein 1

Rims 2: Regulating synaptic membrane exocytosis protein 2

RP: Reserve pool

RRP: Readily releasable pool

PVDF membranes: Polyvinylidene fluoride membranes

Unc 13D: Protein unc-13 homolog D

S62A: phosphodeficiency at Ser62

S9,566,603A: phosphodeficiency at Ser9, 566, 603

SEM: Standard errors

SLP: short-lived plasticity

SNAP-25: Synaptosome-associated protein of 25 kDa

Snapin: SNARE-associated protein Snapin

SNARE: Soluble N-ethyl-maleimide-sensitive factor (NSF) attachment protein

receptor

SON: Supraoptic nucleus

Src: Src family kinases

SV: Synaptic vesicle



Syb: Synaptobrevin

Syb II: Synaptobrevin II

Syns: Synapsins

Syn Ia: Synapsin Ia

Syn Ia-S62A: pCMV-Syn Ia-S62A-IRES2-EGFP

Syn Ia-S9,566,603A: pCMV-Syn Ia-S9,566,603A-IRES2-EGFP

Syp : Synaptophysin

Syt: Synaptotagmin

Syt I: Synaptotagmin I

Stx: Syntaxin

Stx I: Syntaxin I

t-SNARE: target SNARE

VP: Vasopressin

v-SNARE: vesicle SNARE

$X_{KR}$ : The fraction of KR events



# Contents



口試委員審定書.....	i
致謝.....	ii
中文摘要.....	v
Abstract.....	vii
Abbreviations.....	ix

## Chapter I Introduction

1.1 Constitutive and regulated secretion.....	1
1.2 The kinetics of fusion pores.....	3
1.3 Dense-core vesicles (DCVs) and synaptic vesicles (SVs).....	5
1.4 The common machinery in both DCVs and SVs: Synaptotagmin I and the N-ethylmaleimide sensitive factor attachment protein receptor (SNARE) complex.....	7
1.5 The SV-specific protein: Synapsin Ia .....	10
1.6 The vesicle protein present in both DCVs and SVs.....	15
1.7 Objectives of the study.....	16

## Chapter II Materials and Methods

2.1 DNA plasmids.....	20
2.2 Cell culture.....	21
2.3 Transfection .....	22
2.4 Reverse-transcriptase quantitative polymerase chain reaction (RT-qPCR).....	23
2.5 Single-vesicle amperometry.....	25
2.6 Immunofluorescence staining .....	28
2.7 Prediction for protein-protein interaction .....	30
2.8 Co-immunoprecipitation .....	31
2.9 Western blotting.....	33
2.10 Proximity ligation assay.....	35
2.11 Statistics .....	37

### **Chapter III      Results**

3.1 Secretion from DCVs was regulated by Syn Ia or its phosphodeficient mutants..	38
3.2 FF frequency of DCVs was regulated by Syn Ia in a phosphorylation-dependent manner.....	40

3.3 The stabilization of open DCV fusion pores was regulated by Syn Ia or its phosphodeficient mutants .....	42
3.4 Fusion pore kinetics of DCVs was regulated by Syn Ia or its phosphodeficient mutants.....	44
3.5 Syn I mainly localized to SVs, but rarely localized to DCVs in PC12 cells .....	46
3.6 Exploring the putative Syn Ia-interacting proteins by database search and PPI prediction .....	47
3.7 The expression levels of Synaptophysin and SNARE proteins were not altered by overexpressing Syn Ia or its phosphodeficient mutants.....	49
3.8 <i>In vivo</i> interaction between Syn I and Synaptophysin depended on the phosphorylation of Syn Ia.....	50

## Chapter IV Discussion

4.1 Syn Ia dynamically regulates DCV exocytosis via different phosphorylation sites. ....	54
4.2 Syp is selected as the primary putative Syn Ia-interacting protein among top 5 proteins from PPI prediction.....	56

4.3 The potential role of Syn Ia involves in the development of neurological diseases	58
---	----

.....	58
-------	----

4.4 The potential role of Syn Ia in the co-release of neurotransmitters	61
---	----

4.5 Significance	64
------------------	----

<b>Chapter V Conclusion</b>	67
-----------------------------	----

<b>References</b>	69
-------------------	----

## List of Figures

Figure 1. Neurotransmitters are released by $\text{Ca}^{2+}$ -regulated exocytosis	85
--	----

Figure 2. Syn Ia is a key regulator of SV dynamics by modulating the storage and mobilization via its phosphorylation	87
---	----

Figure 3. The scheme of working hypothesis and proposed experiments in this study	89
---	----

Figure 4. Secretion rate of DCVs was regulated by Syn Ia or its phosphodeficient mutants	91
--	----

Figure 5. The mRNA expression in cells overexpressing Syn Ia or its phosphodeficient mutants.....	93
Figure 6. FF frequency and fraction of KR events in cells overexpressing Syn Ia or its phosphodeficient mutants .....	95
Figure 7. Spike characteristics in cells overexpressing Syn Ia or its phosphodeficient mutants.....	97
Figure 8. PSF open time of DCVs was regulated by Syn Ia or its phosphodeficient mutants.....	99
Figure 9. Two fusion events- “kiss and run” v.s. “full fusion” in cells overexpressing Syn Ia or its phosphodeficient mutants.....	101
Figure 10. Fusion pore kinetics of DCVs were regulated by Syn Ia or its phosphodeficient mutants .....	103
Figure 11. Subcellular localization of Syn I and ChB/Syp in cells overexpressing Syn Ia or its phosphodeficient mutants .....	104
Figure 12. Syn Ia-interacting proteins from database search.....	106
Figure 13. The protein-protein interaction prediction of putative Syn Ia-interacting proteins.....	108



Figure 14. The protein levels of Syn I, Syp, or SNAREs in cells overexpressing Syn Ia or its phosphodeficient mutants .....	110
---	-----

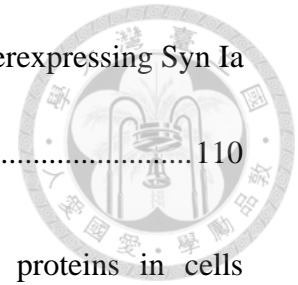


Figure 15. <i>In vivo</i> interaction of Syn I with the interacting proteins in cells overexpressing Syn Ia or its phosphodeficient mutants.....	112
--	-----

Figure 16. <i>In situ</i> interaction of Syn I with the interacting proteins in cells overexpressing Syn Ia or its phosphodeficient mutants.....	114
--	-----

Figure 17. The SV-specific protein Syn Ia regulates the dynamics of DCV exocytosis in a phosphorylation-dependent manner.....	116
---	-----

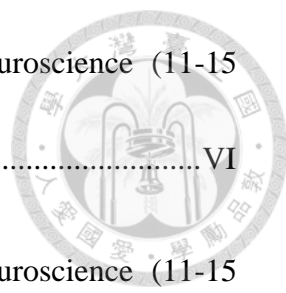
## Appendix

Appendix 1. The 44 <sup>th</sup> Annual Meeting of the Society for Neuroscience (15-19 November 2014, Washington DC, U.S.A.): Abstract.....	II
---	----

Appendix 2. The 44 <sup>th</sup> Annual Meeting of the Society for Neuroscience (15-19 November 2014, Washington DC, U.S.A.): Poster .....	III
--	-----

Appendix 3. The 46 <sup>th</sup> Annual Meeting of the Society for Neuroscience (12-16 November 2016, San Diego, CA, U.S.A.): Abstract .....	IV
--	----

Appendix 4. The 46 <sup>th</sup> Annual Meeting of the Society for Neuroscience (12-16 November 2016, San Diego, CA, U.S.A.): Poster .....	V
--	---



Appendix 5. The 47 <sup>th</sup> Annual Meeting of the Society for Neuroscience (11-15 November 2017, Washington DC, U.S.A.): Abstract.....	VI
Appendix 6. The 47 <sup>th</sup> Annual Meeting of the Society for Neuroscience (11-15 November 2017, Washington DC, U.S.A.): Poster .....	VII
Appendix 7. The Poster Competition of the 2016 GSB Retreat in Genome and Systems Biology (GSB) Degree Program at National Taiwan University, Taipei, Taiwan (8/28-29 2016): Abstract.....	VIII
Appendix 8. The Poster Competition of the 2016 GSB Retreat in Genome and Systems Biology (GSB) Degree Program at National Taiwan University, Taipei, Taiwan (8/28-29 2016): Poster .....	IX
Appendix 9. The 2019 Poster Competition in Genome and Systems Biology (GSB) Degree Program at National Taiwan University, Taipei, Taiwan (5/24, 2019): Poster .....	X

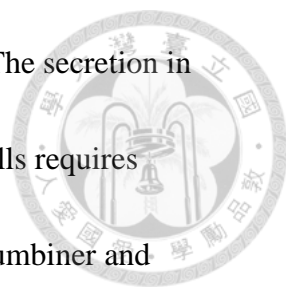


## Chapter I

### Introduction

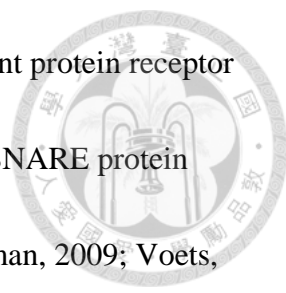
#### 1.1 Constitutive and regulated secretion

In all eukaryotic cells, secretory products are transported and released into extracellular space via two distinct pathways, i.e., constitutive or regulated pathway (Burgess and Kelly, 1987; Kelly, 1985; Levitan and Kaczmarek, 2015; Nicholls, 1994). In constitutive exocytosis, vesicles carrying lipids, cytosolic proteins (e.g., albumin, growth factors, etc), and membrane protein (e.g., receptors) are delivered from trans-Golgi network to cell surface. Subsequently, the arrived vesicles at the cell surface fuse with the plasma membrane, resulting in release of the contents from the vesicles interior into the extracellular space. Particularly, in the constitutive pathway, the movement of lipids and membrane proteins is continuous. Additionally, as the vesicles arrive at the cell surface, constitutive exocytosis immediately occurs without an external stimulus (Dumermuth and Moore, 1998; Gumbiner and Kelly, 1982). Eukaryotic cells rely on this constitutive secretory pathway to maintain growth, survival, and differentiation of cells. On the other hand, the features in regulated



exocytosis are distinguished from those in constitutive exocytosis. The secretion in regulated exocytosis from endocrine cells, neurons, and exocrine cells requires specific signals to trigger release (Dumermuth and Moore, 1998; Gumbiner and Kelly, 1982; Kelly, 1985). For example, neurotransmitters, such as neuropeptides, monoamines, and small molecules, are packaged into vesicles that are transported to presynaptic terminals (the release site). Upon arrival of the appropriate stimulus, the fusion of the vesicles with the plasma membrane allows the packed neurotransmitters released into the extracellular space. The receptors on postsynaptic cells thus receive the neurotransmitters to activate the ligand-gated ion channels and the corresponding downstream signaling pathways. Owing to neurotransmitter release and reception, chemical synaptic transmission, the fundamental process in the nervous systems, can occur among neurons in the network.

Calcium ( $\text{Ca}^{2+}$ ) is mainly regarded as a key regulator in regulated exocytosis (Jahn and Fasshauer, 2012). The process of  $\text{Ca}^{2+}$ -regulated exocytosis (**Fig. 1A**) can be divided into several steps (Sollner et al., 1993a). First, vesicles are initially docked and then primed by chemical energy onto plasma membrane. Subsequently, the supra-threshold stimulus arrived to open voltage-gated channels, allowing  $\text{Ca}^{2+}$  influx. In response to  $\text{Ca}^{2+}$  influx, the  $\text{Ca}^{2+}$  sensor then quickly binds to  $\text{Ca}^{2+}$  and induces the



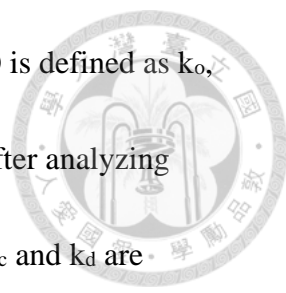
assembly of the soluble N-ethylmaleimide sensitive factor attachment protein receptor (SNARE) complex, comprising two t-SNARE proteins, and one v-SNARE protein (Baker and Hughson, 2016; Sollner et al., 1993b; Sudhof and Rothman, 2009; Voets, 2000). During the initial step of vesicle fusion, a fusion pore, the reversible formation of such a channel, connects the vesicle interior with the extracellular space, allowing vesicles to undergo two types of fusion events — “Full fusion (FF)” or “Kiss and run (KR)” (**Fig. 1B**) (Wang et al., 2006; Wang et al., 2003). The vesicles fuse with the plasma membrane completely termed “FF”, whereas “KR” means transient vesicle fusion, releasing neurotransmitters partially, re-forming vesicles again, and finally leaving the plasma membrane. Vesicle can selectively undergo FF or KR by different molecular mechanisms, thus leading to the diverse dynamics of exocytosis.

## 1.2 The kinetics of fusion pores

During the initial step of vesicle fusion, the vesicle fuse with plasma membrane, thereby forming the narrow “ $\Omega$ ”-shaped structure (**Fig. 1A**). The reversible formation of such a channel connecting the vesicle interior with the extracellular space termed “fusion pore” (Breckenridge and Almers, 1987; Chandler and Heuser, 1980). The intermediate structure before dilation of the fusion pore is under vigorous debate on

whether fusion pores are proteinaceous or lipidic. The proteinaceous pore is a channel-like structure formed by the assembly of hemi-channels (composed of proteins) in the two fusing membranes (Chang et al., 2015). An alternative intermediate is hemifusion diaphragm in which only the proximal leaflets of the proximal membranes are fused while the distal leaflets engage in an extended bilayer region (Zhao et al., 2016). A large body of studies indicated that both proteins and lipid seemed to be necessary for the processes of membrane fusion. Thus, a new hypothetical model of a composite protein–lipid fusion pore has been proposed that the exocytotic fusion pores are neither entirely protein nor entirely lipid (Bao et al., 2016; Chang et al., 2017).

A powerful real-time technique, single-vesicle amperometry (Wightman et al., 1991), provides the most sensitive measurement for vesicular release by detecting oxidized-neurotransmitters released from vesicles (**Fig. 3A**). An efflux of neurotransmitters out of a narrow fusion pore corresponds to the foot signal preceding the spike in amperometric recordings (Chow et al., 1992). Since the opening of fusion pore resembles that of ion channels, the kinetic model for fusion pore is proposed according to single-channel analysis (Wang et al., 2006; Wang et al., 2001). Three transition states of fusion pore were demonstrated as the close state (C), open state



(O), and dilation state (D). The rate constant of the step from C to O is defined as  $k_o$ , for the step from O to C as  $k_c$ , and for the step from O to D as  $k_d$ . After analyzing secretory events from amperometric recordings, the rate constants  $k_c$  and  $k_d$  are calculated by using the specific equations derived from single-channel kinetics in previous studies (Chiang et al., 2014; Wang et al., 2006; Wang et al., 2001). The increase in both  $k_c$  and  $k_d$  suggested that the open fusion pore prefer to enter the close and dilation state. In contrast, the reduction in both  $k_c$  and  $k_d$  suggested that the fusion pore prefer to stay in the open state. The alterations in  $k_c$  or  $k_d$  thus provide information for the changes in fusion pore kinetics during  $\text{Ca}^{2+}$ -regulated exocytosis.

### **1.3 Dense-core vesicles (DCVs) and synaptic vesicles (SVs)**

The neurotransmitters release from vesicles initiate chemical synaptic transmission (De Camilli and Jahn, 1990). Vesicles are divided into two major types. One is “dense-core vesicles” (DCVs) and the other is “synaptic vesicles” (SVs). Despite both DCVs and SVs share the common exocytotic machinery (De Camilli and Jahn, 1990; Sollner, 2003), the sizes, contents, positions relative to plasma membrane, and secretion rates from DCVs and SVs are absolutely different (Gondre-Lewis et al., 2012). The DCVs are comparatively large and contain dense cores inside the vesicles.

DCVs abundantly express at least one member of the chromogranin or secretogranin.

The diameter of DCVs is approximately 100-300 nm. Additionally, DCVs package

slow neurotransmitters, such as neuropeptides [oxytocin (OT) and vasopressin (VP)],

monoamines (e.g., serotonin), and catecholamines [e.g., norepinephrine (NE) and

dopamine]. Unlike DCVs, SVs, much smaller than DCVs, have a clear, circular

appearance under electron microscopy and contain fast neurotransmitters, including

acetylcholine (ACh) and  $\gamma$ -aminobutyric acid (GABA). SVs are located at active

zones in close proximity to plasma membrane, resulting in the fast kinetics of release.

Conversely, DCVs do not dock onto plasma membrane, thus exhibiting longer latency

of vesicle fusion in response to stimulation. Since both DCVs and SVs act as critical

signaling roles to mediate synaptic transmission, the abnormal secretion from SVs and

DCVs could lead to severe, debilitating disorders. For example, the levels of

neuropeptides in the postmortem cerebral cortex (Gabriel et al., 1996) and the levels

of brain-derived neurotrophic factor (BDNF) in prefrontal cortex (Weickert et al.,

2003) from schizophrenic patients are decreased, indicating that defects in neural

transmission may involve in the pathogenesis of schizophrenia. In addition, the

hippocampus of Alzheimer's mouse and the postmortem brain from Alzheimer's

patients show extensively colocalization of chromogranin, the DCV marker, with



amyloid- $\beta$  plaques, suggesting a potential role of the DCV in the Alzheimer's disease pathology (Willis et al., 2011).



#### **1.4 The common machinery in both DCVs and SVs: Synaptotagmin I and the N-ethylmaleimide sensitive factor attachment protein receptor (SNARE) complex**

Syts and SNARE proteins have central roles in mediating  $\text{Ca}^{2+}$ -regulated exocytosis (**Fig. 1A**), essential for many physiological processes and effective neuronal communication. Syts constitute a large protein family of at least seventeen isoforms (Craxton, 2010). Most of Syt isoforms are present in the central nervous system (CNS). Among these isoforms, Syt I serves as a  $\text{Ca}^{2+}$  sensor that is essential in depolarization-induced  $\text{Ca}^{2+}$ -regulated exocytosis (Koh and Bellen, 2003). Syt I is a vesicle-associated protein most localized to vesicles or plasma membrane. Syt I consists of a short N-terminal luminal segment, a single transmembrane (TM), and  $\alpha$ -helix region containing two cytosolic  $\text{Ca}^{2+}$ -binding C2 domains, i.e., C2A and C2B (Shao et al., 1996). Upon binding to  $\text{Ca}^{2+}$ , Syt I first binds to phosphatidylserine (PS)-containing lipid bilayers via its C2B domain to mediate vesicle membrane attachment (Chang et al., 2018; Honigsmann et al., 2013). Subsequently, Syt I further binds to

soluble SNARE proteins to trigger assembly of SNARE complex (Kreutzberger et al., 2017). The highly stable four-helical SNARE complex provides the energy for membrane fusion (Zhou et al., 2015).



Previous studies showed that knockout of Syt I dramatically blocks  $\text{Ca}^{2+}$ -regulated exocytosis (Bacaj et al., 2013). Deletion of Syt I leads to a drastic reduction in the membrane docking of vesicles (de Wit et al., 2009; Kedar et al., 2015). Moreover, the mutation in the  $\text{Ca}^{2+}$ -binding sites of Syt I alters the release in both synapses (Fernandez-Chacon et al., 2001; Mackler et al., 2002; Nishiki and Augustine, 2004; Stevens and Sullivan, 2003) and neuroendocrine cells (Wang et al., 2006), by impairing PS binding (van den Bogaart et al., 2012) and  $\text{Ca}^{2+}$ -stimulated SNARE binding (Lynch et al., 2008; Pang et al., 2006). As for the role in regulating the kinetics of fusion pore, Syt I controls the choice between kiss-and-run and full-fusion events through  $\text{Ca}^{2+}$  binding to different C2 domains (Wang et al., 2003). In addition, Syt I promotes the open fusion pore towards full dilation compared to Syt VII or Syt IX, consistent with its significant role in enhancing  $\text{Ca}^{2+}$ -regulated exocytosis (Zhang et al., 2010).

The SNAREs, the key proteins involved in vesicle fusion, consist of the v-SNARE (Synaptobrevin II, Syb II, or also known as vesicle-associated membrane protein II,

VAMP-II), the t-SNAREs (Synaptosome-associated protein of size 25 kDa, SNAP-25 and Syntaxin I, Stx I) (Schiavo et al., 1992; Sollner et al., 1993b; Sollner, 2003; Sorensen, 2005; Stojilkovic, 2005). Syb II and Stx I localize to the vesicle and plasma membrane, respectively, via transmembrane domain (TM) domains. Unlike Syb II and Stx I, SNAP-25 only anchors plasma membrane via palmitoyl side chains at the center of protein.

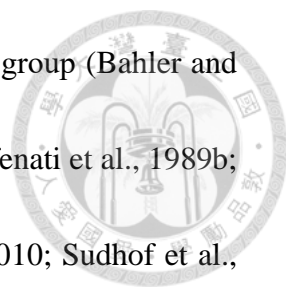
A series of studies showed that manipulations of the TM domains of SNARE proteins affect the fusion pore properties during exocytosis, consistent with the important roles of SNAREs in regulating membrane fusion (Wu et al., 2017). For example, mutations at residues of the TM domain in Syb II (Chang et al., 2015) or Stx I (Han and Jackson, 2005; Han et al., 2004) influence the release passing through exocytotic fusion pores, suggesting that Syb II and Stx I are the structural components of the fusion pore. During membrane fusion, SNAP-25, Syb II, and Stx I pull the membranes together. The TM domain of Syb complementing the TM domain of Stx I may line the nascent proteinaceous fusion pore through the plasma membrane (Chang et al., 2017). The three-dimensional architectural evidence of one study (Adams et al., 2015) showed six Syb II dimers bind to six Synaptophysin (Syp) molecules,

assembling into a hexameric ring involved in the SNARE-mediated membrane fusion, implicating the potential role of the TM domain of Syp in regulating vesicle fusion.

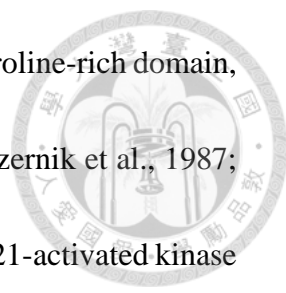


### **1.5 The SV-specific protein: Synapsin Ia**

Synapsins (Syns), abundantly neuronal phosphoproteins, localize to SVs exclusively with the well-known function in recruiting of SVs in a phosphorylation-dependent manner (Cesca et al., 2010; Hosaka et al., 1999; Huttner and Greengard, 1979). Moreover, Syns also contribute to synapse formation, maturation, and plasticity. Syns are widespread in the nervous system and also found in neuroendocrine cells, such as chromaffin cells and PC12 cells (Haycock et al., 1988; Romano et al., 1987a; Romano et al., 1987b), and other non-neuronal cell types, including astrocytes (Cahoy et al., 2008; Maienschein et al., 1999), pancreatic  $\beta$  cells (Matsumoto et al., 1999), osteoblasts, epithelial cells (Bustos et al., 2001), HeLa cells, and NIH/3T3 cells (Hurley et al., 2004). The Syn family consists of ten isoforms, i.e., Syn Ia-b, IIa-b and IIIa-f (Sudhof et al., 1989), with a highly conserved N-terminal region and a relatively variable C-terminus. Among all the homologous proteins, Syn Ia is the best studied in the nervous system. Here, we would give a comprehensive description of Syn Ia, regarding its structure, function, and potential role in relevant neurological diseases.



Syn Ia is first identified and characterized by Paul Greengard's group (Bahler and Greengard, 1987; Baldelli et al., 2007; Benfenati et al., 1989a; Benfenati et al., 1989b; Benfenati et al., 1990; De Camilli et al., 1983; Fornasiero et al., 2010; Sudhof et al., 1989; Yang et al., 2002). Syn I, encoded by the *SYN1*, is originally named as the neuron specific protein I, but later termed Synapsin I. The structure of Syn Ia, of about 700 aa, consists of five domains (**Fig. 2A**). The N-terminal region can be divided into three domains, A, B and C, whereas the C-terminal region can be divided into two domains, D, and E. In addition, nine phosphorylation site are found in the whole Syn Ia structure. Domain A, the highly conserved region among all Syns, contains the phosphorylation site Ser-9 for protein kinase A (PKA) and  $\text{Ca}^{2+}$  / calmodulin-dependent protein kinase (CaMK) I/IV (Czernik et al., 1987; Huttner and Greengard, 1979). In particular, the Ser-9 site is the major phosphorylation site conserved between Syns of both vertebrate and invertebrate animals. Domain B, considered as a linker region connecting domain A to domain C, contains the phosphorylation sites Ser-62 and Ser-67 for mitogen-activated protein kinase (MAPK)/Extracellular signal-regulated kinase (Erk) (Jovanovic et al., 1996). Domain C, the largest region of Syn Ia, contains both hydrophobic and highly charged sequences, used for the interaction of Syn Ia with other molecules. The phosphorylation site Tyr-301 in domain C is activated by Src family



kinases (Src) (Messa et al., 2010; Onofri et al., 2007). Domain D, a proline-rich domain, contains phosphorylation sites Ser-556 and Ser-603 for CaMKII (Czernik et al., 1987; Jovanovic et al., 1996). The Ser-603 site is also phosphorylated by p21-activated kinase (PAK) (Sakurada et al., 2002). Moreover, domain D also contains phosphorylation sites Ser-549 and Ser-551 for Polo-like kinase Cdk 1/5 (Cdk1/5) and MAPK/Erk (Jovanovic et al., 1996; Matsubara et al., 1996). Lastly, the domain E is present in all the “a” isoforms, but absent in “b” isoforms. The phosphorylation site Ser-682 of domain E is activated by Ataxia telangiectasia mutated kinases (ATMK) (Li et al., 2009).

Syn Ia is a key regulator of SV dynamics by modulating the storage and mobilization via its phosphorylation in presynaptic terminals (**Fig. 2B**). Different phosphorylation sites of Syn Ia drive different functions. Under basal conditions, the levels of phosphorylation on Ser-9 site is at a low degree (Menegon et al., 2000). Upon the depolarization-induced  $\text{Ca}^{2+}$  influx, the Ser-9 site is rapidly phosphorylated by PKA and CaMK I/IV, resulting in dissociation of Syn Ia with SVs (Chi et al., 2001; Chi et al., 2003; Huttner and Greengard, 1979). Furthermore, the Ser-9 phosphorylation triggers subtle conformational changes in the structure of Syn Ia, thus decreasing the binding with actin (Bahler and Greengard, 1987; Benfenati et al., 1990). Moreover, at resting, Syn Ia tethers SVs to actin, forming clusters in the reserve pool (RP). When the

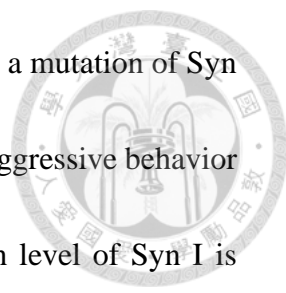
stimulus arrives, phosphorylation of Ser-566 and Ser-603 sites induces major conformational changes in the Syn Ia structure, which contributes to a severe reduction of its binding to both actin and SVs, thus inhibiting the formation of an actin-synapsin-SV ternary complex (Bahler et al., 1990; Bahler and Greengard, 1987; Benfenati et al., 1989a; Ceccaldi et al., 1995; Chi et al., 2003; Petrucci and Morrow, 1987; Valtorta et al., 1992). Hence, the Ser-566 and Ser-603 phosphorylation of Syn Ia recruits SVs to active zones, i.e., readily releasable pool (RRP), thus modulating the mobilization of SVs.

Four phosphorylation sites (Ser-62, Ser-67, Ser-549, and Ser-551) are activated by MAPK and two phosphorylation sites (Ser-549 and Ser-551) are activated by Cdk 1/5. In a previous study, dephosphorylation of Ser-62, Ser-67 and Ser-549 allows Syn Ia to recruit recently recycled SVs back to the clusters, i.e., reserve pool (RP), by increasing their actin-binding affinity, but has no effects on SV binding (Jovanovic et al., 1996). In addition, the phosphorylation of MAPK sites facilitates the SV trafficking in response to high-frequency stimulation (Cesca et al., 2010; Chi et al., 2003). However, the phosphorylation of Syn Ia by Cdk 5 has no effects on the actin binding (Matsubara et al., 1996). The Tyr-301 phosphorylate site, phosphorylated by Src, mediates opposite effects to serine phosphorylation, which increases Syn Ia association to actin and SVs

(Messa et al., 2010; Onofri et al., 2007). Only when the Ser-628 site is phosphorylated by ATMK, the interaction between ATMK and Syn I can be detected (Li et al., 2009). Taken together, these findings show that Syn Ia can diversely regulate the dynamics of SV release via phosphorylation on multiple sites.

Syn Ia plays an important role in maintaining the activity of the neuronal network. The impaired Syn Ia function can result in pathological conditions of the relevant neurological diseases. In addition, Syn influences the behavior and learning ability in flies. The Syn-null flies showed the increased wing beat frequency, elevated walking activity, faster olfactory jump response, enhanced ethanol tolerance, and significant defects in learning and memory (Godenschwege et al., 2004; Michels et al., 2005). Particularly, the Syn-null flies reached only a half of the score of wild-type flies in olfactory associative learning experiments (Michels et al., 2005). In the Syn I-knockout mice, the fine balance of neuronal activity moves towards excitability, leading to severe epilepsy in an age-dependent manner (Cambiaghi et al., 2013; Etholm et al., 2011; Ketzev et al., 2011; Li et al., 1995; Rosahl et al., 1995). Moreover, Syn I-knockout mice displayed abnormalities in short-lived plasticity (SLP), which is responsible for temporary memory storage. However, Syn I-knockout mice apparently displayed normal long-term potentiation (LTP), which is important for learning and memory

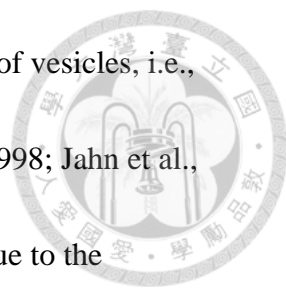




(Silva et al., 1996). In fact, genetic analysis in human identified that a mutation of Syn I is associated with the cause of epilepsy, learning difficulties, and aggressive behavior (Garcia et al., 2004). Previous studies reported that the expression level of Syn I is significantly reduced in the patient brains of schizophrenia (Browning et al., 1993) and bipolar disorder (Vawter et al., 2002). An area-specific reduction in chromogranin B is paralleled with a decrease in Syn I from the hippocampus of schizophrenia patients (Nowakowski et al., 2002), thus providing additional support to the association of Syn I with schizophrenia. Similar to schizophrenia, the relatively low Syn I levels are also found in Alzheimer's disease patients (Ho et al., 2001; Perdahl et al., 1984; Qin et al., 2004). Furthermore, abnormal phosphorylation of Syn I is identified in the striatum and cerebral cortex of Huntington's disease mice (Lievens et al., 2002). Taken together, Syn Ia plays a vital role in regulating the dynamics of SVs and the activity of the neuronal network, thus maintaining normal function of the nervous system. However, whether Syn Ia may regulate the DCV exocytosis remains elusive.

Taken together, Syn Ia play a vital role in regulating the dynamics of SVs and the activity of the neuronal network.

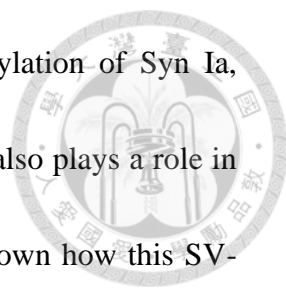
## **1.6 The vesicle protein present in both DCVs and SVs**



Syp, an integral membrane protein, is present in both two types of vesicles, i.e., DCVs and SVs, with four transmembrane domains (Berwin et al., 1998; Jahn et al., 1985; Saegusa et al., 2002; Wheeler et al., 2002; Winkler, 1997). Due to the abundantly presynaptic expression, Syp has thus been implicated in regulation of neurotransmitter release. Recent studies reported that the expression level of Syp is significantly decreased in Alzheimer's disease patients (Hansen et al., 1998). Furthermore, the increased expression of Syp correlates with LTP, suggesting that Syp may contribute to learning and memory (Arthur and Stowell, 2007; Lynch et al., 1994; Mullany and Lynch, 1997). Conversely, the mice lacking Syp exhibited behavioral alterations and learning deficits (Schmitt et al., 2009). Despite of these, the function and molecular mechanism underlying Syp's regulation of neurotransmitter release remains elusive.

### **1.7 Objectives of the study**

Our previous results showed that Syn Ia is abundantly concentrated on the axon terminals of the hypothalamic-neurohypophysial system (HNS), where the neuropeptides, oxytocin (OT) and vasopressin (VP) are released from DCVs to regulate social behavior of adult male rats. Surprisingly, the previous results showed that Syn Ia



upregulates the release of OT and VP in the HNS by phosphorylation of Syn Ia, suggesting that Syn Ia is not only essential for SV exocytosis, but also plays a role in regulating DCV exocytosis. However, it remains completely unknown how this SV-specific phosphoprotein Syn Ia may affect the DCV release. Therefore, it is important to unveil the detailed mechanisms underlying Syn Ia's regulation of DCV release. To determine the Syn Ia's regulation of DCV exocytosis at the single-vesicle level, we directly measured NE release from DCVs by performing single-vesicle amperometry in transfected PC12 cells following molecular perturbation. PC12 cells, derived from adrenal chromaffin cells, have been used extensively to study the process of regulated exocytosis. The dynamics of individual releasing events from DCVs can be resolved by virtue of the slow secretion rate in PC12 cells and high temporal-resolved amperometric recordings. To further determine how Syn Ia regulates the dynamics of DCV exocytosis via phosphorylation, the Syn Ia phosphodeficient mutant at the Ser62 site for MAPK (the plasmid pIRES2EGFP-Synapsin Ia-S62A abbreviated as Syn Ia-S62A), used in the previous experiments of adult male rats, will be verified in this study. Besides, the new Syn Ia phosphodeficient mutant at the triple sites (Ser9, Ser566, and Ser603) for CaMK (the plasmid pIRES2EGFP-Synapsin Ia-S9,566,603A; abbreviated as Syn Ia-S9,566,603A) was created by site-directed mutagenesis in this study.

Here, by using PC12 cells as model, we combined molecular perturbation, single-vesicle amperometry, bioinformatics, and biochemical techniques to unveil the molecular mechanism underlying the Syn Ia's regulation of DCV exocytosis. The specific aims to elucidate in this study were shown as follow (**Fig. 3A**):

- I. Determine how Syn Ia regulates the dynamics of DCV exocytosis via phosphorylation at single-vesicle levels.
  - A. Determine the effects of Syn Ia and its phosphodeficient mutants on the secretion rate of DCVs
  - B. Determine the effects of Syn Ia and its phosphodeficient mutants on the occurrences of two distinct fusion events.
  - C. Determine the effects of Syn Ia and its phosphodeficient mutants on the stabilization of open DCV fusion pores.
  - D. Investigate if Syn Ia and its phosphodeficient mutants regulate fusion pore kinetics of DCV exocytosis.
- II. Determine the mechanism underlying the Syn Ia's regulation of DCV exocytosis.
  - A. Determine the subcellular localization of Syn I in transfected cells.
  - B. Explore the candidate Syn Ia-interacting proteins by bioinformatics approaches.

- C. Determine the *in vivo* interaction of the candidate proteins with Syn I in a Syn Ia phosphorylation-dependent manner.



The results from this study would advance our understanding for cellular and molecular basis underlying Syn Ia's regulation of DCV exocytosis.

## Chapter II



### Materials and Methods

#### 2.1 DNA plasmids

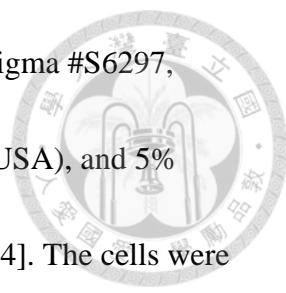
The cDNA encoding the gene of interest, wild-type Syn Ia [from Dr. Paul Greengard's lab (Rockefeller University, USA)] was subcloned into a control vector pCMV-IRES2-EGFP [termed Ctrl (Clontech #6029-1, CA, USA)] by restriction sites, *Bgl* II (Takara #1021A, Shinga, Japan) and *Sac* I (Takara #1080A, Shinga, Japan). The resultant DNA plasmid was pCMV-Syn Ia-IRES2-EGFP (termed Syn Ia). Two phosphodeficient mutants of Syn Ia, including the phosphodeficiency at Ser62 (S62A) or at Ser9, 566, 603 (S9,566,603A), were used in this study. pCMV-Syn Ia-S62A-IRES2-EGFP (termed Syn Ia-S62A), was kindly provided by Dr. Meyer B Jackson's lab (University of Wisconsin-Madison, USA). The other Syn Ia phosphodeficient mutant, pCMV-Syn Ia-S9,566,603A-IRES2-EGFP (termed Syn Ia-S9,566,603A), was acquired by using the QuikChange MultiSite-Directed Mutagenesis Kit (Agilent Technologies # 200514, CA, USA) with designed primers (Forward primer: 5'-CCgCCTggCggACAgCAACTACATggCCAATC-3' and 5'-ATTCgTCAggCCggCCAggCAggT-3'; Reverse primers: 5'-CTggACCAgAgATAgCTgCCTgACgggTAgC-3'). All of the cDNAs in this study

contained a cytomegalovirus (CMV) promoter for expressing the genes of interest (i.e., Syn Ia, Syn Ia-62A, or Syn Ia-S9,566,603A) and the internal ribosome entry site (IRES) for enhanced green fluorescent protein (EGFP). These cDNAs were confirmed by automated sequencing (Genomics, Taiwan) and then amplified by transformation.

To amplify the DNA plasmids, 1  $\mu$ L DNA was added into the 50  $\mu$ L solution containing competent cells, DH-5 $\alpha$ , followed by incubation on ice for 30 min. The heat shock procedure at 42°C for 90 sec was applied, and then 450  $\mu$ L Luria broth (LB) was added into the competent cells, followed by incubation at 37°C with 1-hr shaking for recovery. Subsequently, the mixture of DNA and competent cells was spread on LB agar plates with Kanamycin (50  $\mu$ g/ $\mu$ L from the 1000 $\times$  stock in ddH<sub>2</sub>O; Sigma, Cat. #K4000, St. Louis, MO, USA), followed by incubation at 37°C overnight. The bacterial colonies were further isolated. Finally, all the DNA plasmids were amplified, purified by the MegaPrep kits (Qiagen GmbH #12183, Hilden, Germany), and dissolved in Tris buffer (10 mM, pH 7.6; Sigma #T6966, MO, USA).

## 2.2 Cell culture

PC 12 cells (Hay and Martin, 1992) were cultured in 100-mm dish (Corning® #430167, NY, USA) containing PC12 culture medium [Dulbecco's modified Eagle's

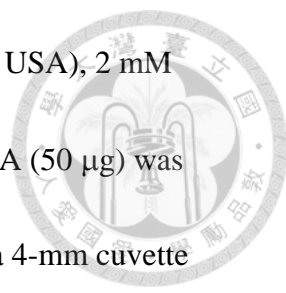


medium (DMEM, Sigma, #D5648, MO, USA), 3.7 g/L NaHCO<sub>3</sub> (Sigma #S6297, MO, USA), 5% equine serum (HyClone#0805-SH30074.03, Utah, USA), and 5% bovine calf serum (HyClone#0805-SH30072.03, Utah, USA), pH 7.4]. The cells were maintained in 10% CO<sub>2</sub> at 37°C and the medium was renewed every two days. When the cells grew full of the dish, the cells were passed into the new dishes. The original medium was discarded and the cells were rinsed and harvested by 1 mL of Hank's solution [Hank's balanced salts modified (Sigma #H4891, MO, USA), 0.35 g/L NaHCO<sub>3</sub>, and 1 mM Ethylenediaminetetraacetic acid disodium salt dehydrate (EDTA, Sigma #E5134, MO, USA, pH 7.2)] using a 22-gauge needle (Terumo #SS-10L2238, Philippines) connected with a syringe. After adding 3 mL new medium, the cell suspension was divided into three new dishes, with each containing 9 mL new fresh PC12 medium.

### **2.3 Transfection**

Cells were rinsed and harvested with Hank's solution. Subsequently, cells were centrifuged at 1,000 g, room temperature, for 3 min. After discarding supernatants, the cell pellets were resuspended with 500 µL cytomix solution [120 mM KCl (Sigma #P9333, MO, USA), 0.15 mM CaCl<sub>2</sub> (Fluka #21108, MO, USA), 10 mM KH<sub>2</sub>PO<sub>4</sub>



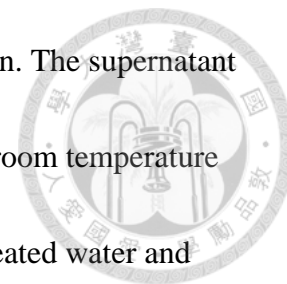


(Sigma #P5655, MO, USA). 2.5 mM HEPES (Sigma #H7523, MO, USA), 2 mM EGTA and 5 mM MgCl<sub>2</sub> (Sigma #M1028, MO, USA), pH 7.6]. DNA (50 µg) was mixed with cell solution, and then the mixture was transferred into a 4-mm cuvette (BTX ECM830, Harvard Apparatus #45-0052, MA, USA) for electroporation by using a 230 V-square pulse for 5 ms (BTX ECM830, square-pulse electroporator, Harvard Apparatus #45-0052, MA, USA). After electroporation, the cells were immediately transferred into recovery medium [PC12 culture medium containing 10% fetal bovine serum (Biological Industries Ltd. #04-004-1A, Beit-Haemek, Israel)]. Recovery medium was replaced with new fresh PC12 medium on the following day.

#### **2.4 Reverse-transcriptase quantitative polymerase chain reaction (RT-qPCR)**

After 72 hr post transfection, the RNA samples from transfected cells were homogenized and extracted by TRIzol reagent (Invitrogen #15596-018, CA, USA), with phase-separation by chloroform (Sigma #C2432-500mL, MO, USA). Followed by centrifugation at 12,000 g, 4°C for 15 min, about 0.6 mL of the RNA in the upper aqueous phase was collected and further precipitated by mixing with 500 µL isopropanol (Sigma #I9516-500 mL, MO, USA). After centrifuging at 12,000 g, 4°C for 10 min, the supernatant was discarded. The RNA pellets were washed once with

75% ethanol, followed by centrifugation at 12,000 g, 4°C for 10 min. The supernatant was then discarded completely. The RNA pellets were air-dried at room temperature for 20 min, dissolved in 20 µL of diethyl pyrocarbonate (DEPC)-treated water and incubated at 60°C for 15 min. The RNA samples were stored at -80°C for further experiments.



The cDNAs were synthesized from RNA samples by using the ProtoScript II First Strand cDNA Synthesis Kit (New England BioLabs, MA, USA). RT-qPCR was performed on the cDNA samples by LabStar SYBR qPCR Kit (TAIGEN Bioscience Corporation, Taiwan) with specific primer sequences to recognize the target gene, Syn Ia (Forward primer: 5'-AgCTCAACAAATCCCAGTCTCT-3' and Reverse primers: 5'-CggATggTCTCAgCTTTCAC-3'), or the reference gene,  $\beta$ -actin (Forward primer: 5'-TgCTCTggCTCCTAgCACCATgAAgATCAA-3' and Reverse primers: 5'-AAACgC AgCTCAgTAACAgTCCgCCTAgAA-3'). The RT-qPCR was performed by the following condition (denaturation at 94°C for 15 s; annealing at 60°C for 30 s; extension at 72°C for 30 s) for 40 cycles.

The cycle threshold (Ct) values were evaluated from the SYBR fluorescence data by using the qPCR machine (Qiagen Rotor-Gene Q, Hilden, Germany) and the supplemental software (Qiagen Rotor-Gene Series Software 1.7, Hilden, Germany).

The mRNA level ( $\Delta C_t$ ) was acquired by subtracting the  $C_t$  of the reference gene ( $\beta$ -actin) from the  $C_t$  of the target gene (Syn Ia). The  $\Delta\Delta C_t$  was obtained by subtracting the median of the  $\Delta C_t$  of the control group from the  $\Delta C_t$  of the transfection group.

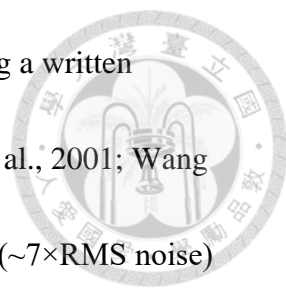
The relative mRNA expression levels of Syn Ia were calculated as  $2^{(-\Delta\Delta C_t)}$ .

## 2.5 Single-vesicle amperometry

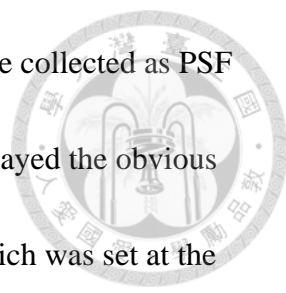
To pre-coat the coverslips in the 35-mm dishes (Corning® #430165, NY, USA) for attaching cells, 1 mL poly-d-lysine (50  $\mu\text{g/mL}$ ; BD Biosciences #354210, Bedford, MA, USA) and collagen I (50  $\mu\text{g/mL}$ ; BD Biosciences #354246, Bedford, MA, USA) were added into each dish with the coverslips, followed by incubation for 1 hr. After discarding the poly-d-lysine and collagen I, the dishes were rinsed by the fresh serum-free PC12 culture medium. After 60-96 hr post transfection, the transfected cells were seeded at the density of  $2 \times 10^5$  per pre-coated dish. The cells on the coverslips were incubated with PC12 culture medium containing 1.5 mM norepinephrine (NE; Sigma #A5785, MO, USA) and 0.5 mM ascorbate (Sigma #A5960, MO, USA) for 16 hr [NE was previously prepared in 20 mM HEPES (Sigma #H7523, MO, USA) as 1,000 $\times$  stocks and ascorbate (Sigma #A5960, MO, USA) was

previously dissolved in ddH<sub>2</sub>O as 1,000× stocks]. The culture medium was replaced by the fresh PC12 culture medium at least 1 hr before amperometric recordings.

The bathing solution [(in mM) 150 NaCl (Sigma #S5011, MO, USA), 4.2 KCl (Sigma #P9333, MO, USA), 1 NaH<sub>2</sub>PO<sub>4</sub> (Sigma #A5785, MO, USA), 0.7 MgCl<sub>2</sub> (Sigma #M1028, MO, USA), 2 CaCl<sub>2</sub> (Fluka #21108, MO, USA), and 10 HEPES (Sigma #H7523, MO, USA), pH 7.4] and high KCl solution (140 mM KCl to replace NaCl in the bathing solution) were prepared for amperometric recordings. During recordings, the cells were bathed in the bathing solution. A 5-μm carbon fiber electrode (CFE-1 or CFE-2, ALA Scientific Instruments, NY, USA) was attached onto the cell. Secretion from cells was induced by the pressure ejection of the high KCl solution from a 2-μm micropipette. A carbon fiber electrode connected with a VA-10X amplifier (ALA Scientific Instruments, NY, USA) at a polarization of 650 mV can record the NE-oxidized current upon the DCV release. The signals were amplified by the VA-10X amplifier (ALA Scientific Instruments, NY, USA), sent to the interface Digidata1440A (MDS Analytical Technologies, CA, USA), and processed by software pClamp10 (Axon Instruments, Molecular Devices Corp., CA, USA).



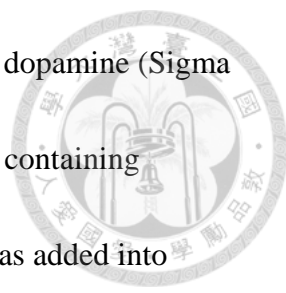
Amperometry data were analyzed as previously described using a written computer program (Chiang et al., 2014; Wang et al., 2006; Wang et al., 2001; Wang et al., 2003). The amperometric events with peak amplitude  $\geq 2$  pA ( $\sim 7 \times \text{RMS noise}$ ) were collected for the calculation of all secretion events. Notably, the same dataset (**Fig. 4 and Fig. 6-10**) was used for this study. Two specific temporal parameters,  $t_1$  and  $t_2$ , were defined as previously reported (Chiang et al., 2014) and used to separate the KR and FF events. The  $t_1$  was the duration from onset to the signal falling back to the average value of 50-100% peak amplitude of events [mean value (50-100%)]. The  $t_2$  was the duration from onset to the signal falling back to the baseline. The  $t_1/t_2$  ratio at 3.5 pA was very sensitive to the event shape of two types of fusion events, full fusion (FF) and kiss and run (KR). The amperometric recordings of FF shaped like a spike. On the other hand, KR was square or rectangular-like shape. Therefore, the cut-off peak amplitude of 3.5 pA was used to divide FF events from KR events (**Fig. 6-7 and Fig. 9**). As the results, the events with peak amplitude  $\geq 3.5$  pA were FF events, and those with peak amplitude with 2-3.5 pA were KR events. The spike characteristics, i.e., peak amplitude, whole area, half width, 35-90% rise time, and decay time, were analyzed by the written computer program according to the criterion illustrated in **Fig. 7** and calculated by the cellular mean method (Chiang et al., 2014;



Wang et al., 2006). The events with peak amplitude  $\geq 13$  pA were collected as PSF events, because the events with large peak amplitude normally displayed the obvious characteristics of PSF. The duration from onset to the end point, which was set at the intersection between the baseline and the line going through the 35-60% peak amplitude (**Fig. 8**), was measured as PSF duration. To further evaluate mean PSF duration ( $\tau$ ), the histograms of PSF duration were constructed in the semi-log plots and fitted by a single-exponential decay function [ $N(t) = N(0) \times \exp(-t/\tau)$ ] to yield the  $\tau$  (Origin8, OriginLab Crop, MA, USA). PSF mean amplitude and area were calculated by taking the cellular means. Subsequently, we resolved the rate constants of fusion pore closure ( $k_c$ ) and dilation ( $k_d$ ) to perform kinetic analysis. The rate constant  $k_c$  and  $k_d$  in the kinetic model were resolved from the mean PSF duration [ $\tau = 1/(k_c + k_d)$ ] and the KR fraction ( $X_{KR}$ ) [ $X_{KR} = k_c / (k_c + k_d)$ ] as previously reported (Chiang et al., 2014; Wang et al., 2006; Wang et al., 2001).

## 2.6 Immunofluorescence staining

After 48 hr post transfection, the transfected cells were seeded at the density of  $2 \times 10^5$  per pre-coated dish with the coverslips. The original medium was discarded from the dishes on the following day. For dopamine staining, the PC12 culture



medium of dishes were replaced by the medium containing 0.7 mM dopamine (Sigma #H8502, MO, USA) for 1 hr-incubation. Subsequently, the medium containing dopamine was discarded and the new fresh PC12 culture medium was added into dishes. After incubating 1 hr, the following procedure was performed. For ChB/Syp staining, the cells on the coverslips were incubated with the high KCl solution for 5 min. Cells (for dopamine or ChB/Syp staining) were washed with phosphate buffered saline (1×PBS: 137mM NaCl, 2.7 mM KCl, 4.3mM Na<sub>2</sub>HPO<sub>4</sub>·2H<sub>2</sub>O, and 1.47 mM KH<sub>2</sub>PO<sub>4</sub>; pH 7.4 by NaOH for 1L) and then fixed by paraformaldehyde (Alfa Aesar #A11313, Great Britain) in 1×PBS at room temperature for 10 min, followed by washout with 1×PBS for 10 min twice. The cells were permeabilized by 0.1% Triton X-100 (Sigma #TB532, MO. U.S.A) in 1×PBS for 10 min, followed by washout with 1×PBS three times. The cell-containing coverslips were transferred onto a parafilm sheet. Cells were incubated in the blocking buffer [3% normal donkey serum (Jackson Lab #017000121, ME, USA) and 0.1% Triton X-100 (Sigma #T8532, MO. U.S.A) in 1×PBS] at room temperature for 1 hr. After blocking, cells were incubated with primary antibodies [rabbit anti-Syn I (Cell Signaling Technology, MA, USA); mouse anti-Chromogranin B (BD Biosciences, NJ, USA); mouse anti-Synaptophysin (Merck Millipore, Darmstadt, Germany)] in the blocking buffer at 4°C overnight, followed by

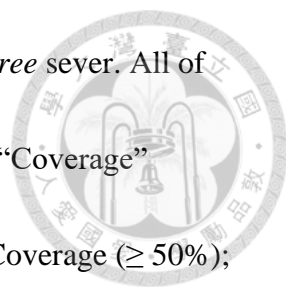
washout with 1×PBS six times (5, 5, 10, 10, 15, and 15 min). Subsequently, cells were incubated with secondary antibodies in the blocking buffer at room temperature in dark for 1 hr, followed by washout with 1×PBS six times (5, 5, 10, 10, 15, and 15 min). The 4',6-diamidino-2-phenylindole (DAPI; Sigma #D9542, MO, U.S.A) was then added to stain the nuclei at room temperature in dark for 10 min. Finally, the coverslips were mounted onto the glass slides with Fluoromount G (Electron Microscopy Sciences #17984-25, PA, USA).

Images were acquired by the Leica TCS SP5 or SP8 Confocal Spectral Microscope Imaging System (Leica, Germany). Quantification of colocalization was determined with the MetaMorph software (Molecular Devices).

## 2.7 Prediction for protein-protein interaction

The possibility of interactions for protein pairs of interest were predicted by the *MirrorTree* sever [<http://csbg.cnb.csic.es/mtserver/>, Computational Systems Biology Group (CNB-CSIC, Madrid, Spain)] (Ochoa and Pazos, 2010). *MirrorTree*, a computational technique, was developed to predict protein interactions through the characteristics of co-evolution between two protein families of around 800 residues long from 120 species. Individual pairs (Syn Ia and putative-interacting proteins; n =

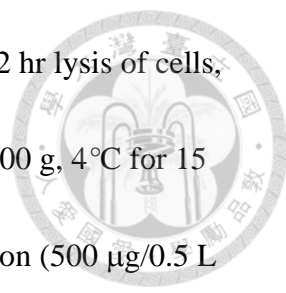




66) of query protein sequences were first imported into the *MirrorTree* server. All of the parameters were remained as the original setting, except for the “Coverage” [Homologs selection: % identity ( $\geq 30\%$ ), e-value ( $\leq 1e-5$ ), and % Coverage ( $\geq 50\%$ ); Orthologs selection: % identity ( $\geq 30\%$ ), and % Gap ( $\leq 90\%$ )]. The highest identity sequence comparing to the query sequence was selected from the Multiple Sequence Alignment (MSA). Only the protein sequences of the organisms present in both trees are used to calculate the similarities. Correlation coefficients [from scoring from 1 (yellow) to 0 (dark blue)], reflecting the possibility of interaction for every pairs of proteins, were acquired from the tree similarity between the two families, according to the standard equation from the PPI prediction of *MirrorTree*.

## 2.8 Co-immunoprecipitation

After 72 hr post transfection, transfected cells were incubated with the high KCl solution for 1 min. The cells were further lysed in the ice-cold RIPA lysis buffer [1% NP-40, 150 NaCl (Sigma #S5011, MO, USA), 1 EDTA (Sigma #E5134, MO, USA), 1 phenylmethylsulfonyl fluoride (Sigma #P7626, MO, U.S.A), 1 sodium orthovanadate (Sigma #S6508, MO, U.S.A), 10 sodium fluoride (Sigma #S7920, MO, U.S.A), and 50 HEPES (Sigma #H7523, MO, USA) (in mM), pH 7.4, supplemented

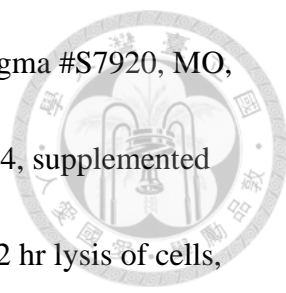


with protease inhibitor cocktail (Sigma #P2714, MO, USA)]. After 2 hr lysis of cells, the proteins from cell lysates were isolated by centrifugation at 12,000 g, 4°C for 15 min. After that, the soluble fraction was acquired. The soluble fraction (500 µg/0.5 L each tube) was preincubated with the antibody [1 µg, rabbit anti-Syn I (Cell Signaling Technology, MA, USA)] to immunoprecipitate Syn I at 4°C overnight. The complex was then incubated with protein G sepharose beads (GE Healthcare Life Science #71-7083-00, MA, USA) for 2 hr. After washed with ice-cold 1×PBS (137 mM NaCl, 2.7 mM KCl, 4.3 mM Na<sub>2</sub>HPO<sub>4</sub>·2H<sub>2</sub>O, and 1.47 mM KH<sub>2</sub>PO<sub>4</sub>; pH 7.4 by NaOH for 1L) for 10 min by 3 times, the immunoprecipitates were mixed with 4× sample buffer [250 mM Tris-HCl (Bioshop #TRS001, Ontario, Canada), 8% SDS (Bioshop #SDS001, Ontario, Canada), 40% Glycerol (J. T. Baker #2136-01, PA, USA), 10% β-mercaptoethanol (Sigma #3148, MO, USA), 0.008% bromophenol blue (Sigma #B0126, MO, USA), and 400 mM DTT (Sigma #D0632, MO, USA), pH 6.8], boiled for 5 min, and electrophoresed via SDS polyacrylamide gels. After transferring to polyvinylidene fluoride membranes (PVDF membranes; Immobilon-P, Merck Millipore, Darmstadt, Germany), membranes were blocked in 3% non-fat milk in TBST [100 mM Tris-HCl (Bioshop #TRS001, Ontario, Canada), 150 mM NaCl (Sigma #S5011, MO, USA), and 0.1% Tween-20 (Merck #8.22184, Darmstadt,

Germany), pH 7.4] for 1 hr, and then incubated with chosen primary antibodies [mouse anti-Syn I (Synaptic Systems, Goettingen, Germany); mouse anti-SNAP-25 (Synaptic Systems, Goettingen, Germany); mouse anti-Stx I (Stanta cruz Biotechnology, TX, USA); mouse anti-Synaptophysin (Synaptic Systems, Goettingen, Germany); mouse anti-Synaptobrevin (Synaptic Systems, Goettingen, Germany)] at 4°C overnight. Membranes were washed with TBST for 10 min three times and then incubated with chosen secondary antibodies in 3% milk in TBST at room temperature for 1 hr. Finally, membranes were washed with TBST for 10 min three times, and signals were visualized and photographed by using enhanced chemiluminescence (ECL; Merck Millipore #WBKLS0500, Darmstadt, Germany) and the FluorChem M Chemiluminescent Western Imaging System (ProteinSimple, CA, USA). Image J (NIH, MD, USA) was used for quantification of protein levels.

## 2.9 Western blotting

After 72 hr post transfection, transfected cells were incubated with the high KCl solution for 1 min. The cells were further lysed in the ice-cold RIPA lysis buffer [1% NP-40, 150 NaCl (Sigma #S5011, MO, USA), 1 EDTA (Sigma #E5134, MO, USA), 1 phenylmethylsulfonyl fluoride (Sigma #P7626, MO, U.S.A), 1 sodium

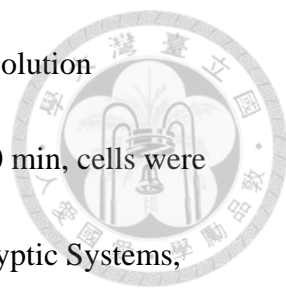


orthovanadate (Sigma #S6508, MO, U.S.A), 10 sodium fluoride (Sigma #S7920, MO, U.S.A), and 50 HEPES (Sigma #H7523, MO, USA) (in mM), pH 7.4, supplemented with protease inhibitor cocktail (Sigma #P2714, MO, USA)]. After 2 hr lysis of cells, the proteins were isolated by centrifugation at 12,000 g, 4°C for 15 min, and the soluble fraction was acquired. The soluble fraction (30 µg) was mixed with 4× sample buffer [250 mM Tris-HCl (Bioshop #TRS001, Ontario, Canada), 8% SDS (Bioshop #SDS001, Ontario, Canada), 40% Glycerol (J. T. Baker #2136-01, PA, USA), 10% β-mercaptoethanol (Sigma #3148, MO, USA), 0.008% bromophenol blue (Sigma #B0126, MO, USA), and 400 mM DTT (Sigma #D0632, MO, USA), pH 6.8], boiled for 5 min, and electrophoresed via SDS polyacrylamide gels. After transferring to polyvinylidene fluoride membranes (PVDF membranes; Immobilon-P, Merck Millipore, Darmstadt, Germany), membranes were blocked in 3% non-fat milk in TBST [100 mM Tris-HCl (Bioshop #TRS001, Ontario, Canada), 150 mM NaCl (Sigma #S5011, MO, USA), and 0.1% Tween-20 (Merck #8.22184, Darmstadt, Germany), pH 7.4] for 1 hr, and then incubated with chosen primary antibodies [mouse anti-Syn I (Synaptic Systems, Goettingen, Germany); mouse anti-SNAP-25 (Synaptic Systems, Goettingen, Germany); mouse anti-Stx I (Stanta cruz Biotechnology, TX, USA); mouse anti-Synaptophysin (Synaptic Systems, Goettingen,

Germany); mouse anti-Synaptobrevin (Synaptic Systems, Goettingen, Germany)] at 4°C overnight. Membranes were then washed with TBST for 10 min three times and then incubated with chosen secondary antibodies in 3% milk in TBST at room temperature for 1 hr. Finally, membranes were washed with TBST for 10 min three times, and signals were visualized and photographed by using enhanced chemiluminescence (ECL; Merck Millipore #WBKLS0500, Darmstadt, Germany) and the FluorChem M Chemiluminescent Western Imaging System (ProteinSimple, CA, USA). Image J (NIH, MD, USA) was used for quantification of protein levels.

## **2.10 Proximity ligation assay**

Intact or transfected cells on the coated-coverslips were washed with ice-cold 1×PBS (137 mM NaCl, 2.7 mM KCl, 4.3 mM Na<sub>2</sub>HPO<sub>4</sub>·2H<sub>2</sub>O, and 1.47 mM KH<sub>2</sub>PO<sub>4</sub>; pH 7.4 by NaOH for 1 L) and further fixed by 4% paraformaldehyde (Alfa Aesar #A11313, Great Britain). After washed with ice-cold 1×PBS for 10 min twice, cells were quickly washed with ddH<sub>2</sub>O to remove salts, followed by permeabilization by 0.1% Triton X-100. Subsequently, the cells were washed with ice-cold 1×PBS for 10 min twice, and then the cell-containing coverslips were transferred onto a parafilm sheet. Cells were stained according to the protocol of the Duolink® proximity ligation



assay (PLA) kit (Sigma, MO, U.S.A). After blocking [1× blocking solution (Duolink® in situ PLA® probe, Sigma, MO, U.S.A)] at 37°C for 30 min, cells were incubated with two chosen primary antibodies [mouse anti-Syn I (Syptic Systems, Goettingen, Germany); mouse anti-Stx I (Santa cruz Biotechnology, TX, USA); rabbit anti-SNAP-25 (Synaptic Systems, Goettingen, Germany); mouse anti-Synaptophysin (Synaptic Systems, Goettingen, Germany)] in the antibody diluent (PLA kit, Sigma, MO, U.S.A) at 4°C overnight, followed by washout with 1× wash buffer A [0.01 M Tris-HCl (Bioshop #TRS001, Ontario, Canada), 0.15 M NaCl (Sigma #S5011, MO, USA), and 0.05% Tween 20 (Merck #8.22184, Darmstadt, Germany), pH 7.4] for 5 min twice. Subsequently, cells were incubated with PLA probes (Sigma #DUO92002 and #DUO92004, MO, U.S.A)) in the PLA probe solution (PLA kit, Sigma, MO, U.S.A) at 37°C in dark for 1 hr, followed by washout with 1× wash buffer A for 5 min twice. The ligation-ligase solution (Sigma # DUO92008, MO, U.S.A)) was added to samples at 37°C in dark for 30 min. Subsequently, cells were incubated with the amplification-polymerase solution (Sigma # DUO92008, MO, U.S.A)) at 37°C in dark for 100 min, followed by washout with 1× wash buffer B (0.2 M Tris-HCl (Bioshop #TRS001, Ontario, Canada) and 0.11 M NaCl (Sigma #S5011, MO, USA), pH 7.5) for 10 min twice. DAPI (Sigma #D9542, MO, U.S.A) was subsequently

added to stain the nuclei at room temperature in dark for 10 min, followed by washout with 0.01× wash buffer B in dark for 1 min. Finally, the coverslips were mounted onto the glass slides with Fluoromount G (Electron Microscopy Sciences #17984-25, PA, USA).

Images were acquired by the Leica TCS SP5 or SP8 Confocal Spectral Microscope Imaging System (Leica, Germany).

## 2.11 Statistics

The data are displayed as means or as medians (the results of mRNA levels) with standard errors (SEM). To further evaluating the statistical significance between two different transfected groups, we used the two-tailed Student's unpaired *t*-test for the parametric method and the Mann-Whitney method for the nonparametric method (InStat 3, GraphPad, CA, USA). The significance is represented with asterisks with the following notation: \**p* < 0.05; \*\**p* < 0.01; \*\*\**p* < 0.001 compared to Syn Ia. #*p* < 0.05; ##*p* < 0.01; ###*p* < 0.001 compared to Ctrl. n.s., not significant.

## Chapter III



### Results

#### 3.1 Secretion from DCVs was regulated by Syn Ia or its phosphodeficient mutants

To determine how Syn Ia regulates the dynamic of DCV exocytosis via phosphorylation at single-vesicle levels, the effects of Syn Ia on DCV secretion were examined first. NE release from individual DCVs are triggered by KCl depolarization, and oxidized through high voltage delivered by potentiated carbon fiber electrode (CFE) (**Fig. 3A**). Individual DCV release revealed as single peak in amperometric recordings. Representative amperometric traces (**Fig. 4A**) in cells overexpressing Ctrl, Syn Ia, Syn Ia-S62A or Syn Ia-S9,566,603A exhibited diverse secretion rates triggered by KCl depolarization (**Fig. 4A**; black bottom line) during the recording time. To further quantify the secretion rate, the plots of cumulative events across the recording time from all cells recorded in various transfected groups (**Fig. 4B**) were constructed and subsequently applied linear fittings from 0 to 10 sec or from 10 to 20 sec (**Fig. 4C**). Based on the results, overexpressing Syn Ia in PC12 cells increased the fitted secretion rate in both early and late stages compared to Ctrl ( $p < 0.001$ ). By contrast, the level of fitted secretion rate in cells overexpressing Syn Ia-S62A was



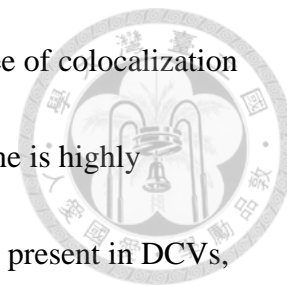
decreased in both early and late stages compared to Syn Ia ( $p < 0.01$ ), but without reaching significant differences of level compared to Ctrl. Moreover, the dramatic reduction of fitted secretion rate in both stages was showed in cells overexpressing Syn Ia-S9,566,603A by two-fold compared to Syn Ia or Ctrl ( $p < 0.001$ ).

Additionally, another method, the cellular mean method, was exerted to calculate the bulk secretion rate in this study (**Fig. 4D**). Overexpressing Syn Ia-S9,566,603A significantly decreased the bulk secretion rate compared to Syn Ia, suggesting the phosphodeficiency at these sites may decrease the secretion rate of DCVs ( $p < 0.01$ ). Thus, these findings suggest that secretion from DCVs is regulated by Syn Ia or its phosphodeficient mutants.

To confirm the effectiveness of overexpression, the Syn Ia mRNA levels were examined at 72 hr post transfection by RT-qPCR combining with specific primer targeting to Syn Ia (**Fig. 5A and Methods**). From the results (**Fig. 5B**), the mRNA levels of Syn Ia were significantly increased in cells transfecting with Syn Ia or its phosphodeficient mutants compared to Ctrl ( $p < 0.05$ ), suggesting the well efficiency of overexpression.

To confirm NE is packed into DCVs in PC12 cells, the cells overexpressing Syn Ia were co-stained with the DCV marker, ChB and dopamine after 1-hr incubation of

dopamine (**Fig. 5C**). In the fluorescence images, a significant degree of colocalization of dopamine and ChB (about 80%) was shown, suggesting dopamine is highly concentrated on DCVs. Dopamine- $\beta$ -hydroxylase, the enzyme only present in DCVs, is responsible for converting dopamine into NE (Cooper et al., 2003). As a result, these findings suggest that NE is mainly packed into DCVs.



### **3.2 FF frequency of DCVs was regulated by Syn Ia in a phosphorylation-dependent manner**

To determine the effects of Syn Ia and its phosphodeficient mutants on the occurrences of two distinct fusion events, the whole population of events were divided into two types of fusion events, i.e., FF and KR. From the amperometric recordings, the shapes of FF (spike-like) are different from KR (square-like). The  $t_1/t_2$  ratio at 3.5 pA was very sensitive to the event shape of two types of fusion events, thus set as cut-off for separation of two events (**Fig. 6A and Methods**).

Overexpressing Syn Ia in PC12 cells slightly increased the FF frequency without achieving statistical significances compared to Ctrl (**Fig. 6B**). In addition, the FF frequency in cells overexpressing Syn Ia-S62A showed the similar levels of Syn Ia. Of note, overexpressing Syn Ia-S9,566,603A significantly decreased the FF frequency

( $p < 0.05$ ) compared to Syn Ia or Syn Ia-S62A, suggesting that the FF frequency can be regulated by phosphorylation at these sites of Syn Ia. Next, we further examined the effects of Syn Ia and its phosphodeficient mutants on the occurrence of KR by analyzing the fraction of KR ( $X_{KR}$ ) (**Fig. 6C**). Based on the results, only overexpressing Syn Ia-S62A reached the significant differences for the levels of  $X_{KR}$  compared to Ctrl ( $p < 0.05$ ). Instead, the  $X_{KR}$  for Syn Ia-62A or Syn Ia-S9,566,603A was similar to Syn Ia, suggesting phosphorylation of Syn Ia may have a minor effect on the occurrence of KR.

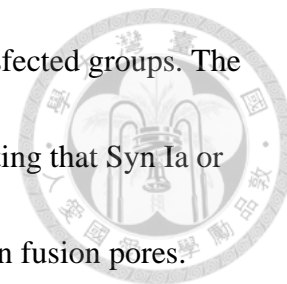
Since the secretion rate and FF frequency were regulated by phosphorylation of Syn Ia, we afterward determined whether Syn Ia and its phosphodeficient mutants affect the post-dilation process of DCVs (**Fig. 7**). Spikes characteristics (**Fig. 7A and Methods**), representing the process of post-dilation of DCVs, was measured from FF events by the cellular mean method. Based on the analysis of spikes characteristics, overexpressing Syn Ia-S62A increased the half width (**Fig. 7D**) compared to Ctrl. However, other spikes characteristics (**Fig. 7B-F**), including peak amplitude, whole area, 35%-90% rise time, and decay time, exhibited little differences among all groups, suggesting that Syn Ia and its phosphodeficient mutants may play a minor role in the post-dilation process of DCV exocytosis.



### 3.3 The stabilization of open DCV fusion pores was regulated by Syn Ia or its phosphodeficient mutants

By zooming in the scale for one amperometric spike (**Fig. 8A and Methods**), there is a foot preceding the spike termed prespike foot (PSF). PSF represents the transient opening of the initial fusion pore prior to dilation. To determine the effects of Syn Ia and its phosphodeficient mutants on the opening of initial fusion pores, the PSF characteristics were analyzed. First of all, PSF open time distributions in various transfected groups were constructed (**Fig. 8B**) and then fitted by single-exponential decay function ( $R^2$  ranging from 0.74 to 0.94) to acquire the PSF mean duration,  $\tau$  (**Fig. 8C**). We found that overexpressing Syn Ia prolonged the PSF mean duration compared to Ctrl ( $p < 0.01$ ), suggesting the effects on stabilizing fusion pores. By contrast, overexpressing Syn Ia-S62A shortened the PSF mean duration (to the similar levels of Ctrl) compared to Syn Ia ( $p < 0.001$ ), suggesting the phosphodeficiency at Ser62 site may destabilize fusion pores. In particular, overexpressing Syn Ia-S9,566,603A significantly prolonged the PSF mean duration compared to Ctrl, Syn Ia, or Syn Ia-S62A, indicating vigorous effects on stabilizing fusion pores by phosphodeficiency at Ser9, Ser566, and Ser603 sites. Secondly, the mean amplitude

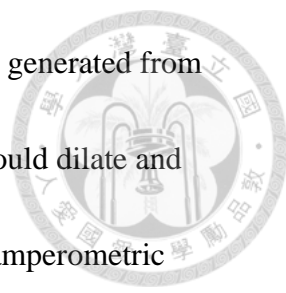
(**Fig. 8D**) and area (**Fig. 8E**) of PSF were measured in various transfected groups. The results showed no significant differences among all groups, suggesting that Syn Ia or its phosphodeficient mutants may not alter the flux through the open fusion pores.



These findings suggest that Syn Ia differentially regulates the stabilization of open fusion pores by phosphorylation at various sites, but without altering the flux through the open fusion pores.

According to previous studies (Chiang et al., 2014; Wang et al., 2006), the mean amplitudes of KR and PSF should be similar because both KR and PSF generated from the same population of non-dilating fusion pores. Moreover, the mean amplitudes of both should not change over the time. To confirm the similarity of the mean amplitudes for KR and PSF in this study, the scatter plots of KR (or PSF) mean amplitude across the KR (or PSF) duration were constructed (**Fig. 9A and 9B**).

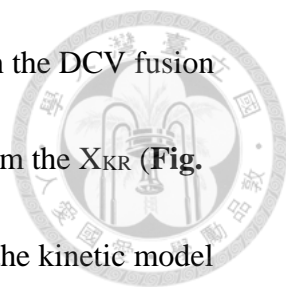
Among the groups, linear fitting of the plots for KR exhibited little correlation ( $R^2$  ranging from -0.01 to 0.02), suggesting the mean amplitudes of KR do not change over the time (**Fig. 9A**). These evidence also confirmed the square-shaped of KR events as shown in amperometric recordings (**Fig. 6A, right**). Consistent with results of KR, little correlation ( $R^2$  ranging from -0.02 to -0.01) was also found in the scatter plots for PSF amplitude versus the PSF duration in various transfected groups (**Fig.**



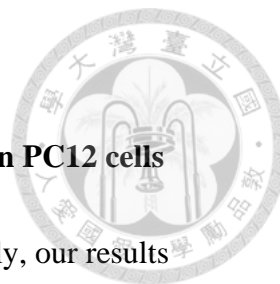
**9B).** Taken together, these results suggest that both PSF and KR are generated from non-dilating fusion pore. Partial fusion pore from this population would dilate and then undergo FF, yielding the PSF followed by spikes as shown in amperometric recordings (**Fig. 6A, left**). Since the population of FF was distinguishable from that of KR events, we next examined the mean amplitude distributions of both events (**Fig. 9C**). Among all groups, the mean amplitude distributions of KR events can be fitted well by single Gaussian distribution ( $R^2$  ranging from 0.90 to 0.98), suggesting these events arise from a single distinct population (**Fig. 9C, insets**). Instead, the mean amplitude distributions of FF exhibited comparatively skewed in various transfected groups (**Fig. 9C**). Given that these results suggest that the population of FF was indeed distinguishable from that of KR events, corresponding to previous studies (Chiang et al., 2014; Wang et al., 2006).

### **3.4 Fusion pore kinetics of DCVs was regulated by Syn Ia or its phosphodeficient mutants**

Since the secretion rate, FF frequency, and stabilization of open fusion pores were regulated by the phosphorylation of Syn Ia, we were interested if Syn Ia and its phosphodeficient mutants further regulate fusion pore kinetics of DCV exocytosis. To



investigate the effects of Syn Ia and its phosphodeficient mutants on the DCV fusion pore kinetics, the specific rate constants  $k_c$  and  $k_d$  were analyzed from the  $X_{KR}$  (**Fig. 6C**) and PSF mean duration,  $\tau$  (**Fig. 8C**) by equations according to the kinetic model of fusion pores defined in previous studies (Chiang et al., 2014; Wang et al., 2006; Wang et al., 2001; Wang et al., 2003) (**Fig. 10 and Methods**). Based on the results of  $k_c$  and  $k_d$ , overexpressing Syn Ia did not change the  $k_c$ , but decreased the  $k_d$  compared to Ctrl, suggesting that Syn Ia prevents the open fusion pores towards the dilation state, thus stabilizes the open fusion pores. By contrast, overexpressing Syn Ia-S62A markedly increased the levels of  $k_c$  compared to Ctrl or Syn Ia, suggesting that Syn Ia-62A strongly promotes the open fusion pores towards the closure state. In addition, overexpressing Syn Ia-S62A lightly increased  $k_d$  compared to Syn Ia. Taken together, these results suggest that Syn Ia-S62A promotes open fusion pores escapes away from the open state (mainly towards the closure state), thus destabilizes the open fusion pores. Instead, overexpressing Syn Ia-S9,566,603A decreased both  $k_c$  and  $k_d$  compared to Ctrl or Syn Ia, suggesting the effects on the prevention of open fusion pores towards the closure or dilation state and the stabilization of open fusion pores. Given that the phosphorylation of Syn Ia may play an important role in regulating fusion pore kinetics of DCVs.



### 3.5 Syn I mainly localized to SVs, but rarely localized to DCVs in PC12 cells

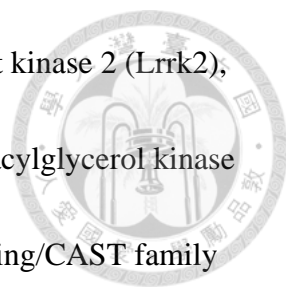
Despite Syn Ia has been considered localized to SVs exclusively, our results from single-vesicle amperometry showed that Syn Ia can regulate DCV exocytosis via its phosphorylation. Thus, the mechanism underlying the Syn Ia's regulation of DCV exocytosis required further exploration. The question here is how a SV-specific protein, Syn Ia regulates DCV release. Does Syn I localize to DCVs to regulate DCV exocytosis? Or, Syn Ia may interact with certain exocytotic proteins that localize to DCV, thus regulating DCV exocytosis. In the latter case, Syn Ia may co-recruit SVs and DCVs to plasma membrane by associating with certain proteins, thus regulating DCV exocytosis. Therefore, to exclude the possibility that Syn Ia localizes to DCVs, we confirmed the subcellular localization of Syn I in PC12 cells (**Fig. 11**). The PC12 cells overexpressing Syn Ia or its phosphodeficient mutants were co-immunostained with Syn I and DCV marker, chromogranin B (ChB) or general vesicle marker, Synaptophysin (Syp) after KCl depolarization. Based on the results from immunofluorescence staining (**Fig. 11A**), Syn I was mainly colocalized with Syp corresponded to previous studies. Conversely, only little levels of colocalization of Syn I and ChB, suggesting Syn I mainly localizes to SVs in PC12 cells. To further



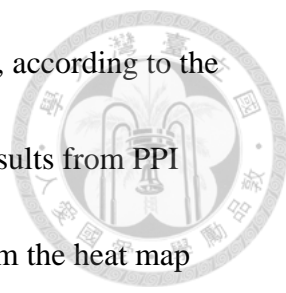
quantify the levels of colocalization, the ratios of the Syn I immunoreactivity overlapping with the ChB or Syp immunoreactivity were analyzed (**Fig. 11B**). We found that Syn I immunoreactivity overlapping with the ChB, reflecting the percentages of Syn I targeting to DCVs, was notably lower than Syp ( $p < 0.001$ ), reflecting the percentages of Syn I targeting to general vesicles. Moreover, the ratios of Syn I/Syp and Syn I/ChB were similar in various transfected groups. Hence, these results suggest that Syn I or its phosphodeficient mutants mainly localize to SVs, but rarely localize to DCVs in PC12 cells.

### **3.6 Exploring the putative Syn Ia-interacting proteins by database search and PPI prediction**

Since Syn I rarely localize to DCVs, we hypothesized that Syn Ia may regulate the dynamics of DCV exocytosis, through the phosphorylation-dependent interaction with certain DCV proteins. Supposedly, the interaction of Syn Ia with Syn Ia-interacting proteins might be regulated by the phosphorylation of Syn Ia. Furthermore, these proteins must be exocytotic proteins, thus can rapidly affect DCV exocytosis. First of all, we explored the putative Syn Ia-interacting proteins by database search (**Fig. 12**). As a result, we found that adaptor-related protein complex 3 subunit delta 1 (Ap3d1),



nitric oxide synthase 1 adaptor protein (Nos1ap), leucine-rich repeat kinase 2 (Lrrk2), calcium-activated potassium channel subunit alpha-1 (Kcnma1), diacylglycerol kinase zeta (Dgkz), diacylglycerol kinase (Dgki), and ELKS/Rab6-interacting/CAST family member 1 (Erc1) in rats can directly interact with rat Syn Ia from IntAct and Mint (**Fig. 12A**). Moreover, Syn Ia can interact with its homologous proteins, Syn Ib and Syn Iib from BIND database. Based on the finding from String database (Szkarczyk et al., 2015), rat Syn I may interact with Nos1ap, CaMK IIa (CaMK II subunit alpha), Erc1, Crk, CaMK IV, CaMK IIg (CaMK II subunit gamma), Syt1, Myristoylated alanine-rich C-kinase substrate (Marcks), Brain-derived neurotrophic factor (BDNF), and Prickle-like protein 1 (Prickle 1) (**Fig. 12B**). All of the results from database search were combined and shown as the pie chart (**Fig. 12C**). Even though three of rat proteins, i.e., Lrrk2, Nos1ap and Erc1, found in the results from two types of databases, these proteins are not associated with DCVs. Therefore, these three proteins were not qualified for the requirement of the putative Syn Ia-interacting proteins in our study. As failing to find the suitable putative Syn Ia-interacting proteins from the database search, we next performed the protein-protein interaction (PPI) predication with the *MirrorTree* (Ochoa and Pazos, 2010; Pazos and Valencia, 2001) (**Fig. 13 and Methods**). The correlation coefficients as the indexes of the



interaction possibility were generated automatically after prediction, according to the criterion of the *MirrorTree* (**Fig. 13A**). The heat map showed the results from PPI prediction for totally 66 protein pairs (**Fig. 13B**). Top 5 proteins from the heat map (with the higher correlation coefficients compared to others) were regulating synaptic membrane exocytosis protein 2 (Rims 2), protein unc-13 homolog D (Unc 13D), SNARE-associated protein Snapin (Snapin), *N*-methyl-D-aspartate receptor subunit 3B (NMDA 3B), and Syp (Chatterton et al., 2002; Ilardi et al., 1999; Jahn et al., 1985; Koch et al., 2000; Shin, 2014). Among the top 5 proteins, the only one reported on the DCV membrane with transmembrane domains is Syp (Berwin et al., 1998; Saegusa et al., 2002; Schilling and Gratzl, 1988; Winkler, 1997). Therefore, Syp was selected as the primary putative Syn Ia-interacting protein. Additionally, three SNARE proteins were also regarded as the putative Syn Ia-interacting proteins in our study, owing to the important roles in regulating DCV exocytosis.

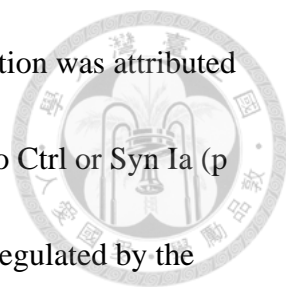
### **3.7 The expression levels of Synaptophysin and SNARE proteins were not altered by overexpressing Syn Ia or its phosphodeficient mutants**

Before verifying of the interaction between Syn Ia and the putative Syn Ia-interacting proteins, the expression levels of Syp and SNARE proteins, i.e., Stx,

SNAP-25, and Syb, were examined in cells overexpressing Syn Ia or its phosphodeficient mutants at 72 hr post transfection (**Fig. 14**). According to the results from western analysis, the expression levels of Syn I protein were markedly increased in cells transfecting with Syn Ia or its phosphodeficient mutants compared to Ctrl ( $p < 0.05$ ) (**Fig. 14A and 14B**), suggesting the well efficiency of overexpression consistent with the results of mRNA levels (**Fig. 5B**). By contrast, similar expression levels of Syp (**Fig. 14A and 14C**), Stx (**Fig. 14A and 14D**), SNAP-25 (**Fig. 14A and 14E**), and Syb (**Fig. 14A and 14F**) were showed in various transfected groups, suggesting overexpressing Syn Ia or its phosphodeficient mutants does not altered the expression levels of these proteins.

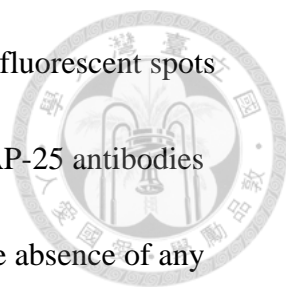
### **3.8 *In vivo* interaction between Syn I and Synaptophysin depended on the phosphorylation of Syn Ia**

To verify the results form PPI prediction (**Fig. 13B**), we performed co-immunoprecipitation (co-IP) from cell overexpressing Syn Ia or its phosphodeficient mutants after KCl depolarization (**Fig. 15**). Based on the results, the interaction between Syn I and Syp was confirmed (**Fig. 15A**). Moreover, overexpressing Syn Ia significantly decreased the levels of interaction between Syn I and Syp compared to



Ctrl ( $p < 0.05$ ). Of note, the dramatic reduction of Syn I-Syp interaction was attributed by overexpressing Syn Ia-S62A or Syn Ia-S9,566,603A compared to Ctrl or Syn Ia ( $p < 0.05$ ), suggesting that the *in vivo* interaction of Syn I with Syp is regulated by the phosphorylation of Syn Ia. Next, we also found the interaction between Syn I and Stx (**Fig. 15B**). In addition, overexpressing Syn Ia or its phosphodeficient mutants significantly decreased the levels of interaction between Syn I and Stx compared to Ctrl ( $p < 0.05$ ). However, Syn I-Stx interaction was not altered by overexpressing Syn Ia-S62A or Syn Ia-S9,566,603A, suggesting that the phosphorylation of Syn Ia may not play an important role in regulating the *in vivo* interaction of Syn I with Stx. Even through the interaction of Syn I with SNAP-25 or Syb also found, the interactions were appeared occasionally (**Fig. 15C and 15D**). Since the expression levels of Syp and SNARE proteins were not altered by overexpressing Syn Ia or its phosphodeficient mutants (**Fig. 14**), the levels of interaction between Syn I and Syp was particularly regulated by the phosphorylation of Syn Ia.

The *in situ* interaction between Syn I and Syn I-interacting proteins was further confirmed by performing the proximity ligation assay (PLA) (Ivanov, 2014; Soderberg et al., 2008) (**Fig. 16**). The explicit red puncta from results of PLA demonstrated the *in situ* interactions of proteins. Since direct interaction of Stx and



SNAP-25 reported previously (Sollner et al., 1993a), the clear PLA fluorescent spots were indeed showed in intact cells with the labeling of Stx and SNAP-25 antibodies (**Fig. 16A1-3**). By contrast, we did not detect any PLA signals in the absence of any primary antibodies (**Fig. 16A4-5**). Here, the interaction between Syn I and Syp confirmed again in cells overexpressing Syn Ia after 1-min KCl depolarization (**Fig. 16B**). As expected, the apparent spots from the results of PLA were detected in transfected cells with the labeling of Syn I and Syp antibodies, suggesting Syn Ia may directly interact with Syp *in situ* in the same cell. Additionally, some PLA signals were found in cells overexpressing Syn Ia with the labeling of Syn I and SNAP-25 antibodies (**Fig. 16C**), but less PLA puncta numbers compared to the labeling of Syn I-Syp (**Fig. 16B**). In summary, our results suggest that the *in vivo* interaction between Syn I and Syp is not attributed to the change in expression levels of proteins, but depends on the phosphorylation of Syn Ia.

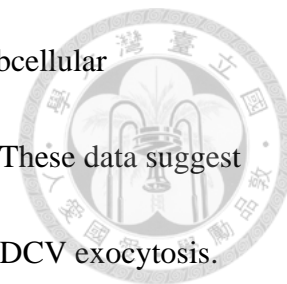
## Chapter IV



### Discussion

In this study, we show that overexpressing Syn Ia-S9,566,603A significantly decreases the secretion rate and FF frequency, suggesting that secretion from DCVs is regulated by the phosphorylation of Syn Ia. In addition, Syn Ia and its phosphodeficient mutants also exert the profound effects on the opening of initial fusion pores. Overexpressing Syn Ia or Syn Ia-S9,566,603A prolongs the PSF mean duration. By contrast, overexpressing Syn Ia-S62A shortens the PSF mean duration. Since Syn Ia or its phosphodeficient mutants do not change the PSF mean amplitude and area, our findings suggest that Syn Ia differentially regulates the stabilization of open fusion pores by its phosphorylation at various sites, without altering the flux through the open fusion pores. Moreover, we further show that Syn Ia and its phosphodeficient mutants regulate fusion pore kinetics, the intermediates during DCV fusion. Overexpressing Syn Ia-S62A increases  $k_c$  and  $k_d$ , thus promoting open fusion pores leaving from the open state mainly towards the close state. Conversely, overexpressing Syn Ia-S9,566,603A decreases both  $k_c$  and  $k_d$ , thus preventing the open fusion pores towards the close or dilation state, leading to stabilizing open fusion pores. Thus, phosphorylation of Syn Ia may play an important role in regulating

fusion pore kinetics of DCVs. Based on the confirmation for the subcellular localization of Syn I in PC12 cells, Syn I rarely localizes to DCVs. These data suggest that Syn Ia may interact certain protein to regulate the dynamics of DCV exocytosis.



Therefore, we further predict and identify certain DCV proteins that can directly interact with Syn I in a phosphorylation-dependent manner, thus affecting DCV exocytosis. From the database search and PPI prediction, Syp and three SNARE proteins was selected as the putative Syn Ia-interacting protein i.e., Stx, SNAP-25, and Syb for further verifying their interactions. Finally, we show that Syn I may directly interact with Syp *in situ* in the same cell. Since the expression levels of Syp protein is not altered by overexpressing Syn Ia or its phosphodeficient mutants, our results suggest that the *in vivo* interaction of Syn I and Syp cannot be attributed to the change in expression levels of proteins.

#### **4.1 Syn Ia dynamically regulates DCV exocytosis via different phosphorylation sites.**

The amperometric results (**Fig. 4**) show that a profound reduction in the secretion rate of DCVs by overexpressing Syn Ia-S9,566,603A compared to Syn Ia-S62A, suggesting that phosphorylation of Ser9, Ser566, and Ser603 may play a vital



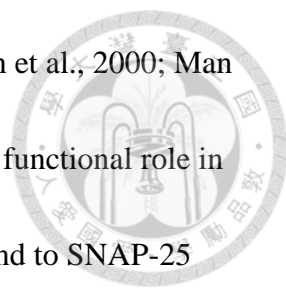
role in regulating the secretion rate of DCVs. Previous studies reported that phosphorylation of Ser9, Ser566, and Ser603 induces major conformational changes in the structure of Syn Ia. By contrast, no effects on the structure of Syn Ia were found due to phosphorylation of Ser62 (Bahler et al., 1990; Bahler and Greengard, 1987; Benfenati et al., 1989a; Ceccaldi et al., 1995; Chi et al., 2003; Petrucci and Morrow, 1987; Valtorta et al., 1992). The different effects on the structure of Syn Ia by different phosphorylation sites seemed to be the underlying mechanisms that phosphorylation of Syn Ia at different sites leads to the different reduction levels in the secretion rate of DCVs.

According to our kinetic model (Chiang et al., 2014; Wang et al., 2006; Wang et al., 2001; Wang et al., 2003), if the  $k_c$  is increased, the opening fusion pore prefer to enter the close state (KR events). By contrast, if  $k_d$  is increased, the opening fusion pore prefers to enter the dilation state (FF events). Syn Ia-S62A increases  $k_c$  compared to Syn Ia (**Fig. 10**), however, Syn Ia-S62A cannot increase the occurrence of KR events compared to Syn Ia (**Fig. 6C**). We speculate that these results may be due to the increased portion in the sum of  $k_c$  and  $k_d$  is similar to the increased portion in  $k_c$  alone, thereby not changing the ratio of  $k_c$  versus  $k_c$  and  $k_d$  ( $X_{KR}$ ). In addition, the decreased PSF mean duration of Syn Ia-S62A (**Fig. 8C**) is consistent with the

inverse of the increased sum of  $k_c$  and  $k_d$ . Similarly, the increased PSF mean duration of Syn Ia-S9,566,603A (**Fig. 8C**) is due to the decreased sum of  $k_c$  and  $k_d$ . Since  $k_d$  in Syn Ia-S9,566,603A is decreased, Syn Ia-S9,566,603A indeed decreases the FF frequency compared to Syn Ia (**Fig. 6B**). The constant  $X_{KR}$  of Syn Ia-S9,566,603A compared to Syn Ia may be presumably due to the decreased portion in the sum of  $k_c$  and  $k_d$  is similar to the decreased portion in  $k_c$  alone.

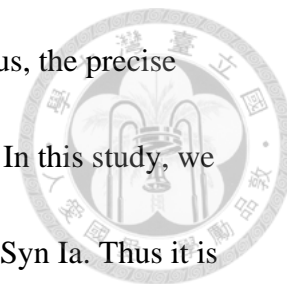
#### **4.2 Syp is selected as the primary putative Syn Ia-interacting protein among top 5 proteins from PPI prediction.**

Based on the results from PPI prediction (**Fig. 13**), the top 5 proteins are Rims 2, Unc 13D, Snapin, NMDA 3B, and Syp. Rims 2 is effector of a group of small GTPases, Ras-related protein Rab, with the main function in regulating SV priming (Koushika et al., 2001; Stevens et al., 2011). NMDA 3B is a postsynaptic protein. Thus, Rims 2 and NMDA 3B are apparently not our putative Syn Ia-interacting proteins. In addition, the Unc 13 family (Unc 13A-D) also plays important role in the first part of the priming step rather than docking or fusion during DCV exocytosis (Ashery et al., 2000; Augustin et al., 1999; Man et al., 2015; Richmond et al., 1999). Previous studies found that Unc13 D is abundantly expressed in lung, spleen, and



testis, regarded as non-neuronal isoform of the Unc 13 family (Koch et al., 2000; Man et al., 2015). Thus, Unc13 D is presumably not considered to play a functional role in exocytosis. Snapin, a ubiquitously expressed soluble protein, can bind to SNAP-25 via phosphorylation (Chheda et al., 2001). Most studies showed that Snapin can enhance the interactions of SNAREs and Syt I, thus playing an important role in priming step during exocytosis (Ilardi et al., 1999; Stevens et al., 2011). However, Snapin is not enriched in SV fractions, raising the question whether Snapin may function as a general regulator of neurotransmitter release (Vites et al., 2004). Since Syp is the only one of top 5 proteins from PPI prediction that was reported on the DCV membrane with four transmembrane domains (Berwin et al., 1998; Jahn et al., 1985; Saegusa et al., 2002; Wheeler et al., 2002; Winkler, 1997), Syp is selected as the primary putative Syn Ia-interacting protein in this study. The abundantly expression of Syp in presynaptic terminals and the integral membrane domains of Syp form a hexameric channel-like structure (Gincel and Shoshan-Barmatz, 2002; Thomas et al., 1988), so Syp has been implicated in regulation of neurotransmitter release. Previous studies showed that increased expression of Syp correlates with learning and memory (Arthur and Stowell, 2007; Lynch et al., 1994; Mullany and Lynch, 1997), biogenesis of secretory vesicles (Thiele et al., 2000), and some neurodegenerative

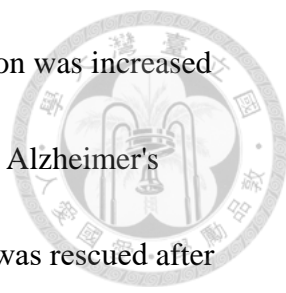
diseases (Eastwood and Harrison, 1995; Heinonen et al., 1995). Thus, the precise function and role of Syp in regulating exocytosis remained elusive. In this study, we show that the Syn I-Syp interaction depends on phosphorylation of Syn Ia. Thus it is likely that the Syn I-Syp interaction is involved in Syn Ia's regulation of DCV exocytosis.



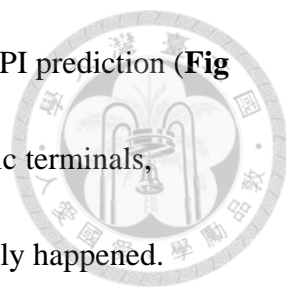
#### **4.3 The potential role of Syn Ia in the development of neurological diseases**

Specific actions of nitric oxide (NO) (Zhou and Zhu, 2009), a major biological messenger molecule with multiple functions in the nervous systems, is generated by neuronal NO synthase (nNOS), at presynaptic sites. The nNOS is determined by the ternary complex, comprising nNOS, CAPON (also named NOS1ap), and Syn I, leading nNOS to target to the precise localization (Jaffrey et al., 2002). Previous studies reported that NO signaling involved in modulating physiological functions such as learning, memory, and neurogenesis, as well as neurological disorders [depression (Lawford et al., 2013), anxiety (Zhu et al., 2014), and autism (Delorme et al., 2010)].

The expression level of nNOS was altered in the mouse model of Alzheimer's disease (Choi et al., 2018), a neurodegenerative disorder involving progressive



memory loss and behavioral changes. The nNOS–CAPON interaction was increased in the hippocampus of APP/PS1 mice (a transgenic mouse model of Alzheimer's disease); however, memory deficits of 4-month-old APP/PS1 mice was rescued after blocking the nNOS–CAPON interaction, suggesting that nNOS–CAPON interaction mediates the development of Alzheimer's disease, especially in the early stages (Zhang et al., 2018). An involvement of nNOS/NOS1ap interaction highly altered the dendritic spine development and filopodial outgrowth that are important neuropathological features of schizophrenia (Candemir et al., 2016), a severe mental disorder, characterized by a variety of symptoms (e.g., delusions, hallucinations, psychosis, paranoia, poor attention, and memory deficits). Moreover, NMDA receptors (NMDAR) signaling through nNOS contributes to excitotoxicity. The hyperactivity of NMDAR occurs in schizophrenia that is thought to be exacerbated by NOS1ap, implicating the roles of nNOS and NOS1ap in schizophrenia (Courtney et al., 2014). Significant linkage disequilibrium between schizophrenia and CAPON gene (Brzustowicz et al., 2004) and increased-expression of CAPON in Dorsolateral Prefrontal Cortex in Schizophrenia and Bipolar Disorder (Xu et al., 2005) support a role of NOS1ap in schizophrenia.



Although the high correlation coefficient of NMDA 3B from PPI prediction (**Fig 13**, the top 4th protein), Syn Ia is exclusively localized to presynaptic terminals, suggesting that the interaction of NMDA 3B-Syn Ia is highly unlikely happened.

Therefore, Syn Ia seemed implausible to participate in NMDA receptor (NMDAR) signaling through nNOS that contributes to the development of schizophrenia (Candemir et al., 2016; Courtney et al., 2014). Since Syn I is one of the key components of the nNOS- NOS1ap-Syn I ternary complex, leading nNOS to target to the precise localization (Jaffrey et al., 2002), Syn Ia may presumably involve in the nNOS–CAPON interaction, thus mediating the neurotoxicity in Alzheimer's disease or Schizophrenia. Moreover, previous studies reported that the levels of neuropeptides, packaged into DCVs, were associated with the pathogenesis of schizophrenia (Gabriel et al., 1996). The paralleled reduction of Syn Ia with the DCV marker was found in the hippocampus from schizophrenia (Nowakowski et al., 2002).

In addition, the colocalization of  $\beta$ -amyloid with the DCV marker was showed in the brain from Alzheimer's patients (Willis et al., 2011). Since these results and our findings in this study showing that Syn Ia regulates the dynamics of DCV exocytosis in a phosphorylation-dependent manner, the deficiency of Syn Ia's regulation

underlying DCV exocytosis may presumably lead to the development of neurological diseases, such as schizophrenia and Alzheimer's diseases.



#### **4.4 The potential role of Syn Ia in the co-release of neurotransmitters.**

In the early 1900s, the scientist, Henry Dale purposed the Dale's Principle (Dale, 1935). The concept in the Dale's Principle is that one neuron makes and releases only one transmitter. Furthermore, it was generally considered that neurotransmitters contained in one neuron are specialized for either inhibitory or excitatory roles, but not both. However, an increasing studies showed that multiple neurotransmitters were shown in the same neurons (Brownstein et al., 1974; Chronwall et al., 1984; Cottrell, 1976; Everitt et al., 1984a; Grimmelikhuijzen, 1983; Hanley et al., 1974; Kerkut et al., 1967; Mains et al., 1977; Osborne, 1977) and can be released from the same nerve terminals (Bartfai et al., 1988; Fulop et al., 2005; Furshpan et al., 1986; Furshpan et al., 1976; Johnson, 1994; Kupfermann, 1991; Potter et al., 1986; Slonimsky et al., 2006; Yang et al., 2002). In addition, the coexistence of multiple neurotransmitters is appeared both in the central (Chronwall et al., 1984; Everitt et al., 1984a; Merighi, 2002) and peripheral nervous system (Burnstock, 1983). These evidences not only

challenged the Dale's Principle, but also implicated in the hypothesis of co-release of neurotransmitters.



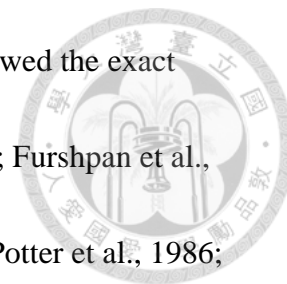
The term “coexistence” was first used in the study in invertebrate isolated ganglia neurons. More than one coexisting neurotransmitters, 5-hydroxytryptamine (5-HT), octopamine, and ACh, found in these neurons (Brownstein et al., 1974).

Coexistence of multiple neurotransmitters in the same neurons is not limited in these neurotransmitters derived from a common gene coding for the prohormone (Mains et al., 1977; Pulst et al., 1986) or the products of distinct genes (Chronwall et al., 1984). Different types of neurotransmitters (Belin et al., 1983; Belin et al., 1981; Everitt et al., 1984b; Johnson, 1994; Kaneko et al., 1990; Li and Bayliss, 1998; Millhorn et al., 1987; Nanopoulos et al., 1981), even that neurotransmitters and neuropeptides (Everitt et al., 1984a; Hanley et al., 1974; Hokfelt et al., 1977; Nicholas et al., 1990), were also found to co-exist in the same neurons.

In the very beginning, the theory of co-release of neurotransmitters is extremely controversial, because some researchers doubt that different neurotransmitters may act different functions at the specific time and targets. For example, if one neurotransmitter has the synergistic effect, the other may act the opposite effect upon their target site. In this concern, two different neurotransmitters seemed unlikely co-



release in the same neurons. However, numerous recent studies showed the exact presence of co-transmission (Dal Bo et al., 2004; Fulop et al., 2005; Furshpan et al., 1986; Furshpan et al., 1976; Johnson, 1994; Li and Bayliss, 1998; Potter et al., 1986; Slonimsky et al., 2006; Yang et al., 2002).



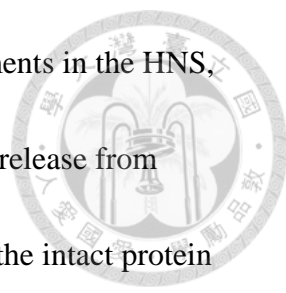
The most direct evidence for the occurrence of co-release of two neurotransmitters is the study by Johnson (Johnson, 1994). They showed that 60% of the serotonergic neurons evoked excitatory glutamatergic potentials, demonstrating co-release of serotonin and glutamate from single raphe neurons. The results from immunocytochemistry and single-cell RT-PCR experiments confirmed that isolated dopamine neurons express vesicular glutamate transporters 2 (VGLUT2), thus providing a basis for dopamine neurons to couple glutamate as a cotransmitter (Dal Bo et al., 2004). The other evidence provided the presence of glutaminase, an enzyme for synthesis of glutamate, in mesencephalic DA neurons of both rat and monkey (Sulzer et al., 1998). Moreover, a number of groups reported that glutamate can be released from monoamine neurons. These studies supported the co-transmission.

Co-transmission of multiple neurotransmitters seemed not such parsimonious than the release of a single transmitter. Nonetheless, co-transmission facilitates the crosstalk between nearby neurons. Therefore, coexistence and co-transmission of

multiple neurotransmitters display a variety of release properties which favor in the diversity of synaptic transmission. However, the molecular mechanism that mediates the co-release of multiple neurotransmitters or co-release of SVs and DCVs remains unknown. In this study, we show that Syn Ia is not only crucial in recruiting SVs, but also plays an important role in regulating the dynamics of DCV exocytosis via its phosphorylation, providing a new conceptual advance regarding the co-release of SVs and DCVs.

#### **4.5 Significance**

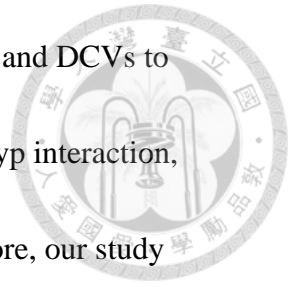
In this study, we provide the first evidence in the literature that Syn Ia, a SV-specific SV protein can regulate the dynamics of DCV exocytosis via phosphorylation of Syn Ia. The DCV-associated protein, Syp, potentially involved in the Syn Ia's regulation of DCVs via interacting with Syn Ia in a phosphorylation-dependent manner. Single-vesicle amperometry is used for the study of molecular mechanisms in distinguishes steps (fusion pore, kiss and run, and full fusion). The characteristics (spike and PSF characteristics) associated with DCVs were used to detect the release of NE as an oxidation current at the surface of a CFE. By virtue of single-vesicle amperometry, we can determine the dynamics of individual releasing events from



DCVs in a highly temporal resolution. By comparing to the experiments in the HNS, we can only detected the overall increased or decreased level in the release from DCVs (OT or VP) by ELISA. Owing to the lack of information for the intact protein structure of Syn Ia, we can just explore the putative Syn Ia-interacting proteins by performing the sequence-based PPI prediction technique, instead of the structure-based techniques. Even with less precision of sequence-based PPI prediction compared to the structure-based techniques, we finally identify Syp as a Syn Ia-interacting protein and further confirm the phosphorylation-dependent interaction of Syp and Syn Ia. We show that phosphorylation of Syn Ia is important in regulating release of both SVs and DCVs. Despite the precise role of Syn Ia-Syp interaction in regulatng DCV exocytosis requires further investigation, the expression level of Syp has been reported to related to some neurological diseases, such as Alzheimer's disease, suggesting the potential role of Syp in regulating neurotransmitter release.

Neurotransmitter release and reception mediate chemical synaptic transmission. Defects in neurotransmitter release lead to various neurological diseases. Advanced understanding of the molecular and cellular mechanisms underlying neurotransmitter release is required to develop appropriate cures for the relevant neurological diseases. In this study, we show the important role of Syn Ia in the regulation of DCV

exocytosis and implicate that Syn Ia may potentially co-recruit SVs and DCVs to plasma membrane together by phosphorylation-dependent Syn Ia-Syp interaction, thus dynamically regulating both of SVs and DCVs release. Therefore, our study provides a new conceptual advance regarding the co-release mechanism of DCVs and SVs, conferring the versatility of neurotransmitter release.



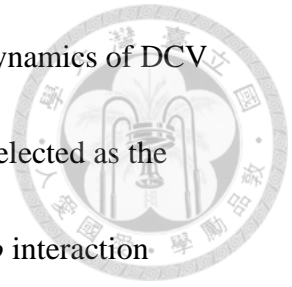
## Chapter V



### Conclusion

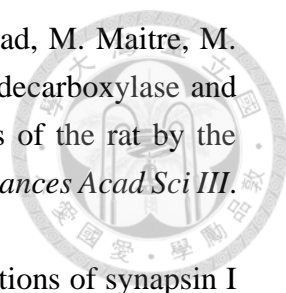
In this study, we provided the first evidence that Syn Ia, a SV-specific SV protein can regulate the dynamics of DCV exocytosis via the phosphorylation of Syn Ia. We showed that Syn Ia decreased  $k_d$  compared to Ctrl, suggesting that Syn Ia promotes DCV fusion pore remaining at the open state. Therefore, Syn Ia stabilized the opening DCV fusion pores, and thus the PSF mean duration of Syn Ia was increased compared to Ctrl. Conversely, the phosphodeficient mutant at the Ser62, Syn Ia-S62A, increased both  $k_c$  and  $k_d$  (the much stronger effects on  $k_c$ ) compared to Syn Ia, suggesting that Syn Ia-S62A promotes the opening DCV fusion pore entering the close or dilation state (mainly towards the close state). On the contrary, the phosphodeficient mutant at the Ser9, Ser566, and Ser603, Syn Ia-S9,566,603A, decreased both  $k_c$  and  $k_d$  compared to Syn Ia, suggesting that Syn Ia-S9,566,603A prevents the opening DCV fusion pore towards the close or dilation state. Hence, Syn Ia differentially regulates the stabilization of the DCV fusion pores via phosphorylation at various sites. Moreover, Syn Ia-S9,566,603A significantly decreased the secretion rate and FF frequency, suggesting that Syn Ia regulates the secretion from DCVs by its phosphorylation. Since Syn I rarely localized to DCVs,

Syn Ia may interact with certain DCV protein, thus regulating the dynamics of DCV exocytosis. From the database search and PPI prediction, Syp was selected as the primary putative Syn Ia-interacting protein. Furthermore, the *in vivo* interaction between Syn I and Syp was identified by co-IP and PLA. Finally, we showed that the *in vivo* interaction between Syn I and Syp is not attributed to the change in expression levels. In conclusion, in this study, we used multiple techniques to unveil how the SV-specific protein Syn Ia regulates the release of DCVs. These results provide not only the cutting-edge understanding for the molecular basis underlying Syn Ia's regulation of DCV exocytosis, but also a new conceptual advance regarding the co-release mechanism of DCVs and SVs, conferring the versatility of neurotransmitter release.

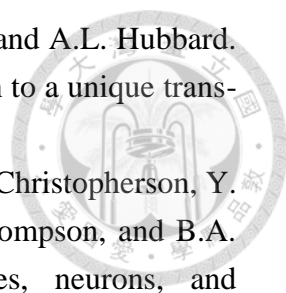


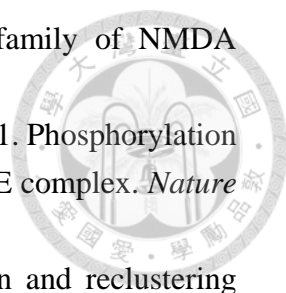
## References

- Adams, D.J., C.P. Arthur, and M.H. Stowell. 2015. Architecture of the Synaptophysin/Synaptobrevin Complex: Structural Evidence for an Entropic Clustering Function at the Synapse. *Scientific reports*. 5:13659.
- Arthur, C.P., and M.H. Stowell. 2007. Structure of synaptophysin: a hexameric MARVEL-domain channel protein. *Structure*. 15:707-714.
- Ashery, U., F. Varoqueaux, T. Voets, A. Betz, P. Thakur, H. Koch, E. Neher, N. Brose, and J. Rettig. 2000. Munc13-1 acts as a priming factor for large dense-core vesicles in bovine chromaffin cells. *The EMBO journal*. 19:3586-3596.
- Augustin, I., C. Rosenmund, T.C. Sudhof, and N. Brose. 1999. Munc13-1 is essential for fusion competence of glutamatergic synaptic vesicles. *Nature*. 400:457-461.
- Bacaj, T., D. Wu, X. Yang, W. Morishita, P. Zhou, W. Xu, R.C. Malenka, and T.C. Sudhof. 2013. Synaptotagmin-1 and synaptotagmin-7 trigger synchronous and asynchronous phases of neurotransmitter release. *Neuron*. 80:947-959.
- Bahler, M., F. Benfenati, F. Valtorta, and P. Greengard. 1990. The synapsins and the regulation of synaptic function. *BioEssays : news and reviews in molecular, cellular and developmental biology*. 12:259-263.
- Bahler, M., and P. Greengard. 1987. Synapsin I bundles F-actin in a phosphorylation-dependent manner. *Nature*. 326:704-707.
- Baker, R.W., and F.M. Hughson. 2016. Chaperoning SNARE assembly and disassembly. *Nature reviews. Molecular cell biology*. 17:465-479.
- Baldelli, P., A. Fassio, F. Valtorta, and F. Benfenati. 2007. Lack of synapsin I reduces the readily releasable pool of synaptic vesicles at central inhibitory synapses. *The Journal of neuroscience : the official journal of the Society for Neuroscience*. 27:13520-13531.
- Bao, H., M. Goldschen-Ohm, P. Jeggle, B. Chanda, J.M. Edwardson, and E.R. Chapman. 2016. Exocytotic fusion pores are composed of both lipids and proteins. *Nature structural & molecular biology*. 23:67-73.
- Bartfai, T., K. Iverfeldt, G. Fisone, and P. Serfozo. 1988. Regulation of the release of coexisting neurotransmitters. *Annu Rev Pharmacol Toxicol*. 28:285-310.
- Belin, M.F., D. Nanopoulos, M. Didier, M. Aguera, H. Steinbusch, A. Verhofstad, M. Maitre, and J.F. Pujol. 1983. Immunohistochemical evidence for the presence of gamma-aminobutyric acid and serotonin in one nerve cell. A study on the raphe nuclei of the rat using antibodies to glutamate decarboxylase and serotonin. *Brain research*. 275:329-339.

- 
- Belin, M.F., D. Weisman-Nanopoulos, H. Steinbusch, A. Verhofstad, M. Maitre, M. Jouvét, and J.F. Pujol. 1981. [Demonstration of glutamate decarboxylase and serotonin in the same neuron of the nucleus raphe dorsalis of the rat by the methods of immunocytochemical doubling labelling]. *C R Seances Acad Sci III*. 293:337-341.
- Benfenati, F., M. Bahler, R. Jahn, and P. Greengard. 1989a. Interactions of synapsin I with small synaptic vesicles: distinct sites in synapsin I bind to vesicle phospholipids and vesicle proteins. *The Journal of cell biology*. 108:1863-1872.
- Benfenati, F., P. Greengard, J. Brunner, and M. Bahler. 1989b. Electrostatic and hydrophobic interactions of synapsin I and synapsin I fragments with phospholipid bilayers. *The Journal of cell biology*. 108:1851-1862.
- Benfenati, F., P. Neyroz, M. Bahler, L. Masotti, and P. Greengard. 1990. Time-resolved fluorescence study of the neuron-specific phosphoprotein synapsin I. Evidence for phosphorylation-dependent conformational changes. *The Journal of biological chemistry*. 265:12584-12595.
- Berwin, B., E. Floor, and T.F. Martin. 1998. CAPS (mammalian UNC-31) protein localizes to membranes involved in dense-core vesicle exocytosis. *Neuron*. 21:137-145.
- Breckenridge, L.J., and W. Almers. 1987. Final steps in exocytosis observed in a cell with giant secretory granules. *Proceedings of the National Academy of Sciences of the United States of America*. 84:1945-1949.
- Browning, M.D., E.M. Dudek, J.L. Rapier, S. Leonard, and R. Freedman. 1993. Significant reductions in synapsin but not synaptophysin specific activity in the brains of some schizophrenics. *Biological psychiatry*. 34:529-535.
- Brownstein, M.J., J.M. Saavedra, J. Axelrod, G.H. Zeman, and D.O. Carpenter. 1974. Coexistence of several putative neurotransmitters in single identified neurons of Aplysia. *Proceedings of the National Academy of Sciences of the United States of America*. 71:4662-4665.
- Brzustowicz, L.M., J. Simone, P. Mohseni, J.E. Hayter, K.A. Hodgkinson, E.W. Chow, and A.S. Bassett. 2004. Linkage disequilibrium mapping of schizophrenia susceptibility to the CAPON region of chromosome 1q22. *American journal of human genetics*. 74:1057-1063.
- Burgess, T.L., and R.B. Kelly. 1987. Constitutive and regulated secretion of proteins. *Annual review of cell biology*. 3:243-293.
- Burnstock, G. 1983. Autonomic neurotransmitters and trophic factors. *J Auton Nerv Syst*. 7:213-217.

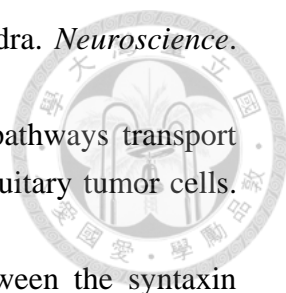


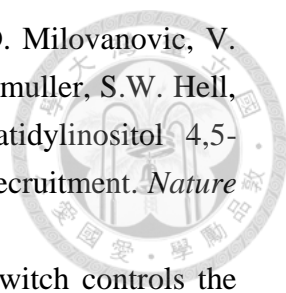
- 
- Bustos, R., E.R. Kolen, L. Braiterman, A.J. Baines, F.S. Gorelick, and A.L. Hubbard. 2001. Synapsin I is expressed in epithelial cells: localization to a unique trans-Golgi compartment. *Journal of cell science*. 114:3695-3704.
- Cahoy, J.D., B. Emery, A. Kaushal, L.C. Foo, J.L. Zamanian, K.S. Christopherson, Y. Xing, J.L. Lubischer, P.A. Krieg, S.A. Krupenko, W.J. Thompson, and B.A. Barres. 2008. A transcriptome database for astrocytes, neurons, and oligodendrocytes: a new resource for understanding brain development and function. *The Journal of neuroscience : the official journal of the Society for Neuroscience*. 28:264-278.
- Cambiaghi, M., M. Cursi, E. Monzani, F. Benfenati, G. Comi, F. Minicucci, F. Valtorta, and L. Leocani. 2013. Temporal evolution of neurophysiological and behavioral features of synapsin I/II/III triple knock-out mice. *Epilepsy research*. 103:153-160.
- Candemir, E., L. Kollert, L. Weissflog, M. Geis, A. Muller, A.M. Post, A. O'Leary, J. Harro, A. Reif, and F. Freudenberg. 2016. Interaction of NOS1AP with the NOS-I PDZ domain: Implications for schizophrenia-related alterations in dendritic morphology. *Eur Neuropsychopharmacol*. 26:741-755.
- Ceccaldi, P.E., F. Grohovaz, F. Benfenati, E. Chieregatti, P. Greengard, and F. Valtorta. 1995. Dephosphorylated synapsin I anchors synaptic vesicles to actin cytoskeleton: an analysis by videomicroscopy. *The Journal of cell biology*. 128:905-912.
- Cesca, F., P. Baldelli, F. Valtorta, and F. Benfenati. 2010. The synapsins: key actors of synapse function and plasticity. *Prog Neurobiol*. 91:313-348.
- Chandler, D.E., and J.E. Heuser. 1980. Arrest of membrane fusion events in mast cells by quick-freezing. *The Journal of cell biology*. 86:666-674.
- Chang, C.W., C.W. Chiang, and M.B. Jackson. 2017. Fusion pores and their control of neurotransmitter and hormone release. *The Journal of general physiology*. 149:301-322.
- Chang, C.W., E. Hui, J. Bai, D. Bruns, E.R. Chapman, and M.B. Jackson. 2015. A structural role for the synaptobrevin 2 transmembrane domain in dense-core vesicle fusion pores. *The Journal of neuroscience : the official journal of the Society for Neuroscience*. 35:5772-5780.
- Chang, S., T. Trimbuch, and C. Rosenmund. 2018. Synaptotagmin-1 drives synchronous Ca(2+)-triggered fusion by C2B-domain-mediated synaptic-vesicle-membrane attachment. *Nature neuroscience*. 21:33-40.
- Chatterton, J.E., M. Awobuluyi, L.S. Premkumar, H. Takahashi, M. Talantova, Y. Shin, J. Cui, S. Tu, K.A. Sevarino, N. Nakanishi, G. Tong, S.A. Lipton, and D. Zhang.

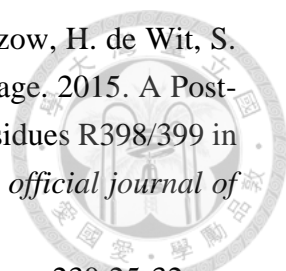
- 
2002. Excitatory glycine receptors containing the NR3 family of NMDA receptor subunits. *Nature*. 415:793-798.
- Chheda, M.G., U. Ashery, P. Thakur, J. Rettig, and Z.H. Sheng. 2001. Phosphorylation of Snapin by PKA modulates its interaction with the SNARE complex. *Nature cell biology*. 3:331-338.
- Chi, P., P. Greengard, and T.A. Ryan. 2001. Synapsin dispersion and reclustering during synaptic activity. *Nature neuroscience*. 4:1187-1193.
- Chi, P., P. Greengard, and T.A. Ryan. 2003. Synaptic vesicle mobilization is regulated by distinct synapsin I phosphorylation pathways at different frequencies. *Neuron*. 38:69-78.
- Chiang, N., Y.T. Hsiao, H.J. Yang, Y.C. Lin, J.C. Lu, and C.T. Wang. 2014. Phosphomimetic Mutation of Cysteine String Protein-alpha Increases the Rate of Regulated Exocytosis by Modulating Fusion Pore Dynamics in PC12 Cells. *PloS one*. 9:e99180.
- Choi, S., J.S. Won, S.L. Carroll, B. Annamalai, I. Singh, and A.K. Singh. 2018. Pathology of nNOS-Expressing GABAergic Neurons in Mouse Model of Alzheimer's Disease. *Neuroscience*. 384:41-53.
- Chow, R.H., L. von Ruden, and E. Neher. 1992. Delay in vesicle fusion revealed by electrochemical monitoring of single secretory events in adrenal chromaffin cells. *Nature*. 356:60-63.
- Chronwall, B.M., T.N. Chase, and T.L. O'Donohue. 1984. Coexistence of neuropeptide Y and somatostatin in rat and human cortical and rat hypothalamic neurons. *Neuroscience letters*. 52:213-217.
- Cooper, J.R., F.E. Bloom, and R.H. Roth. 2003. The biochemical basis of neuropharmacology. Oxford University Press, Oxford ; New York. vii, 405 p. pp.
- Cottrell, G.A. 1976. Proceedings: Does the giant cerebral neurone of *Helix* release two transmitters: ACh and serotonin? *The Journal of physiology*. 259:44P-45P.
- Courtney, M.J., L.L. Li, and Y.Y. Lai. 2014. Mechanisms of NOS1AP action on NMDA receptor-nNOS signaling. *Frontiers in cellular neuroscience*. 8:252.
- Craxton, M. 2010. A manual collection of Syt, Esyt, Rph3a, Rph3al, Doc2, and Dblc2 genes from 46 metazoan genomes--an open access resource for neuroscience and evolutionary biology. *BMC genomics*. 11:37.
- Czernik, A.J., D.T. Pang, and P. Greengard. 1987. Amino acid sequences surrounding the cAMP-dependent and calcium/calmodulin-dependent phosphorylation sites in rat and bovine synapsin I. *Proceedings of the National Academy of Sciences of the United States of America*. 84:7518-7522.

- Dal Bo, G., F. St-Gelais, M. Danik, S. Williams, M. Cotton, and L.E. Trudeau. 2004. Dopamine neurons in culture express VGLUT2 explaining their capacity to release glutamate at synapses in addition to dopamine. *Journal of neurochemistry*. 88:1398-1405.
- Dale, H. 1935. Pharmacology and Nerve-endings (Walter Ernest Dixon Memorial Lecture): (Section of Therapeutics and Pharmacology). *Proc R Soc Med*. 28:319-332.
- De Camilli, P., R. Cameron, and P. Greengard. 1983. Synapsin I (protein I), a nerve terminal-specific phosphoprotein. I. Its general distribution in synapses of the central and peripheral nervous system demonstrated by immunofluorescence in frozen and plastic sections. *The Journal of cell biology*. 96:1337-1354.
- De Camilli, P., and R. Jahn. 1990. Pathways to regulated exocytosis in neurons. *Annual review of physiology*. 52:625-645.
- de Wit, H., A.M. Walter, I. Milosevic, A. Gulyas-Kovacs, D. Riedel, J.B. Sorensen, and M. Verhage. 2009. Synaptotagmin-1 docks secretory vesicles to syntaxin-1/SNAP-25 acceptor complexes. *Cell*. 138:935-946.
- Delorme, R., C. Betancur, I. Scheid, H. Anckarsater, P. Chaste, S. Jamain, F. Schuroff, G. Nygren, E. Herbrecht, A. Dumaine, M.C. Mouren, M. Rastam, M. Leboyer, C. Gillberg, and T. Bourgeron. 2010. Mutation screening of NOS1AP gene in a large sample of psychiatric patients and controls. *Bmc Med Genet*. 11.
- Dumermuth, E., and H.P. Moore. 1998. Analysis of constitutive and constitutive-like secretion in semi-intact pituitary cells. *Methods*. 16:188-197.
- Eastwood, S.L., and P.J. Harrison. 1995. Decreased synaptophysin in the medial temporal lobe in schizophrenia demonstrated using immunoautoradiography. *Neuroscience*. 69:339-343.
- Etholm, L., H. Linden, T. Eken, and P. Heggelund. 2011. Electroencephalographic characterization of seizure activity in the synapsin I/II double knockout mouse. *Brain research*. 1383:270-288.
- Everitt, B.J., T. Hokfelt, L. Terenius, K. Tatemoto, V. Mutt, and M. Goldstein. 1984a. Differential co-existence of neuropeptide Y (NPY)-like immunoreactivity with catecholamines in the central nervous system of the rat. *Neuroscience*. 11:443-462.
- Everitt, B.J., T. Hokfelt, J.Y. Wu, and M. Goldstein. 1984b. Coexistence of tyrosine hydroxylase-like and gamma-aminobutyric acid-like immunoreactivities in neurons of the arcuate nucleus. *Neuroendocrinology*. 39:189-191.
- Fernandez-Chacon, R., A. Konigstorfer, S.H. Gerber, J. Garcia, M.F. Matos, C.F. Stevens, N. Brose, J. Rizo, C. Rosenmund, and T.C. Sudhof. 2001.

- Synaptotagmin I functions as a calcium regulator of release probability. *Nature*. 410:41-49.
- Fornasiero, E.F., D. Bonanomi, F. Benfenati, and F. Valtorta. 2010. The role of synapsins in neuronal development. *Cellular and molecular life sciences : CMLS*. 67:1383-1396.
- Fulop, T., S. Radabaugh, and C. Smith. 2005. Activity-dependent differential transmitter release in mouse adrenal chromaffin cells. *The Journal of neuroscience : the official journal of the Society for Neuroscience*. 25:7324-7332.
- Furshpan, E.J., S.C. Landis, S.G. Matsumoto, and D.D. Potter. 1986. Synaptic functions in rat sympathetic neurons in microcultures. I. Secretion of norepinephrine and acetylcholine. *The Journal of neuroscience : the official journal of the Society for Neuroscience*. 6:1061-1079.
- Furshpan, E.J., P.R. MacLeish, P.H. O'Lague, and D.D. Potter. 1976. Chemical transmission between rat sympathetic neurons and cardiac myocytes developing in microcultures: evidence for cholinergic, adrenergic, and dual-function neurons. *Proceedings of the National Academy of Sciences of the United States of America*. 73:4225-4229.
- Gabriel, S.M., M. Davidson, V. Haroutunian, P. Powchik, L.M. Bierer, D.P. Purohit, D.P. Perl, and K.L. Davis. 1996. Neuropeptide deficits in schizophrenia vs. Alzheimer's disease cerebral cortex. *Biological psychiatry*. 39:82-91.
- Garcia, C.C., H.J. Blair, M. Seager, A. Coulthard, S. Tennant, M. Buddles, A. Curtis, and J.A. Goodship. 2004. Identification of a mutation in synapsin I, a synaptic vesicle protein, in a family with epilepsy. *Journal of medical genetics*. 41:183-186.
- Gincel, D., and V. Shoshan-Barmatz. 2002. The synaptic vesicle protein synaptophysin: purification and characterization of its channel activity. *Biophysical journal*. 83:3223-3229.
- Godenschwege, T.A., D. Reisch, S. Diegelmann, K. Eberle, N. Funk, M. Heisenberg, V. Hoppe, J. Hoppe, B.R. Klagges, J.R. Martin, E.A. Nikitina, G. Putz, R. Reifegerste, N. Reisch, J. Rister, M. Schaupp, H. Scholz, M. Schwarzel, U. Werner, T.D. Zars, S. Buchner, and E. Buchner. 2004. Flies lacking all synapsins are unexpectedly healthy but are impaired in complex behaviour. *The European journal of neuroscience*. 20:611-622.
- Gondre-Lewis, M.C., J.J. Park, and Y.P. Loh. 2012. Cellular mechanisms for the biogenesis and transport of synaptic and dense-core vesicles. *International review of cell and molecular biology*. 299:27-115.

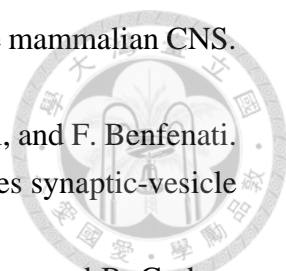
- 
- Grimmelikhuijzen, C.J. 1983. Coexistence of neuropeptides in hydra. *Neuroscience*. 9:837-845.
- Gumbiner, B., and R.B. Kelly. 1982. Two distinct intracellular pathways transport secretory and membrane glycoproteins to the surface of pituitary tumor cells. *Cell*. 28:51-59.
- Han, X., and M.B. Jackson. 2005. Electrostatic interactions between the syntaxin membrane anchor and neurotransmitter passing through the fusion pore. *Biophysical journal*. 88:L20-22.
- Han, X., C.T. Wang, J. Bai, E.R. Chapman, and M.B. Jackson. 2004. Transmembrane segments of syntaxin line the fusion pore of Ca<sup>2+</sup>-triggered exocytosis. *Science*. 304:289-292.
- Hanley, M.R., G.A. Cottrell, P.C. Emson, and F. Fonnum. 1974. Enzymatic synthesis of acetylcholine by a serotonin-containing neurone from Helix. *Nature*. 251:631-633.
- Hansen, L.A., S.E. Daniel, G.K. Wilcock, and S. Love. 1998. Frontal cortical synaptophysin in Lewy body diseases: relation to Alzheimer's disease and dementia. *J Neurol Neurosurg Psychiatry*. 64:653-656.
- Hay, J.C., and T.F. Martin. 1992. Resolution of regulated secretion into sequential MgATP-dependent and calcium-dependent stages mediated by distinct cytosolic proteins. *The Journal of cell biology*. 119:139-151.
- Haycock, J.W., P. Greengard, and M.D. Browning. 1988. Cholinergic regulation of protein III phosphorylation in bovine adrenal chromaffin cells. *The Journal of neuroscience : the official journal of the Society for Neuroscience*. 8:3233-3239.
- Heinonen, O., H. Soininen, H. Sorvari, O. Kosunen, L. Paljarvi, E. Koivisto, and P.J. Riekkinen, Sr. 1995. Loss of synaptophysin-like immunoreactivity in the hippocampal formation is an early phenomenon in Alzheimer's disease. *Neuroscience*. 64:375-384.
- Ho, L., Y. Guo, L. Spielman, O. Petrescu, V. Haroutunian, D. Purohit, A. Czernik, S. Yemul, P.S. Aisen, R. Mohs, and G.M. Pasinetti. 2001. Altered expression of a-type but not b-type synapsin isoform in the brain of patients at high risk for Alzheimer's disease assessed by DNA microarray technique. *Neuroscience letters*. 298:191-194.
- Hokfelt, T., L.G. Elfvin, R. Elde, M. Schultzberg, M. Goldstein, and R. Luft. 1977. Occurrence of somatostatin-like immunoreactivity in some peripheral sympathetic noradrenergic neurons. *Proceedings of the National Academy of Sciences of the United States of America*. 74:3587-3591.

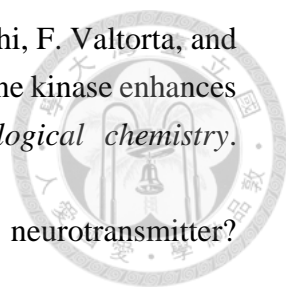
- 
- Honigsmann, A., G. van den Bogaart, E. Iraheta, H.J. Risselada, D. Milovanovic, V. Mueller, S. Mullar, U. Diederichsen, D. Fasshauer, H. Grubmuller, S.W. Hell, C. Eggeling, K. Kuhnel, and R. Jahn. 2013. Phosphatidylinositol 4,5-bisphosphate clusters act as molecular beacons for vesicle recruitment. *Nature structural & molecular biology*. 20:679-686.
- Hosaka, M., R.E. Hammer, and T.C. Sudhof. 1999. A phospho-switch controls the dynamic association of synapsins with synaptic vesicles. *Neuron*. 24:377-387.
- Hurley, S.L., D.L. Brown, and J.J. Cheetham. 2004. Cytoskeletal interactions of synapsin I in non-neuronal cells. *Biochemical and biophysical research communications*. 317:16-23.
- Huttner, W.B., and P. Greengard. 1979. Multiple phosphorylation sites in protein I and their differential regulation by cyclic AMP and calcium. *Proceedings of the National Academy of Sciences of the United States of America*. 76:5402-5406.
- Ilardi, J.M., S. Mochida, and Z.H. Sheng. 1999. Snapin: a SNARE-associated protein implicated in synaptic transmission. *Nature neuroscience*. 2:119-124.
- Ivanov, A.I. 2014. Exocytosis and endocytosis. Humana Press, New York. xiii, 435 pages pp.
- Jaffrey, S.R., F. Benfenati, A.M. Snowman, A.J. Czernik, and S.H. Snyder. 2002. Neuronal nitric-oxide synthase localization mediated by a ternary complex with synapsin and CAPON. *Proceedings of the National Academy of Sciences of the United States of America*. 99:3199-3204.
- Jahn, R., and D. Fasshauer. 2012. Molecular machines governing exocytosis of synaptic vesicles. *Nature*. 490:201-207.
- Jahn, R., W. Schiebler, C. Ouimet, and P. Greengard. 1985. A 38,000-dalton membrane protein (p38) present in synaptic vesicles. *Proceedings of the National Academy of Sciences of the United States of America*. 82:4137-4141.
- Johnson, M.D. 1994. Synaptic glutamate release by postnatal rat serotonergic neurons in microculture. *Neuron*. 12:433-442.
- Jovanovic, J.N., F. Benfenati, Y.L. Siow, T.S. Sihra, J.S. Sanghera, S.L. Pelech, P. Greengard, and A.J. Czernik. 1996. Neurotrophins stimulate phosphorylation of synapsin I by MAP kinase and regulate synapsin I-actin interactions. *Proceedings of the National Academy of Sciences of the United States of America*. 93:3679-3683.
- Kaneko, T., H. Akiyama, I. Nagatsu, and N. Mizuno. 1990. Immunohistochemical demonstration of glutaminase in catecholaminergic and serotonergic neurons of rat brain. *Brain research*. 507:151-154.

- 
- Kedar, G.H., A.S. Munch, J.R. van Weering, J. Malsam, A. Scheutzw, H. de Wit, S. Houy, B. Tawfik, T.H. Sollner, J.B. Sorensen, and M. Verhage. 2015. A Post-Docking Role of Synaptotagmin 1-C2B Domain Bottom Residues R398/399 in Mouse Chromaffin Cells. *The Journal of neuroscience : the official journal of the Society for Neuroscience*. 35:14172-14182.
- Kelly, R.B. 1985. Pathways of protein secretion in eukaryotes. *Science*. 230:25-32.
- Kerkut, G.A., C.B. Sedden, and R.J. Walker. 1967. Uptake of DOPA and 5-hydroxytryptophan by monoamine-forming neurones in the brain of *Helix aspersa*. *Comp Biochem Physiol*. 23:159-162.
- Ketzef, M., J. Kahn, I. Weissberg, A.J. Becker, A. Friedman, and D. Gitler. 2011. Compensatory network alterations upon onset of epilepsy in synapsin triple knock-out mice. *Neuroscience*. 189:108-122.
- Koch, H., K. Hofmann, and N. Brose. 2000. Definition of Munc13-homology-domains and characterization of a novel ubiquitously expressed Munc13 isoform. *The Biochemical journal*. 349:247-253.
- Koh, T.W., and H.J. Bellen. 2003. Synaptotagmin I, a Ca<sup>2+</sup> sensor for neurotransmitter release. *Trends in neurosciences*. 26:413-422.
- Koushika, S.P., J.E. Richmond, G. Hadwiger, R.M. Weimer, E.M. Jorgensen, and M.L. Nonet. 2001. A post-docking role for active zone protein Rim. *Nature neuroscience*. 4:997-1005.
- Kreutzberger, A.J.B., V. Kiessling, B. Liang, P. Seelheim, S. Jakhanwal, R. Jahn, J.D. Castle, and L.K. Tamm. 2017. Reconstitution of calcium-mediated exocytosis of dense-core vesicles. *Science advances*. 3:e1603208.
- Kupfermann, I. 1991. Functional studies of cotransmission. *Physiological reviews*. 71:683-732.
- Lawford, B.R., C.P. Morris, C.D. Swagell, I.P. Hughes, R.M. Young, and J. Voisey. 2013. NOS1AP is associated with increased severity of PTSD and depression in untreated combat veterans. *J Affect Disord*. 147:87-93.
- Levitan, I.B., and L.K. Kaczmarek. 2015. The neuron : cell and molecular biology. Oxford University Press, Oxford ; New York. xvi, 579 pages pp.
- Li, J., Y.R. Han, M.R. Plummer, and K. Herrup. 2009. Cytoplasmic ATM in neurons modulates synaptic function. *Current biology : CB*. 19:2091-2096.
- Li, L., L.S. Chin, O. Shupliakov, L. Brodin, T.S. Sihra, O. Hvalby, V. Jensen, D. Zheng, J.O. McNamara, P. Greengard, and et al. 1995. Impairment of synaptic vesicle clustering and of synaptic transmission, and increased seizure propensity, in synapsin I-deficient mice. *Proceedings of the National Academy of Sciences of the United States of America*. 92:9235-9239.

- Li, Y.W., and D.A. Bayliss. 1998. Presynaptic inhibition by 5-HT<sub>1B</sub> receptors of glutamatergic synaptic inputs onto serotonergic caudal raphe neurones in rat. *The Journal of physiology*. 510 ( Pt 1):121-134.
- Lievens, J.C., B. Woodman, A. Mahal, and G.P. Bates. 2002. Abnormal phosphorylation of synapsin I predicts a neuronal transmission impairment in the R6/2 Huntington's disease transgenic mice. *Molecular and cellular neurosciences*. 20:638-648.
- Lynch, K.L., R.R. Gerona, D.M. Kielar, S. Martens, H.T. McMahon, and T.F. Martin. 2008. Synaptotagmin-1 utilizes membrane bending and SNARE binding to drive fusion pore expansion. *Molecular biology of the cell*. 19:5093-5103.
- Lynch, M.A., K.L. Voss, J. Rodriguez, and T.V. Bliss. 1994. Increase in synaptic vesicle proteins accompanies long-term potentiation in the dentate gyrus. *Neuroscience*. 60:1-5.
- Mackler, J.M., J.A. Drummond, C.A. Loewen, I.M. Robinson, and N.E. Reist. 2002. The C(2)B Ca(2+)-binding motif of synaptotagmin is required for synaptic transmission in vivo. *Nature*. 418:340-344.
- Maienschein, V., M. Marxen, W. Volknandt, and H. Zimmermann. 1999. A plethora of presynaptic proteins associated with ATP-storing organelles in cultured astrocytes. *Glia*. 26:233-244.
- Mains, R.E., B.A. Eipper, and N. Ling. 1977. Common precursor to corticotropins and endorphins. *Proceedings of the National Academy of Sciences of the United States of America*. 74:3014-3018.
- Man, K.N., C. Imig, A.M. Walter, P.S. Pinheiro, D.R. Stevens, J. Rettig, J.B. Sorensen, B.H. Cooper, N. Brose, and S.M. Wojcik. 2015. Identification of a Munc13-sensitive step in chromaffin cell large dense-core vesicle exocytosis. *eLife*. 4.
- Matsubara, M., M. Kusubata, K. Ishiguro, T. Uchida, K. Titani, and H. Taniguchi. 1996. Site-specific phosphorylation of synapsin I by mitogen-activated protein kinase and Cdk5 and its effects on physiological functions. *The Journal of biological chemistry*. 271:21108-21113.
- Matsumoto, K., K. Ebihara, H. Yamamoto, H. Tabuchi, K. Fukunaga, M. Yasunami, H. Ohkubo, M. Shichiri, and E. Miyamoto. 1999. Cloning from insulinoma cells of synapsin I associated with insulin secretory granules. *The Journal of biological chemistry*. 274:2053-2059.
- Menegon, A., D.D. Dunlap, F. Castano, F. Benfenati, A.J. Czernik, P. Greengard, and F. Valtorta. 2000. Use of phosphosynapsin I-specific antibodies for image analysis of signal transduction in single nerve terminals. *Journal of cell science*. 113 ( Pt 20):3573-3582.



- 
- Merighi, A. 2002. Costorage and coexistence of neuropeptides in the mammalian CNS. *Prog Neurobiol.* 66:161-190.
- Messa, M., S. Congia, E. Defranchi, F. Valtorta, A. Fassio, F. Onofri, and F. Benfenati. 2010. Tyrosine phosphorylation of synapsin I by Src regulates synaptic-vesicle trafficking. *Journal of cell science.* 123:2256-2265.
- Michels, B., S. Diegelmann, H. Tanimoto, I. Schwenkert, E. Buchner, and B. Gerber. 2005. A role for Synapsin in associative learning: the *Drosophila* larva as a study case. *Learn Mem.* 12:224-231.
- Millhorn, D.E., T. Hokfelt, K. Seroogy, W. Oertel, A.A. Verhofstad, and J.Y. Wu. 1987. Immunohistochemical evidence for colocalization of gamma-aminobutyric acid and serotonin in neurons of the ventral medulla oblongata projecting to the spinal cord. *Brain research.* 410:179-185.
- Mullany, P., and M.A. Lynch. 1997. Changes in protein synthesis and synthesis of the synaptic vesicle protein, synaptophysin, in entorhinal cortex following induction of long-term potentiation in dentate gyrus: an age-related study in the rat. *Neuropharmacology.* 36:973-980.
- Nanopoulos, D., M. Maitre, M.F. Belin, M. Aguera, J.F. Pujol, H. Gamrani, and A. Calas. 1981. Autoradiographic and immunocytochemical evidence for the existence of GABAergic neurons in the nucleus raphe dorsalis--possible existence of neurons containing 5HT and glutamate decarboxylase. *Adv Biochem Psychopharmacol.* 29:519-525.
- Nicholas, A.P., A.C. Cuellar, M. Goldstein, and T. Hokfelt. 1990. Glutamate-like immunoreactivity in medulla oblongata catecholamine/substance P neurons. *Neuroreport.* 1:235-238.
- Nicholls, D.G. 1994. Proteins, transmitters, and synapses. Blackwell Scientific Publications, Oxford ; Boston. xii, 253 p., 254 p. of plates pp.
- Nishiki, T., and G.J. Augustine. 2004. Dual roles of the C2B domain of synaptotagmin I in synchronizing  $\text{Ca}^{2+}$ -dependent neurotransmitter release. *The Journal of neuroscience : the official journal of the Society for Neuroscience.* 24:8542-8550.
- Nowakowski, C., W.A. Kaufmann, C. Adlassnig, H. Maier, K. Salimi, K.A. Jellinger, and J. Marksteiner. 2002. Reduction of chromogranin B-like immunoreactivity in distinct subregions of the hippocampus from individuals with schizophrenia. *Schizophr Res.* 58:43-53.
- Ochoa, D., and F. Pazos. 2010. Studying the co-evolution of protein families with the Mirrortree web server. *Bioinformatics.* 26:1370-1371.

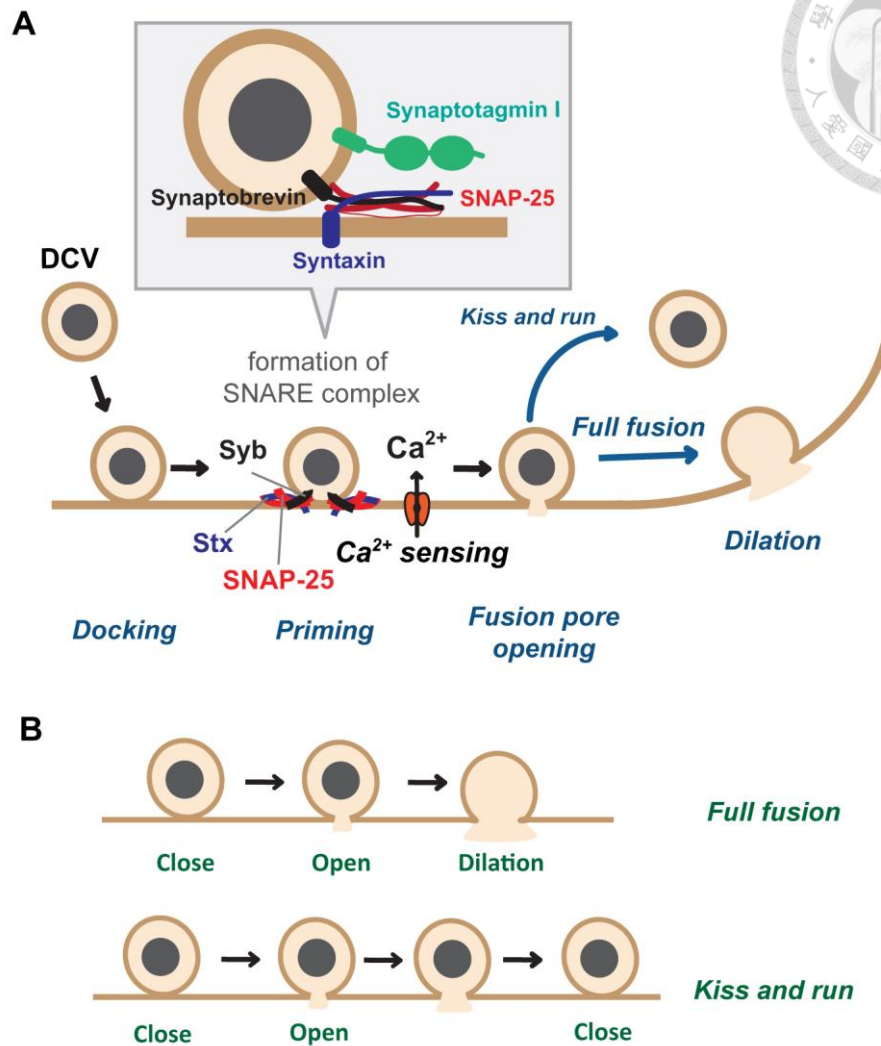
- 
- Onofri, F., M. Messa, V. Matafora, G. Bonanno, A. Corradi, A. Bachi, F. Valtorta, and F. Benfenati. 2007. Synapsin phosphorylation by SRC tyrosine kinase enhances SRC activity in synaptic vesicles. *The Journal of biological chemistry*. 282:15754-15767.
- Osborne, N.N. 1977. Do snail neurones contain more than one neurotransmitter? *Nature*. 270:622-623.
- Pang, Z.P., O.H. Shin, A.C. Meyer, C. Rosenmund, and T.C. Sudhof. 2006. A gain-of-function mutation in synaptotagmin-1 reveals a critical role of Ca<sup>2+</sup>-dependent soluble N-ethylmaleimide-sensitive factor attachment protein receptor complex binding in synaptic exocytosis. *The Journal of neuroscience : the official journal of the Society for Neuroscience*. 26:12556-12565.
- Pazos, F., and A. Valencia. 2001. Similarity of phylogenetic trees as indicator of protein-protein interaction. *Protein engineering*. 14:609-614.
- Perdahl, E., R. Adolfsson, I. Alafuzoff, K.A. Albert, E.J. Nestler, P. Greengard, and B. Winblad. 1984. Synapsin I (protein I) in different brain regions in senile dementia of Alzheimer type and in multi-infarct dementia. *J Neural Transm*. 60:133-141.
- Petrucci, T.C., and J.S. Morrow. 1987. Synapsin I: an actin-bundling protein under phosphorylation control. *The Journal of cell biology*. 105:1355-1363.
- Potter, D.D., S.C. Landis, S.G. Matsumoto, and E.J. Furshpan. 1986. Synaptic functions in rat sympathetic neurons in microcultures. II. Adrenergic/cholinergic dual status and plasticity. *The Journal of neuroscience : the official journal of the Society for Neuroscience*. 6:1080-1098.
- Pulst, S.M., D. Gusman, B.S. Rothman, and E. Mayeri. 1986. Coexistence of egg-laying hormone and alpha-bag cell peptide in bag cell neurons of *Aplysia* indicates that they are a peptidergic multitransmitter system. *Neuroscience letters*. 70:40-45.
- Qin, S., X.Y. Hu, H. Xu, and J.N. Zhou. 2004. Regional alteration of synapsin I in the hippocampal formation of Alzheimer's disease patients. *Acta Neuropathol*. 107:209-215.
- Richmond, J.E., W.S. Davis, and E.M. Jorgensen. 1999. UNC-13 is required for synaptic vesicle fusion in *C. elegans*. *Nature neuroscience*. 2:959-964.
- Romano, C., R.A. Nichols, and P. Greengard. 1987a. Synapsin I in PC12 cells. II. Evidence for regulation by NGF of phosphorylation at a novel site. *The Journal of neuroscience : the official journal of the Society for Neuroscience*. 7:1300-1306.
- Romano, C., R.A. Nichols, P. Greengard, and L.A. Greene. 1987b. Synapsin I in PC12 cells. I. Characterization of the phosphoprotein and effect of chronic NGF

- treatment. *The Journal of neuroscience : the official journal of the Society for Neuroscience*. 7:1294-1299.
- Rosahl, T.W., D. Spillane, M. Missler, J. Herz, D.K. Selig, J.R. Wolff, R.E. Hammer, R.C. Malenka, and T.C. Sudhof. 1995. Essential functions of synapsins I and II in synaptic vesicle regulation. *Nature*. 375:488-493.
- Saegusa, C., M. Fukuda, and K. Mikoshiba. 2002. Synaptotagmin V is targeted to dense-core vesicles that undergo calcium-dependent exocytosis in PC12 cells. *J Biol Chem*. 277:24499-24505.
- Sakurada, K., H. Kato, H. Nagumo, H. Hiraoka, K. Furuya, T. Ikuhara, Y. Yamakita, K. Fukunaga, E. Miyamoto, F. Matsumura, Y.I. Matsuo, Y. Naito, and Y. Sasaki. 2002. Synapsin I is phosphorylated at Ser603 by p21-activated kinases (PAKs) in vitro and in PC12 cells stimulated with bradykinin. *The Journal of biological chemistry*. 277:45473-45479.
- Schiavo, G., F. Benfenati, B. Poulain, O. Rossetto, P. Polverino de Laureto, B.R. DasGupta, and C. Montecucco. 1992. Tetanus and botulinum-B neurotoxins block neurotransmitter release by proteolytic cleavage of synaptobrevin. *Nature*. 359:832-835.
- Schilling, K., and M. Gratzl. 1988. Quantification of p38/synaptophysin in highly purified adrenal medullary chromaffin vesicles. *FEBS letters*. 233:22-24.
- Schmitt, U., N. Tanimoto, M. Seeliger, F. Schaeffel, and R.E. Leube. 2009. Detection of behavioral alterations and learning deficits in mice lacking synaptophysin. *Neuroscience*. 162:234-243.
- Shao, X., B.A. Davletov, R.B. Sutton, T.C. Sudhof, and J. Rizo. 1996. Bipartite Ca<sup>2+</sup>-binding motif in C2 domains of synaptotagmin and protein kinase C. *Science*. 273:248-251.
- Shin, O.H. 2014. Exocytosis and synaptic vesicle function. *Comprehensive Physiology*. 4:149-175.
- Silva, A.J., T.W. Rosahl, P.F. Chapman, Z. Marowitz, E. Friedman, P.W. Frankland, V. Cestari, D. Cioffi, T.C. Sudhof, and R. Bourtschuladze. 1996. Impaired learning in mice with abnormal short-lived plasticity. *Current biology : CB*. 6:1509-1518.
- Slonimsky, J.D., M.D. Mattaliano, J.I. Moon, L.C. Griffith, and S.J. Birren. 2006. Role for calcium/calmodulin-dependent protein kinase II in the p75-mediated regulation of sympathetic cholinergic transmission. *Proceedings of the National Academy of Sciences of the United States of America*. 103:2915-2919.

- Soderberg, O., K.J. Leuchowius, M. Gullberg, M. Jarvius, I. Weibrecht, L.G. Larsson, and U. Landegren. 2008. Characterizing proteins and their interactions in cells and tissues using the in situ proximity ligation assay. *Methods*. 45:227-232.
- Sollner, T., M.K. Bennett, S.W. Whiteheart, R.H. Scheller, and J.E. Rothman. 1993a. A protein assembly-disassembly pathway in vitro that may correspond to sequential steps of synaptic vesicle docking, activation, and fusion. *Cell*. 75:409-418.
- Sollner, T., S.W. Whiteheart, M. Brunner, H. Erdjument-Bromage, S. Geromanos, P. Tempst, and J.E. Rothman. 1993b. SNAP receptors implicated in vesicle targeting and fusion. *Nature*. 362:318-324.
- Sollner, T.H. 2003. Regulated exocytosis and SNARE function (Review). *Mol Membr Biol*. 20:209-220.
- Sorensen, J.B. 2005. SNARE complexes prepare for membrane fusion. *Trends in neurosciences*. 28:453-455.
- Stevens, C.F., and J.M. Sullivan. 2003. The synaptotagmin C2A domain is part of the calcium sensor controlling fast synaptic transmission. *Neuron*. 39:299-308.
- Stevens, D.R., C. Schirra, U. Becherer, and J. Rettig. 2011. Vesicle pools: lessons from adrenal chromaffin cells. *Front Synaptic Neurosci*. 3:2.
- Stojilkovic, S.S. 2005. Ca<sup>2+</sup>-regulated exocytosis and SNARE function. *Trends Endocrinol Metab*. 16:81-83.
- Sudhof, T.C., A.J. Czernik, H.T. Kao, K. Takei, P.A. Johnston, A. Horiuchi, S.D. Kanazir, M.A. Wagner, M.S. Perin, P. De Camilli, and et al. 1989. Synapsins: mosaics of shared and individual domains in a family of synaptic vesicle phosphoproteins. *Science*. 245:1474-1480.
- Sudhof, T.C., and J.E. Rothman. 2009. Membrane fusion: grappling with SNARE and SM proteins. *Science*. 323:474-477.
- Sulzer, D., M.P. Joyce, L. Lin, D. Geldwert, S.N. Haber, T. Hattori, and S. Rayport. 1998. Dopamine neurons make glutamatergic synapses in vitro. *The Journal of neuroscience : the official journal of the Society for Neuroscience*. 18:4588-4602.
- Szklarczyk, D., A. Franceschini, S. Wyder, K. Forslund, D. Heller, J. Huerta-Cepas, M. Simonovic, A. Roth, A. Santos, K.P. Tsafou, M. Kuhn, P. Bork, L.J. Jensen, and C. von Mering. 2015. STRING v10: protein-protein interaction networks, integrated over the tree of life. *Nucleic acids research*. 43:D447-452.
- Thiele, C., M.J. Hannah, F. Fahrenholz, and W.B. Huttner. 2000. Cholesterol binds to synaptophysin and is required for biogenesis of synaptic vesicles. *Nature cell biology*. 2:42-49.

- Thomas, L., K. Hartung, D. Langosch, H. Rehm, E. Bamberg, W.W. Franke, and H. Betz. 1988. Identification of synaptophysin as a hexameric channel protein of the synaptic vesicle membrane. *Science*. 242:1050-1053.
- Valtorta, F., P. Greengard, R. Fesce, E. Chieregatti, and F. Benfenati. 1992. Effects of the neuronal phosphoprotein synapsin I on actin polymerization. I. Evidence for a phosphorylation-dependent nucleating effect. *The Journal of biological chemistry*. 267:11281-11288.
- van den Bogaart, G., K. Meyenberg, U. Diederichsen, and R. Jahn. 2012. Phosphatidylinositol 4,5-bisphosphate increases Ca<sup>2+</sup> affinity of synaptotagmin-1 by 40-fold. *The Journal of biological chemistry*. 287:16447-16453.
- Vawter, M.P., L. Thatcher, N. Usen, T.M. Hyde, J.E. Kleinman, and W.J. Freed. 2002. Reduction of synapsin in the hippocampus of patients with bipolar disorder and schizophrenia. *Mol Psychiatry*. 7:571-578.
- Vites, O., J.S. Rhee, M. Schwarz, C. Rosenmund, and R. Jahn. 2004. Reinvestigation of the role of snapin in neurotransmitter release. *The Journal of biological chemistry*. 279:26251-26256.
- Voets, T. 2000. Dissection of three Ca<sup>2+</sup>-dependent steps leading to secretion in chromaffin cells from mouse adrenal slices. *Neuron*. 28:537-545.
- Wang, C.T., J. Bai, P.Y. Chang, E.R. Chapman, and M.B. Jackson. 2006. Synaptotagmin-Ca<sup>2+</sup> triggers two sequential steps in regulated exocytosis in rat PC12 cells: fusion pore opening and fusion pore dilation. *J Physiol*. 570:295-307.
- Wang, C.T., R. Grishanin, C.A. Earles, P.Y. Chang, T.F. Martin, E.R. Chapman, and M.B. Jackson. 2001. Synaptotagmin modulation of fusion pore kinetics in regulated exocytosis of dense-core vesicles. *Science*. 294:1111-1115.
- Wang, C.T., J.C. Lu, J. Bai, P.Y. Chang, T.F. Martin, E.R. Chapman, and M.B. Jackson. 2003. Different domains of synaptotagmin control the choice between kiss-and-run and full fusion. *Nature*. 424:943-947.
- Weickert, C.S., T.M. Hyde, B.K. Lipska, M.M. Herman, D.R. Weinberger, and J.E. Kleinman. 2003. Reduced brain-derived neurotrophic factor in prefrontal cortex of patients with schizophrenia. *Mol Psychiatry*. 8:592-610.
- Wheeler, T.C., L.S. Chin, Y. Li, F.L. Roudabush, and L. Li. 2002. Regulation of synaptophysin degradation by mammalian homologues of seven in absentia. *The Journal of biological chemistry*. 277:10273-10282.
- Wightman, R.M., J.A. Jankowski, R.T. Kennedy, K.T. Kawagoe, T.J. Schroeder, D.J. Leszczyszyn, J.A. Near, E.J. Diliberto, Jr., and O.H. Viveros. 1991. Temporally

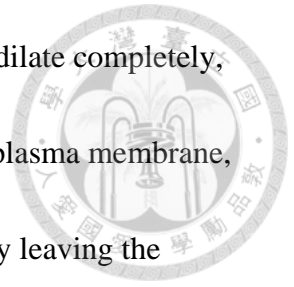
- resolved catecholamine spikes correspond to single vesicle release from individual chromaffin cells. *Proceedings of the National Academy of Sciences of the United States of America*. 88:10754-10758.
- Willis, M., I. Leitner, K.A. Jellinger, and J. Marksteiner. 2011. Chromogranin peptides in brain diseases. *Journal of neural transmission*. 118:727-735.
- Winkler, H. 1997. Membrane composition of adrenergic large and small dense cored vesicles and of synaptic vesicles: consequences for their biogenesis. *Neurochemical research*. 22:921-932.
- Wu, Z., S. Thiagarajan, B. O'Shaughnessy, and E. Karatekin. 2017. Regulation of Exocytotic Fusion Pores by SNARE Protein Transmembrane Domains. *Frontiers in molecular neuroscience*. 10:315.
- Xu, B., N. Wratten, E.I. Charych, S. Buyske, B.L. Firestein, and L.M. Brzustowicz. 2005. Increased expression in dorsolateral prefrontal cortex of CAPON in schizophrenia and bipolar disorder. *PLoS Med*. 2:e263.
- Yang, B., J.D. Slonimsky, and S.J. Birren. 2002. A rapid switch in sympathetic neurotransmitter release properties mediated by the p75 receptor. *Nature neuroscience*. 5:539-545.
- Zhang, Y., Z. Zhu, H.Y. Liang, L. Zhang, Q.G. Zhou, H.Y. Ni, C.X. Luo, and D.Y. Zhu. 2018. nNOS-CAPON interaction mediates amyloid-beta-induced neurotoxicity, especially in the early stages. *Aging Cell*. 17:e12754.
- Zhang, Z., E. Hui, E.R. Chapman, and M.B. Jackson. 2010. Regulation of exocytosis and fusion pores by synaptotagmin-effector interactions. *Molecular biology of the cell*. 21:2821-2831.
- Zhao, W.D., E. Hamid, W. Shin, P.J. Wen, E.S. Krystofiak, S.A. Villarreal, H.C. Chiang, B. Kachar, and L.G. Wu. 2016. Hemi-fused structure mediates and controls fusion and fission in live cells. *Nature*. 534:548-552.
- Zhou, L., and D.Y. Zhu. 2009. Neuronal nitric oxide synthase: structure, subcellular localization, regulation, and clinical implications. *Nitric Oxide*. 20:223-230.
- Zhou, Q., Y. Lai, T. Bacaj, M. Zhao, A.Y. Lyubimov, M. Uervirojnangkoorn, O.B. Zeldin, A.S. Brewster, N.K. Sauter, A.E. Cohen, S.M. Soltis, R. Alonso-Mori, M. Chollet, H.T. Lemke, R.A. Pfuetzner, U.B. Choi, W.I. Weis, J. Diao, T.C. Sudhof, and A.T. Brunger. 2015. Architecture of the synaptotagmin-SNARE machinery for neuronal exocytosis. *Nature*. 525:62-67.
- Zhu, L.J., T.Y. Li, C.X. Luo, N. Jiang, L. Chang, Y.H. Lin, H.H. Zhou, C. Chen, Y. Zhang, W. Lu, L.Y. Gao, Y. Ma, Q.G. Zhou, Q. Hu, X.L. Hu, J. Zhang, H.Y. Wu, and D.Y. Zhu. 2014. CAPON-nNOS coupling can serve as a target for developing new anxiolytics. *Nat Med*. 20:1050-1054.



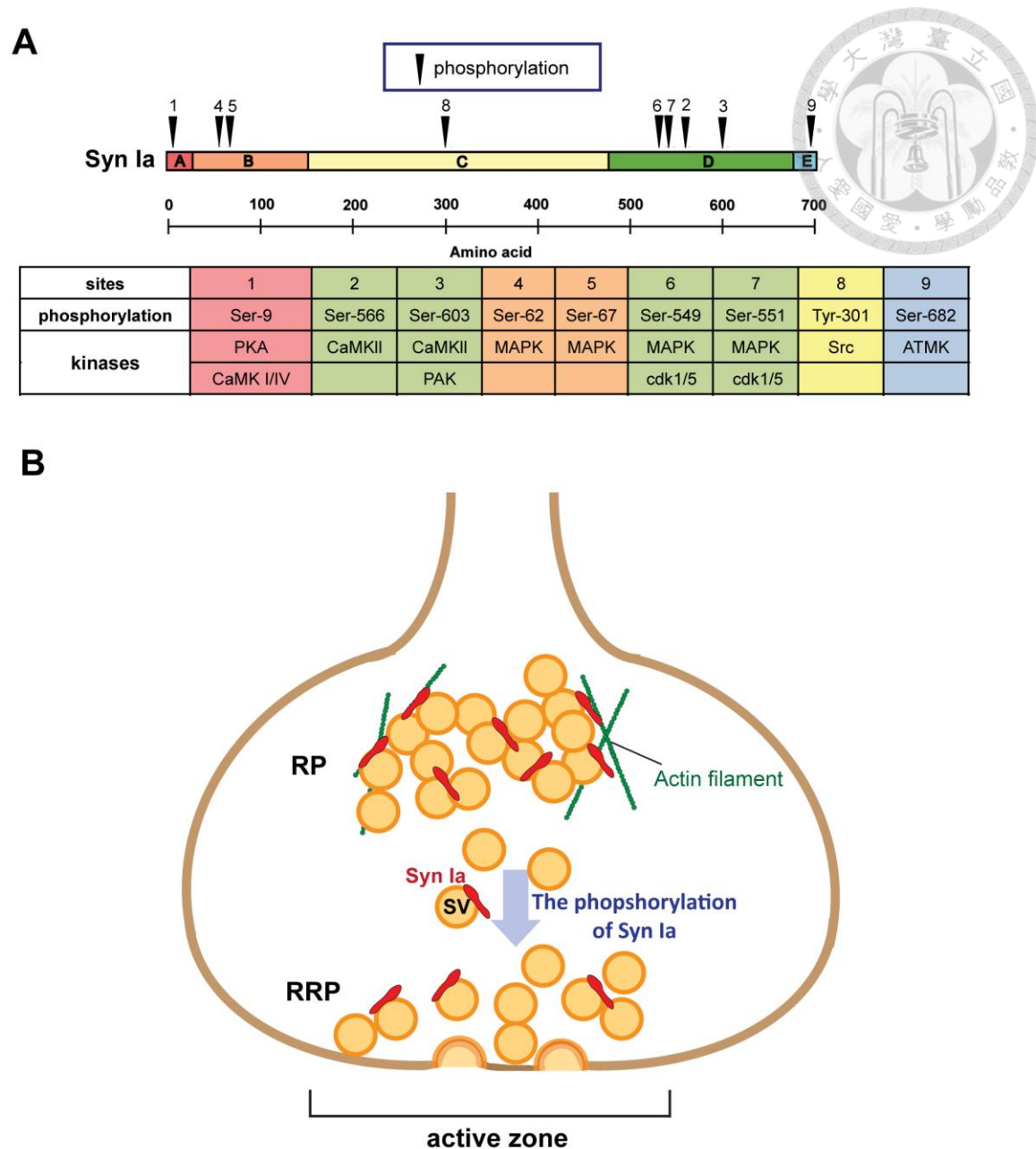
**Figure 1. Neurotransmitters are released by Ca<sup>2+</sup>-regulated exocytosis.**

**A**, The process of Ca<sup>2+</sup>-regulated exocytosis can be divided into several steps, including docking, priming, and fusion. Synaptotagmin I and SNARE complex (formed by Syntaxin, Synaptobrevin, and SNAP-25) help DCVs fused with plasma membrane. **B**, Two distinct fusion events in Ca<sup>2+</sup>-regulated exocytosis. After fusion pores form, DCVs can undergo two distinct fusion events, i.e., full fusion (FF) and

kiss and run (KR). DCVs fuse with the plasma membrane and then dilate completely, termed “FF”, whereas “KR” is that DCVs transiently fuse with the plasma membrane, release neurotransmitter partially, and then become vesicles again by leaving the plasma membrane.



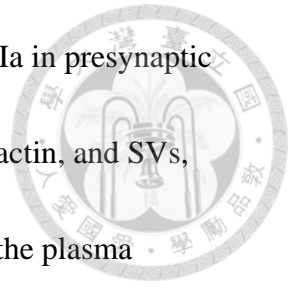




**Figure 2. Syn Ia is a key regulator of SV dynamics by modulating the storage and mobilization via its phosphorylation.**

**A**, The domain structure of Synapsin Ia and distinct phosphorylation sites. The structure of Syn Ia can be divided into five domains, A, B, C, D, and, E. The arrows represented nine phosphorylation sites regulated by different protein kinases. **B**, The

process of SV exocytosis modulated by the phosphorylation of Syn Ia in presynaptic terminals. Syn Ia (represented in red) acts as a linker between SVs, actin, and SVs, forming the clusters in a reserve pool (RP), which is far away from the plasma membrane. Upon the appropriate stimulus, Syn Ia is phosphorylated and then recruits SVs to active zone to form readily releasable pool (RRP). SVs in RRP are ready to dock, prime, and fusion.



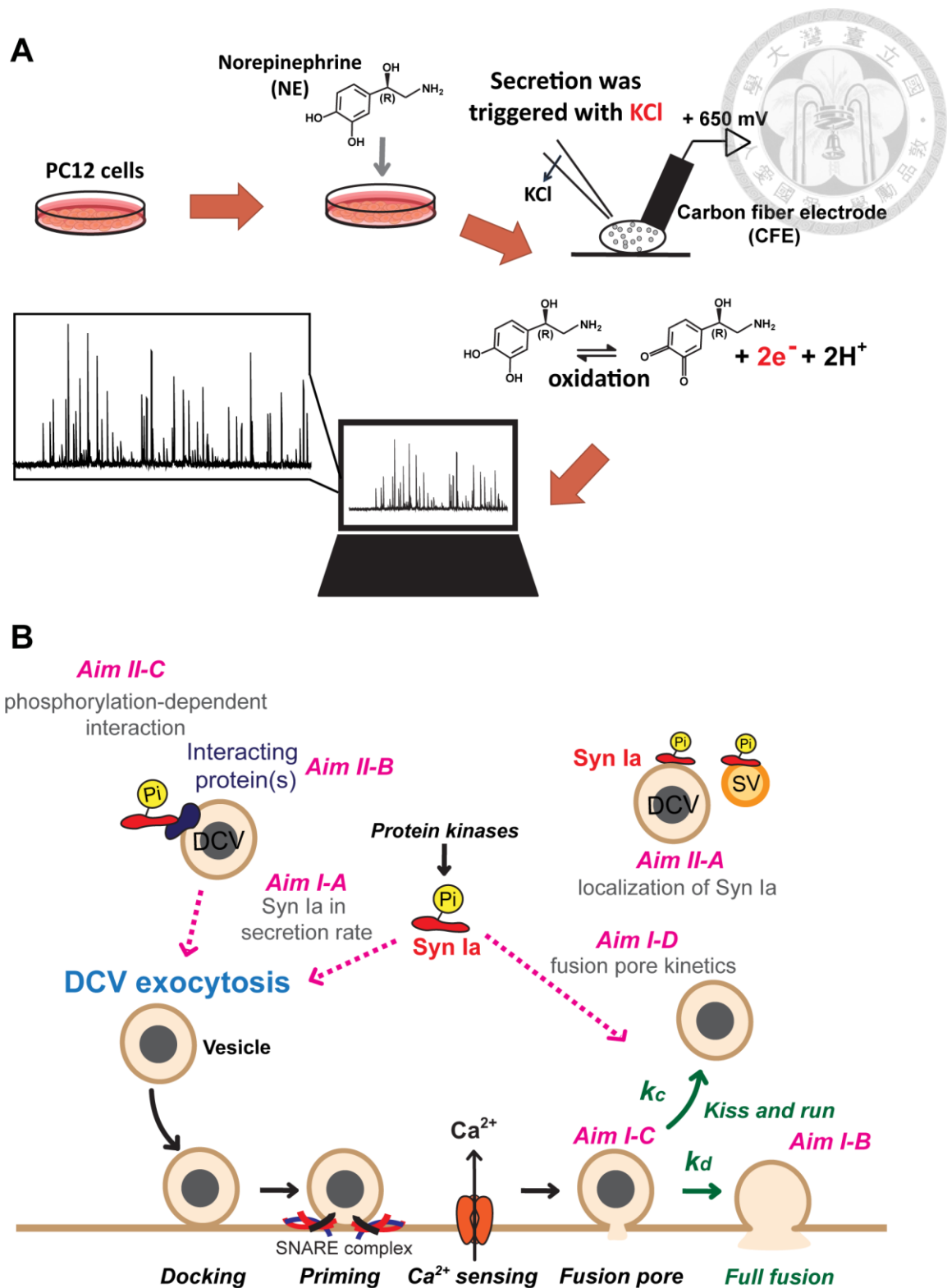


**Figure 3. The scheme of the working hypothesis and proposed experiments in this study.**

**A**, Single-vesicle amperometry provides the sensitive measurement for DCV release by detecting oxidized-neurotransmitters released from DCVs. PC12 Cells were incubated with norepinephrine (NE) prior to single-vesicle amperometric recordings.

The release of NE from individual DCVs was induced by high KCl and detected as an oxidation current at the potentiated carbon fiber electrode (CFE) with +650 mV. An efflux of neurotransmitters out of DCVs corresponds to the signal in amperometric recordings. **B**, In this study, we would determine how Syn Ia regulates the dynamics of DCV exocytosis via phosphorylation at single-vesicle levels and further determine the mechanism underlying the Syn Ia's regulation of DCV exocytosis.

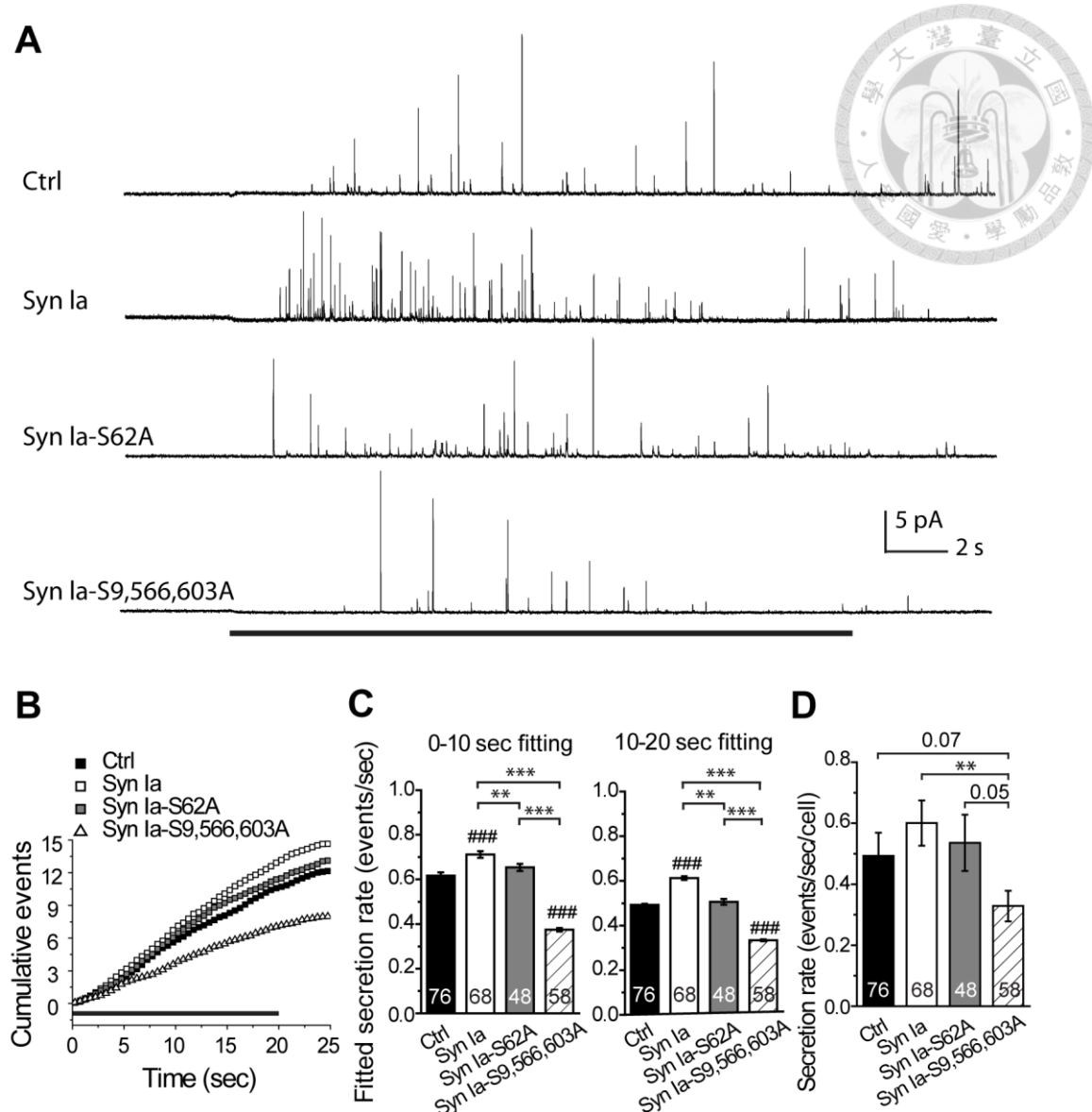


**Figure 4. Secretion rate of DCVs was regulated by Syn Ia or its phosphodeficient mutants.**

**A**, Representative secretion events in cells overexpressing control (Ctrl), wild-type

Syn Ia (Syn Ia), or the phosphodeficient mutants (Syn Ia-S62A or Syn Ia-

S9,566,603A). The Black bottom line showed the period of KCl application (20 sec).

**B**, Cumulative events (peak amplitude  $\geq 2$  pA) normalized by a number of cells from

the onset of KCl application (black bottom line) to the end of recordings (total 25 sec). **C**, Fitted secretion rate obtained from (**B**) by linear fits for the 0-10 sec (left) or 10-20 sec (right).  $R^2$  were ranging from 0.988 to 0.998 for these groups. **D**, Bulk secretion rate was acquired from the same dataset in (**B**) by taking the cellular means (numbers in columns as cell numbers).

All data are presented as mean  $\pm$  SEM. Numbers in columns as cell numbers. \*\* $p < 0.01$ ; \*\*\* $p < 0.001$  vs. Syn Ia; #### $p < 0.001$  vs. Ctrl, two-tailed Student's unpaired t test.

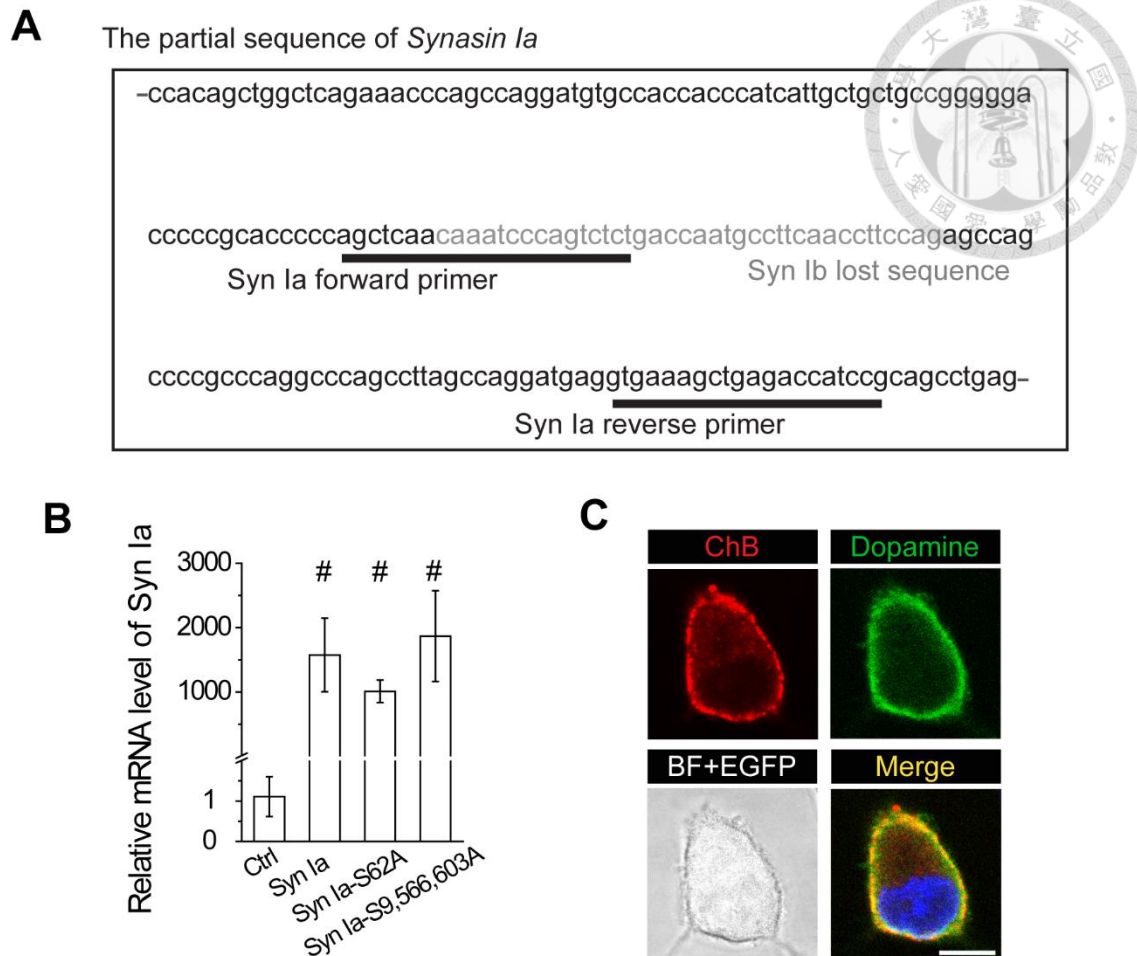
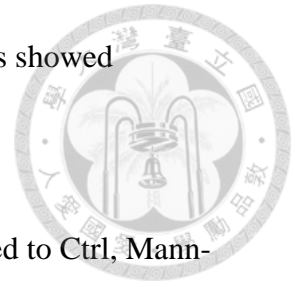


**Figure 5. The mRNA expression in cells overexpressing Syn Ia or its phosphodeficient mutants.**

**A**, The design of the specific primers targeting to Syn Ia. **B**, Relative mRNA levels of Syn Ia determined by performing qPCR with the specific primers targeting to Syn Ia in cells overexpressing Ctrl, Syn Ia, or the phosphodeficient mutants (Syn Ia-S62A or Syn Ia-S9,566,603A). **C**, Immunofluorescent images for the distribution of the DCV marker chromogranin B (ChB) (red) and dopamine (green) after 1 hr-incubation of

dopamine. EGFP (white) indicated transfected cells. Merged images showed colocalization (yellow). BF, bright field. Scale bar, 5  $\mu$ m.

All data are presented as median  $\pm$  SEM (n = 4). <sup>#</sup>p < 0.05, compared to Ctrl, Mann-Whitney test.





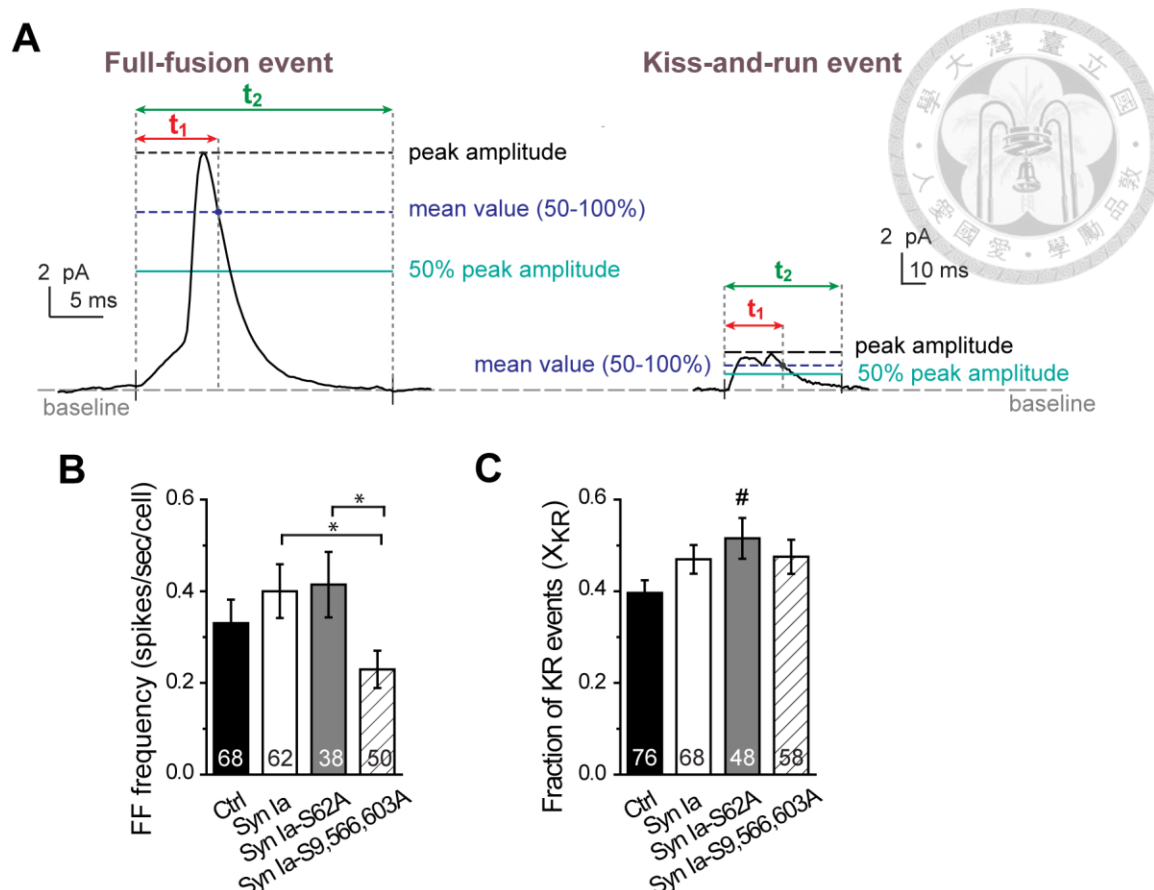


**Figure 6. FF frequency and fraction of KR events in cells overexpressing Syn Ia or its phosphodeficient mutants.**

**A**, Two specific temporal parameters,  $t_1$  (red) and  $t_2$  (green) were defined as previously reported (Chiang et al., 2014). The  $t_1$  was the duration from onset to the signal falls back to the average value of 50-100% peak amplitude of events [mean value (50-100%), blue]. The  $t_2$  was the duration from onset to the signal falls back to the baseline. The  $t_1/t_2$  ratio at 3.5 pA was very sensitive to the event shape of two types of fusion events, FF (exhibiting the spike-like shape with smaller  $t_1/t_2$  ratios) and KR (exhibiting the square-like shape with larger  $t_1/t_2$  ratios), so the peak

amplitudes of 3.5 pA was set as cut-off for separation of two events. **B**, FF frequency was acquired from the FF events (peak amplitude  $\geq 3.5$  pA) from the onset of KCl application (black bottom line) to the end of recording (total 25 sec) by taking the cellular means (numbers in columns as cell numbers). **C**, Fraction of KR events ( $X_{KR}$ ) as the ratios of the numbers of KR events (peak amplitude 2-3.5 pA) vs. the numbers of total events (peak amplitude  $\geq 2$  pA; **Figure 4**) by taking the cellular means (numbers in columns as cell numbers).

All data are presented as mean  $\pm$  SEM. Numbers in columns as cell numbers. \* $p < 0.05$  vs. Syn Ia; # $p < 0.05$  vs. Ctrl, two-tailed Student's unpaired t test.

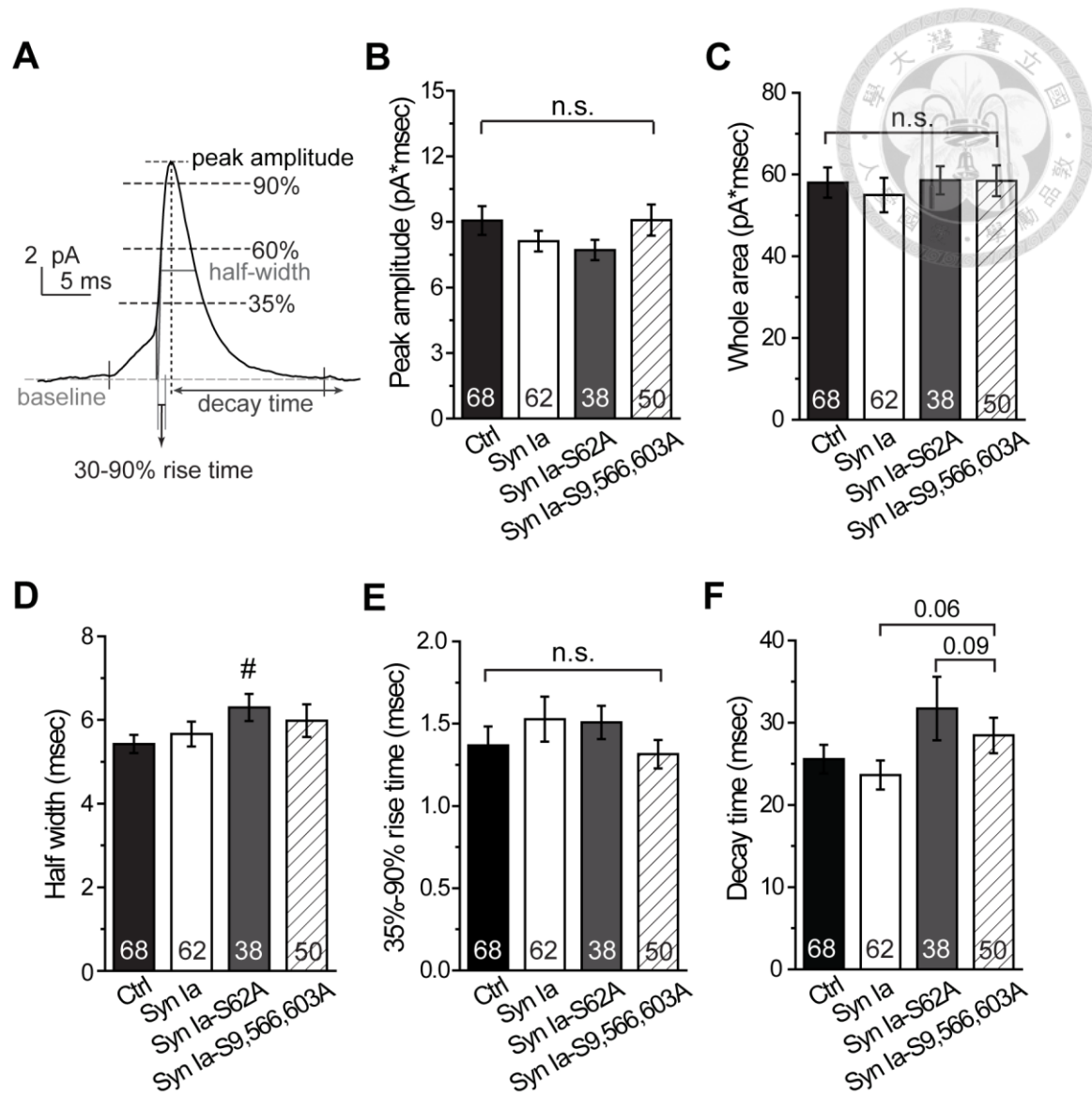


**Figure 7. Spike characteristics in cells overexpressing Syn Ia or its phosphodeficient mutants.**

**A**, The criteria of spike characteristics. **B**, Peak amplitude, **C**, Whole area, **D**, Half width, **E**, Rise time and **F**, Decay time for FF events (peak amplitude  $\geq 3.5$  pA) by taking the cellular means.

All data are presented as mean  $\pm$  SEM. Numbers in columns as cell numbers. #p <

0.05 vs. Ctrl, two-tailed Student's unpaired t test.



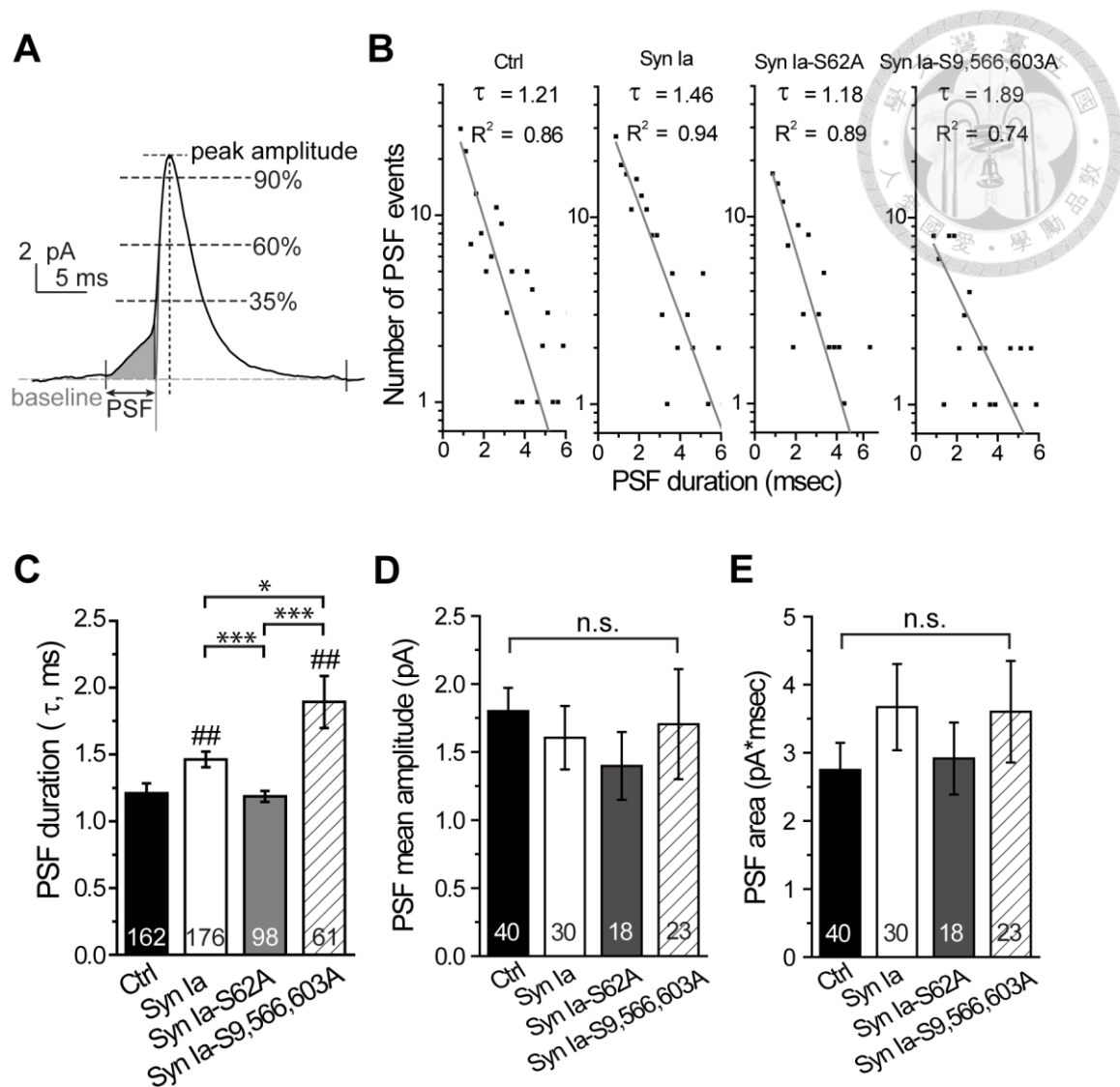


**Figure 8. PSF open time of DCVs was regulated by Syn Ia or its phosphodeficient mutants.**

**A**, PSF characteristics were acquired from large amperometric spikes (peak amplitude  $\geq 13$  pA). The shaded area a prespike foot (PSF). The PSF open time was measured from onset to end point, which is the intersection between the baseline and the gray line (The line from the 35% to 60% height of spike). **B**, PSF open time distributions

(semi-log plots for the histograms of PSF duration) were fitted by a single-exponential decay function,  $N(t) = N(0) \times \exp(-t/\tau)$ , to yield the PSF mean duration,  $\tau$  (msec).  $R^2$ , the goodness of fits. **C**, PSF mean duration,  $\tau$  obtained in **(B)**. **D**, PSF mean amplitudes and **E**, PSF areas obtained from the cellular means.

All data are presented as mean  $\pm$  SEM. Numbers in columns as cell numbers. \* $p < 0.05$ ; \*\*\* $p < 0.001$  vs. Syn Ia; ## $p < 0.01$  vs. Ctrl; n.s., not significant, two-tailed Student's unpaired t test.

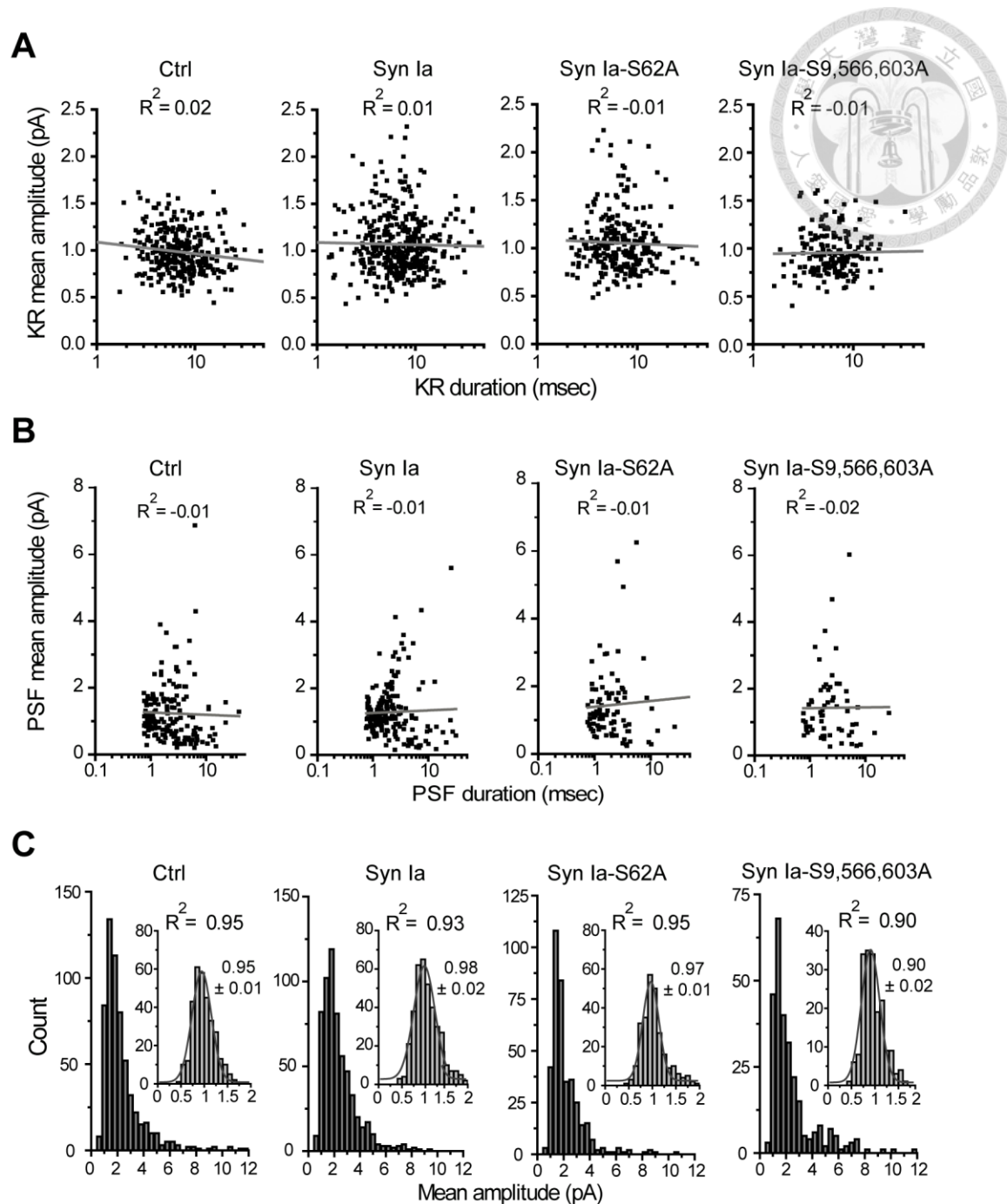
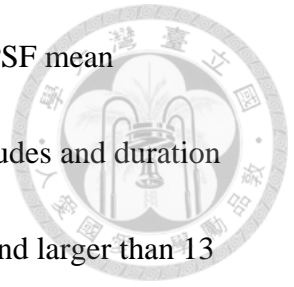


**Figure 9. Two fusion events- “kiss and run” v.s. “full fusion” in cells**

**overexpressing Syn Ia or its phosphodeficient mutants.**

**A**, Scatter plots of KR mean amplitudes v.s. KR duration for different groups. KR mean amplitudes and duration obtained from individual KR events (dots). The  $R^2$

from linear regression (gray) were as indicated. **B**, Scatter plots of PSF mean amplitudes v.s. PSF duration for different groups. PSF mean amplitudes and duration obtained from individual FF events with the peak amplitude equal and larger than 13 pA (dots). The  $R^2$  from linear regression (gray) was as indicated. **C**, Histograms of the mean amplitudes from individual FF events ( $\geq 3.5$  pA). Insets, histograms of KR mean amplitudes from individual KR events fitted by Gaussian distribution (gray). Mean  $\pm$  SEM and  $R^2$  from Gaussian distributions were as indicated.





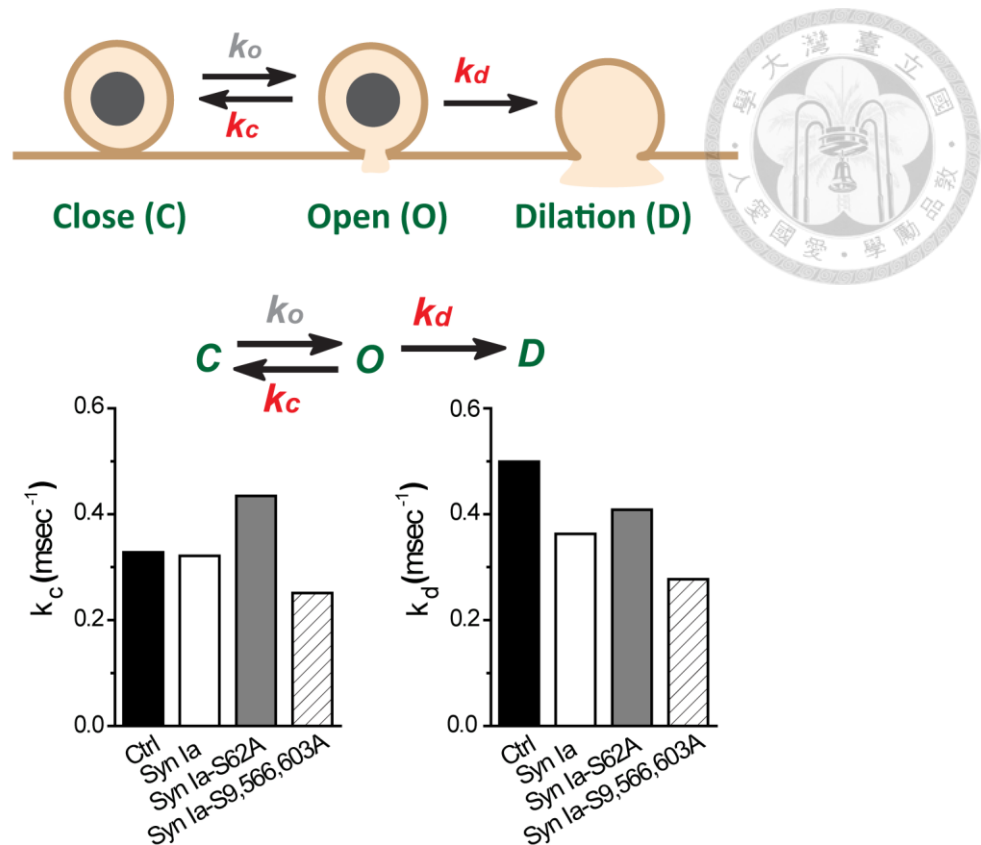


**Figure 10. Fusion pore kinetics of DCVs was regulated by Syn Ia or its phosphodeficient mutants.**

The kinetic model of fusion pores. An opening fusion pore (O: open state) can transiently toward closure (C: close state) or dilation (D: dilation state). The rate constant  $k_o$  represents the rate from O towards C, the rate constant  $k_c$  represents the rate from O towards C, and the rate constant  $k_d$  represents the rate from O towards D. Both  $k_c$  and  $k_d$  were resolved from the  $X_{KR}$  (**Figure 6C**) and PSF mean duration (**Figure 8C**) using the equations ( $X_{KR} = k_c / (k_c + k_d)$ ;  $\tau = 1 / (k_c + k_d)$ ) as previously reported (Chiang et al., 2014; Wang et al., 2006; Wang et al., 2001).

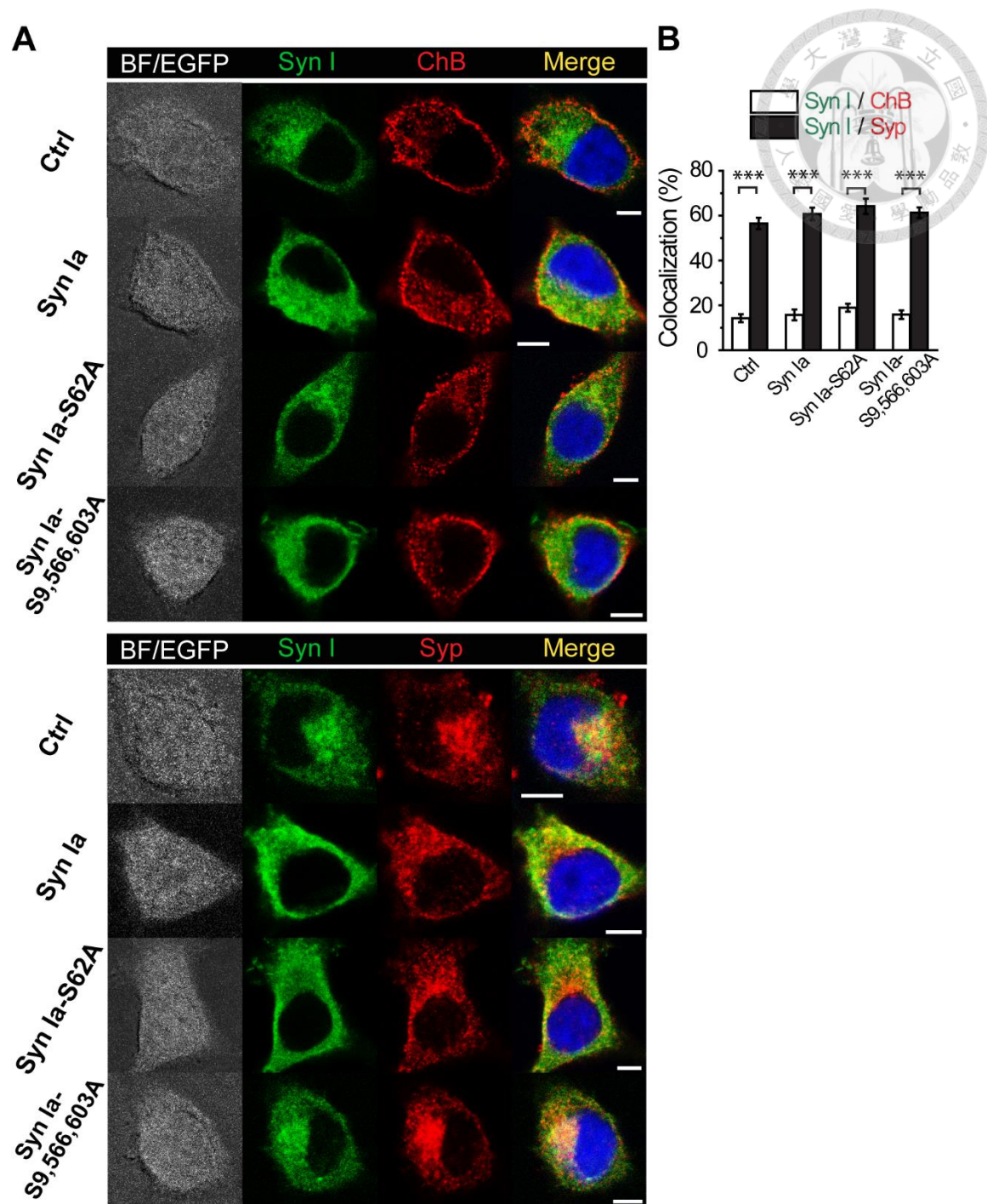


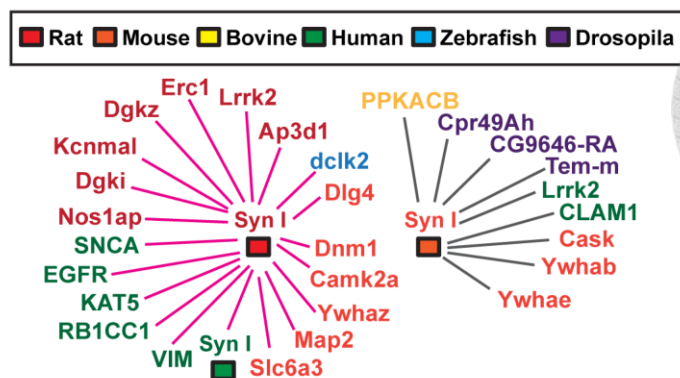
**Figure 11. Subcellular localization of Syn I and ChB/Syp in cells overexpressing Syn Ia or its phosphodeficient mutants.**

**A**, Immunofluorescent images for the distribution of Syn I (green) and the DCV marker chromogranin B (ChB) / vesicle marker Synaptophysin (Syp) (red) after 5-min KCl depolarization. EGFP (white) indicated transfected cells. Merged images showed colocalization of Syn I and ChB/Syp immunoreactivities (yellow). BF, bright field.

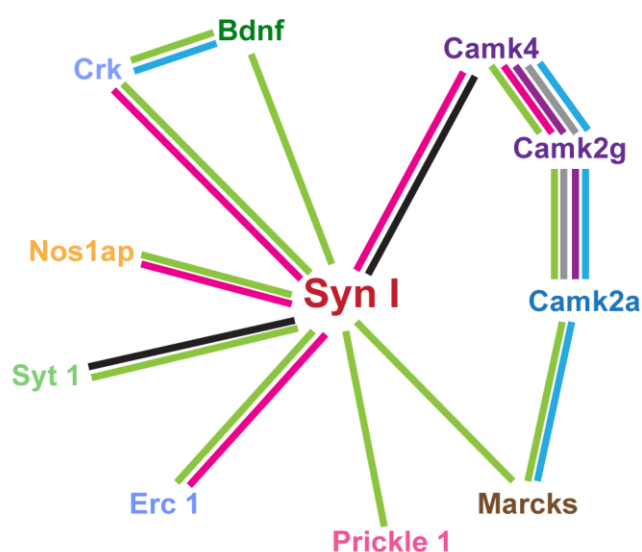
DAPI, the labeling of nucleus (blue). Scale bars, 5  $\mu$ m. **B**, White columns, the ratios of Syn I immunoreactivity overlapping with ChB immunoreactivity, reflecting the percentage of Syn I targeting to DCVs; black columns, the ratios of Syn I immunoreactivity overlapping with Syp immunoreactivity, reflecting the percentage of Syn I targeting to general vesicles.

All data are presented as mean  $\pm$  SEM. Total 9-19 cells for these groups (10 for Ctrl, 9 for Syn Ia, 10 for Syn Ia-S62A, and 11 for Syn Ia-S9,566,603A in Syn I/ChB groups; 9 for Ctrl, 15 for Syn Ia, 18 for Syn Ia-S62A, and 12 for Syn Ia-S9,566,603A in Syn I/Syp groups). \*\*\* $p < 0.001$  vs. Syn Ia, two-tailed Student's unpaired t test.

A



B



C

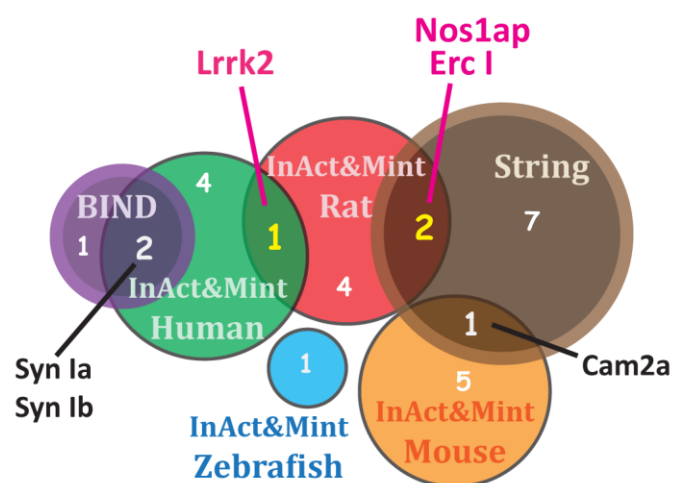
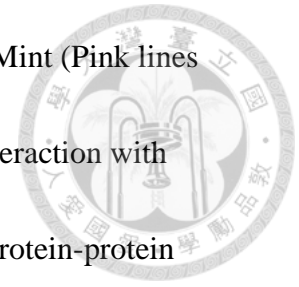
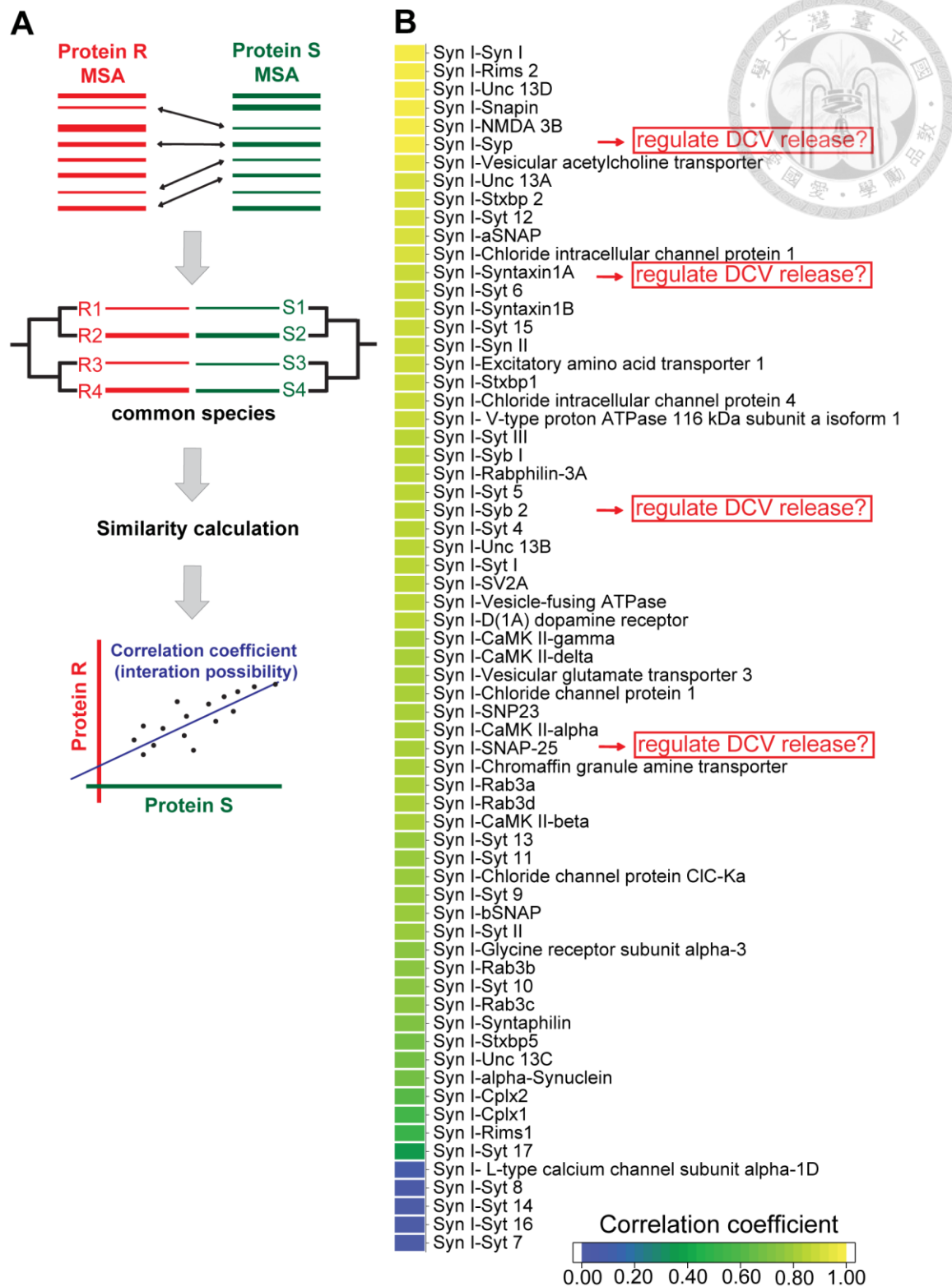


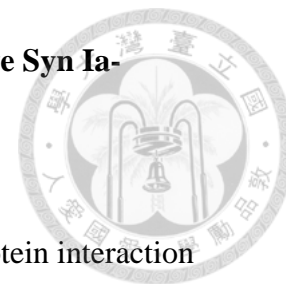
Figure 12. Syn Ia-interacting proteins from database search.

**A**, Syn Ia-interacting proteins in different species from IntAct and Mint (Pink lines represent the interaction with rat Syn Ia; gray lines represent the interaction with mouse Syn Ia. **B**, The STRING database can collect the results of protein-protein interaction via multiple resources (included Neighborhood, Fusion, Occurrence, Coexpression, Experiment, Database, or Textmining) to construct a summary network for results. **C**, Combining the results from IntAct, Mint, BIND, and String. The colors represented different databases. The numbers showed as the numbers of proteins.





**Figure 13. The protein-protein interaction prediction of putative Syn Ia-interacting proteins.**



**A**, The workflow of the *MirrorTree* for sequence-based protein-protein interaction prediction. After acquiring multiple sequence alignment (MSA) of the orthologs from different species for two query sequences (protein R and S), only the proteins of the organisms present in both trees are used to calculate the similarities. Correlation coefficients [from scoring from 1 (yellow) to 0 (dark blue)], the possibility of interaction from protein pair (protein R and S), acquired from the tree similarity between the two families. The higher correlation coefficient represents the higher possibility of interaction between protein R and S. **B**, The heat map showed the correlation coefficients from 66 predictions of individual protein pairs (Syn Ia and putative-interacting proteins) by *MirrorTree* in this study.

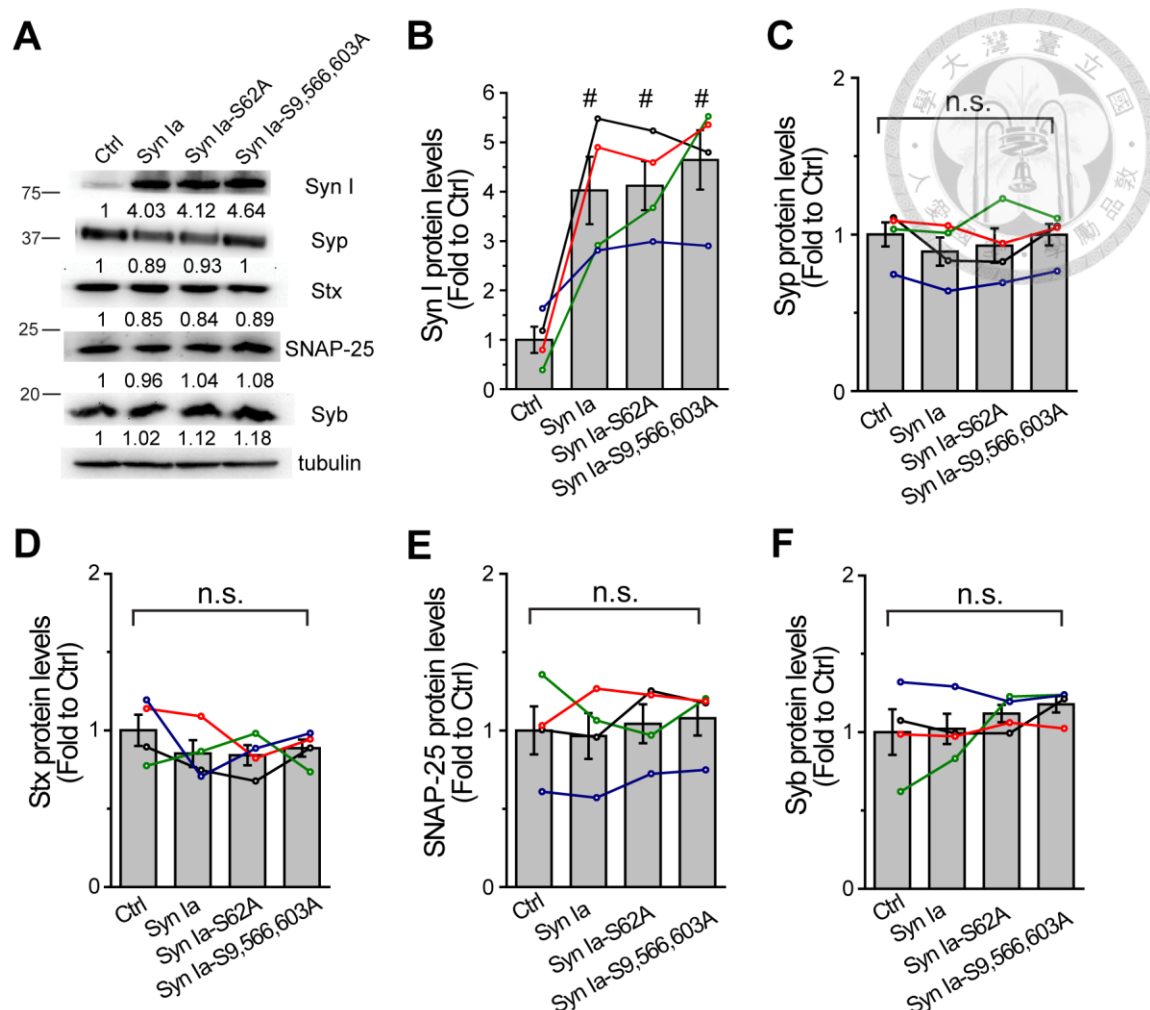


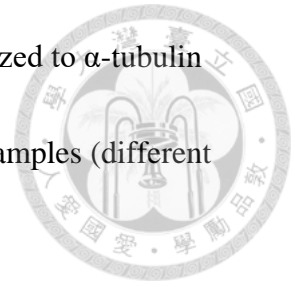
**Figure 14. The protein levels of Syn I, Syp, or SNAREs in cells overexpressing Syn Ia or its phosphodeficient mutants.**

**A**, Representative blots of Syn I, Syp, or SNAREs expression levels at 72 hr post transfection. Cell lysates after 1-min KCl depolarization were used for immunoblots, using the antibodies against Syn I (**B**), Syp (**C**), Stx (**D**), SN25 (**E**), Syb (**F**), or  $\alpha$ -tubulin. The values in the middle row indicate the protein levels first normalized to  $\alpha$ -tubulin and then to the mean value of the corresponding Ctrl.



**B-F**, Quantitative analysis of protein levels. Data were first normalized to  $\alpha$ -tubulin and then to the corresponding Ctrl. Dots, the data from individual samples (different colors). The dots from same sample are connected by lines.

All data are ( $n = 4$ ) and presented as mean  $\pm$  SEM.  $^{\#}p < 0.05$  vs. Ctrl; n.s., not significant; two-tailed Student's unpaired t test.



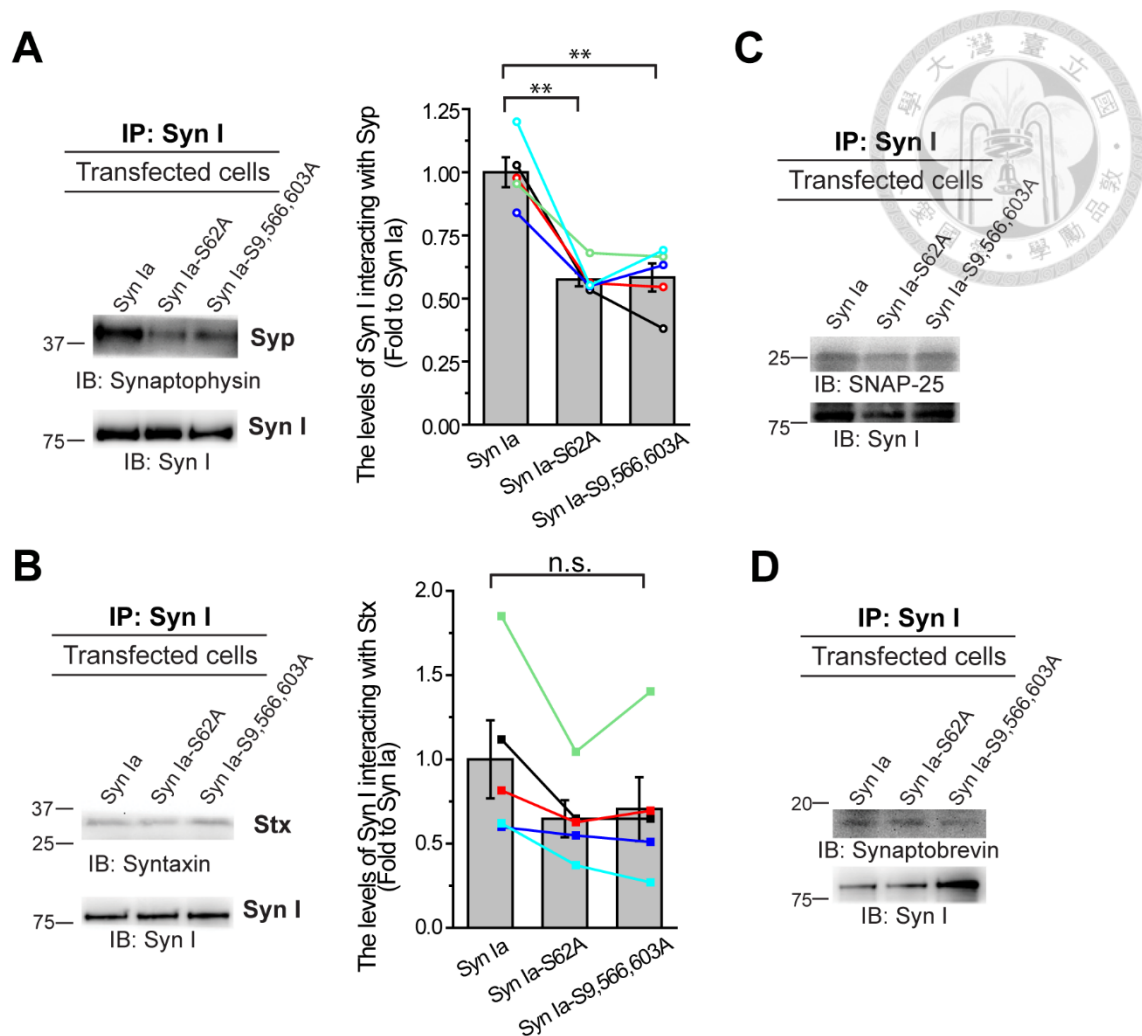


**Figure 15. *In vivo* interaction of Syn I with the interacting proteins in cells**

**overexpressing Syn Ia or its phosphodeficient mutants.**

**A-D**, Representative blots for the interaction of Syn I with Syp (**A**), Stx (**B**), SNAP-25

(**C**) or Syb (**D**) at 72 hr post transfection. Cell lysates after 1-min KCl depolarization

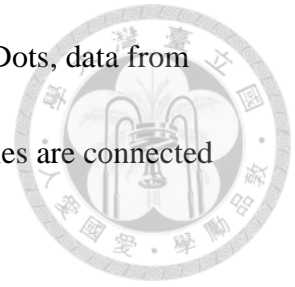
were first immunoprecipated (IP) by Syn I and then the binding of Syn I with putative

proteins was determined by immunoblotting (IB).

**A-B**, Quantitative analysis of the changes in the interaction levels. Dots, data from individual samples (different colors). The dots from the same samples are connected by lines.  $n = 5$  for Syp and Stx.

All data are presented as mean  $\pm$  SEM.

\* $p < 0.05$  vs. Syn Ia; two-tailed Student's unpaired t test.



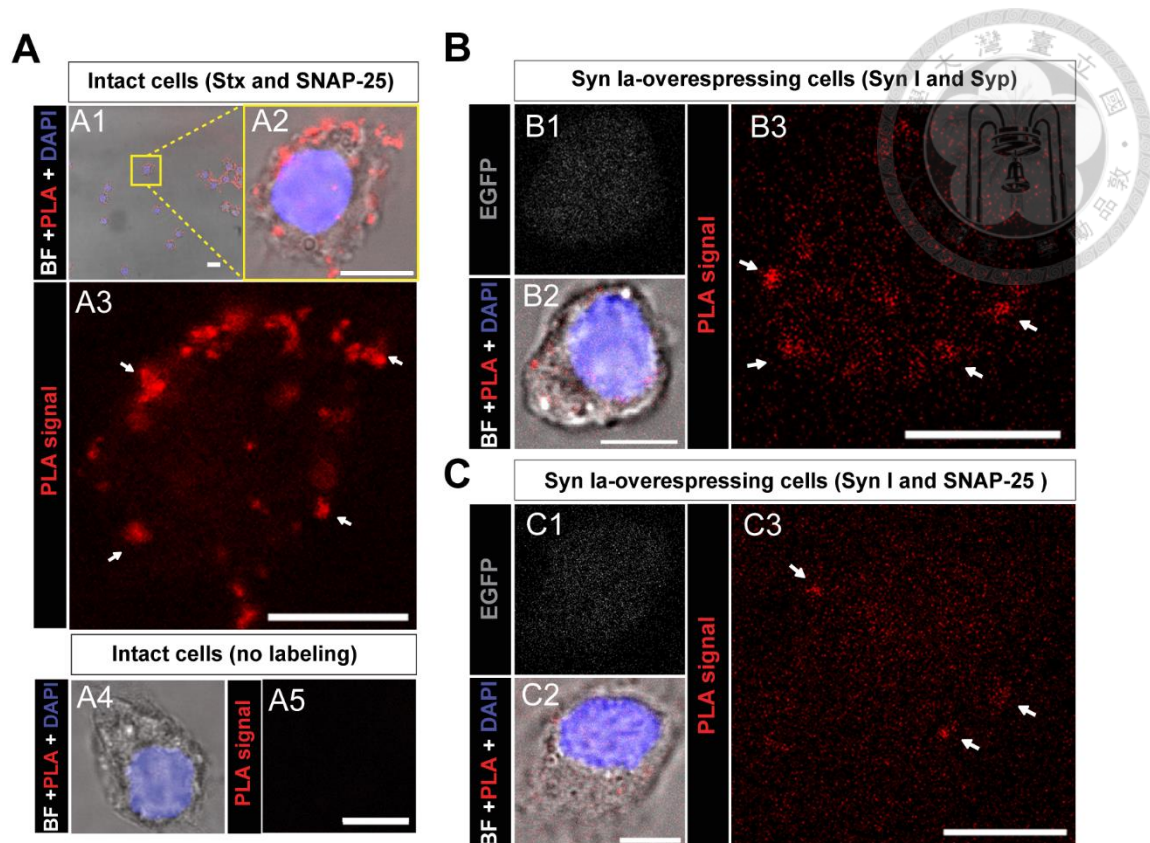


**Figure 16. *In situ* interaction of Syn I with the interacting proteins in cells overexpressing Syn Ia or its phosphodeficient mutants.**

**A-C**, Representative images for the *in situ* interaction of protein pairs detected by PLA. Individual PLA fluorescent spots (red) showed the interaction (white arrows).

**A**, Stx interacted with SNAP-25 in intact cells. **A2-3**, Enlarged images from the yellow box in **A1**. **A4-5**, Absence of PLA fluorescent signal in intact cells without the labeling of primary antibodies. **B-C**, Syn I interacted with Syp (**B**) or with SNAP-25 (**C**) in cells overexpressing Syn Ia (72 hr post transfection) after 1-min KCl depolarization.

BF, bright field; PLA (red), *in situ* interaction of protein pairs; EGFP (white)

indicated transfected cells; DAPI, the labeling of nucleus (blue). Scale bars, 5  $\mu\text{m}$ .



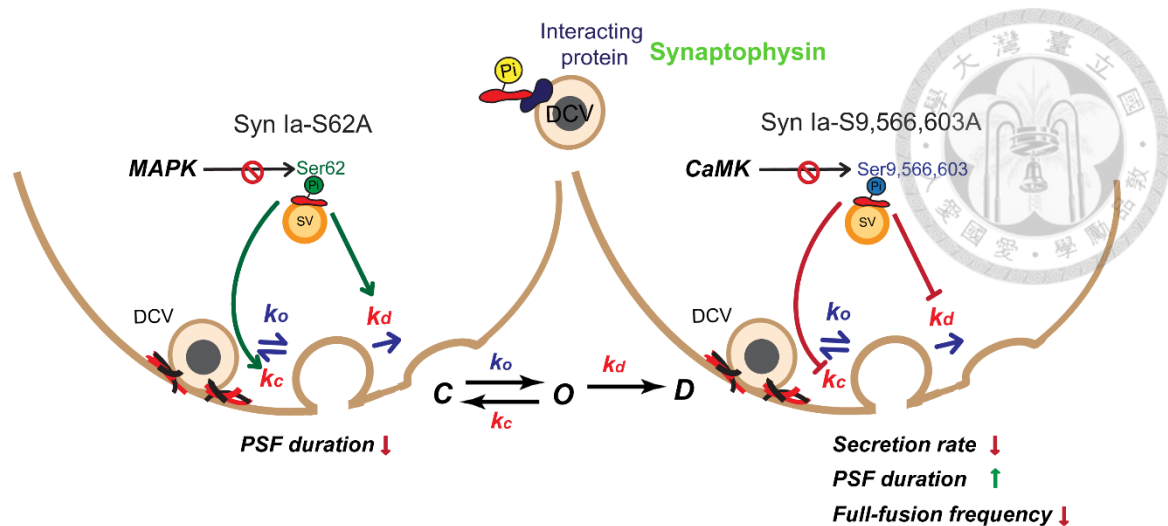


**Figure 17. The SV-specific protein Syn Ia regulates the dynamics of DCV**

**exocytosis in a phosphorylation-dependent manner.**

The phosphorylation of the SV-specific protein Syn Ia can regulate DCV release and the kinetics of fusion pores. Syn Ia-S62A increased both  $k_c$  and  $k_d$ , thus shortening the PSF mean duration. Syn Ia-S9,566,603A decreased the secretion rate and FF frequency. Moreover, Syn Ia-S9,566,603A decreased both  $k_c$  and  $k_d$ , thus prolonging the PSF mean duration. The *in vivo* interaction between Syn I and Syp was dependent on the phosphorylation of Syn Ia.



# Appendix



NEUROSCIENCE

2014

Print this Page for Your Records

[Close Window](#)

Control/Tracking Number: 2014-S-7119-SfN

Activity: Scientific Abstract

Current Date/Time: 5/7/2014 5:34:08 AM

Synapsin Ia, a synaptic vesicle protein, regulates the dynamics of dense-core vesicle exocytosis

AUTHOR BLOCK: \*H.-J. YANG, Y.-C. CHANG, C.-T. WANG;  
Inst. of Mol. and Cell. Biol., Natl. Taiwan Univ., Taipei, Taiwan

*Abstract:*

Neurotransmitters are packaged into two distinct classes of vesicles, synaptic vesicles (SVs) and dense-core vesicles (DCVs). Although the release from both vesicle classes shares a common mechanism of  $\text{Ca}^{2+}$ -dependent exocytosis, a particular phosphoprotein, synapsin (Syn), localizes to SVs exclusively. The Syn protein family consists of ten homologous proteins, of which Syn Ia is the best studied. Upon phosphorylation by various protein kinases, Syn Ia can recruit SVs to plasma membrane, thereby increasing the dynamics of SV exocytosis. However, it remains unknown whether SV recruitment to plasma membrane may also facilitate the dynamics of DCV exocytosis. Our preliminary results showed that in the rat hypothalamic-neurohypophyseal system (HNS), Syn Ia increased oxytocin release by phosphorylation at the serine 62 site (Ser-62), suggesting that that Syn Ia phosphorylation may facilitate the release from DCVs. To further determine the Syn Ia's regulation of DCV exocytosis at the single-vesicle level, we directly measured norepinephrine release from DCVs by performing single-vesicle amperometry in PC12 cells. The foot signal preceding amperometric spikes (prespike foot, PSF) has been shown to represent the fusion pore dynamics. Secretory events were triggered by direct application of high extracellular KCl onto the cells. We found that Syn Ia significantly increased the secretion rate by phosphorylation at multiple serine sites (Ser-9, Ser-566, and Ser-603). These results suggested that Syn Ia may facilitate the secretion rate of DCVs by CaMK phosphorylation. In contrast, Syn Ia significantly increased the PSF lifetime by phosphorylation at Ser-62, suggesting that Syn Ia may stabilize fusion pores by MAPK phosphorylation. Immunostainings confirmed that Syn Ia did not localize to the DCVs in PC12 cells. Thus, our results suggest that the SV-specific protein Syn Ia may play an important role in regulating the dynamics of DCV exocytosis.

:

Presentation Preference (Complete): Poster Only

Linking Group (Complete): None selected

Nanosymposium Information (Complete):

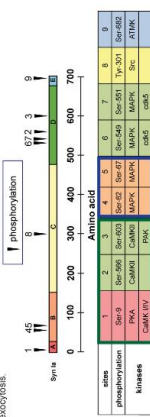
Theme and Topic (Complete): B.06.a. Docking and fusion

**Appendix 1. The 44<sup>th</sup> Annual Meeting of the Society for Neuroscience (15-19****November 2014, Washington DC, U.S.A.): Abstract****II**

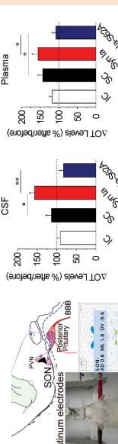


## Introduction

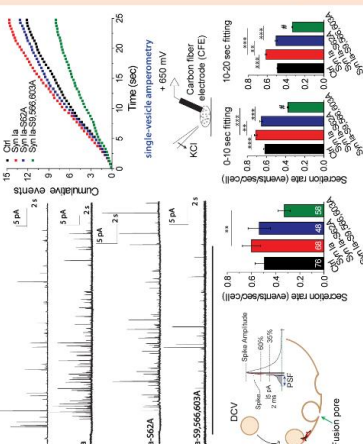
Neurotransmitters are packed into two distinct classes of vesicles, synaptic vesicles (SVs) and dense-core vesicles (DCVs). Although the release from both vesicle classes shares a common mechanism of  $\text{Ca}^{2+}$ -dependent exocytosis, a particular phosphoprotein, synapsin (Syn), localizes to SVs exclusively. The Syn protein family consists of ten homologous proteins, of which Syn Ia is the best studied. Upon phosphorylation by various protein kinases, Syn Ia can recruit SVs to plasma membrane, thereby increasing the dynamics of SV exocytosis. However, it remains unknown whether phosphorylation of Syn Ia may also facilitate the dynamics of DCV exocytosis.



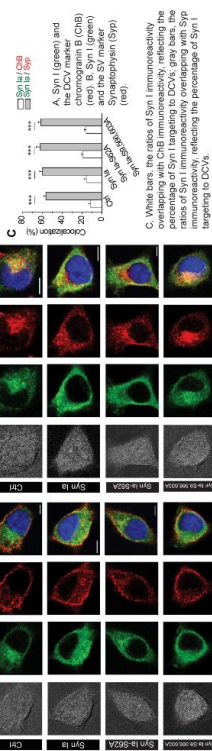
### The changed OT levels in CSF and plasma after HNS transfection



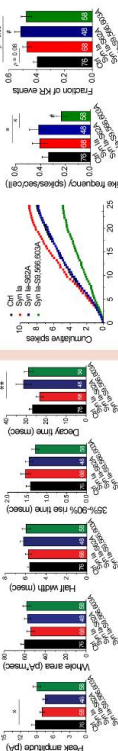
Secretion rate in PC12 cells overexpressing Syn Ia or its phosphomutants



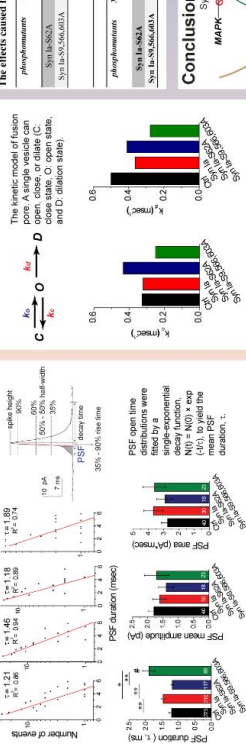
### Subcellular localization of Syn I



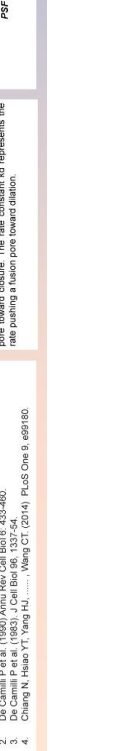
### KR events and spike frequency



Core kinetics	Summary
---------------	---------



step from C to O is defined as  $k_{CO}$ , and for the step from O to D as  $k_{OD}$ .  $k_{CO}$  represents the rate for a fusion



## KR events v.s. full-fusion events

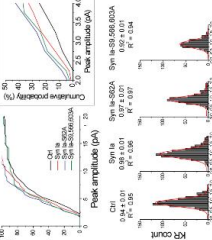


Figure 1 consists of four bar graphs showing the effect of Syn 1a on the growth of Syn 1a-562A and Syn 1a-562A-603A. The y-axis is 'Growth (μg)' ranging from 0 to 30. The x-axis is 'Concentration (μg)' with values 0, 0.01, 0.1, 1, 10, 100, 1000, 10000. The legend indicates: Ctr (white), Syn 1a (black), Syn 1a-562A (hatched), and Syn 1a-562A-603A (dotted). Error bars represent standard deviation. Statistical significance is indicated by asterisks (\* p < 0.05, \*\* p < 0.01, \*\*\* p < 0.001).

Concentration (μg)	Ctr (μg)	Syn 1a (μg)	Syn 1a-562A (μg)	Syn 1a-562A-603A (μg)
0	~25	~25	~25	~25
0.01	~25	~25	~25	~25
0.1	~25	~25	~25	~25
1	~25	~25	~25	~25
10	~25	~25	~25	~25
100	~25	~25	~25	~25
1000	~25	~25	~25	~25
10000	~25	~25	~25	~25

**acknowledgements**

m	PSF duration (s)		Full-spectrum frequency	$k_c$	$k_d$	Decay time (spike characteristics)
	↓	↑				
1	↓	↑	**	↑	↓	**
2	↓	↑		↑	↓	↑
3	↓	↑		↑	↓	↑
4	↓	↑		↑	↓	↑
5	↓	↑		↑	↓	↑
6	↓	↑		↑	↓	↑
7	↓	↑		↑	↓	↑
8	↓	↑		↑	↓	↑
9	↓	↑		↑	↓	↑
10	↓	↑		↑	↓	↑
11	↓	↑		↑	↓	↑
12	↓	↑		↑	↓	↑
13	↓	↑		↑	↓	↑
14	↓	↑		↑	↓	↑
15	↓	↑		↑	↓	↑
16	↓	↑		↑	↓	↑
17	↓	↑		↑	↓	↑
18	↓	↑		↑	↓	↑
19	↓	↑		↑	↓	↑
20	↓	↑		↑	↓	↑
21	↓	↑		↑	↓	↑
22	↓	↑		↑	↓	↑
23	↓	↑		↑	↓	↑
24	↓	↑		↑	↓	↑
25	↓	↑		↑	↓	↑
26	↓	↑		↑	↓	↑
27	↓	↑		↑	↓	↑
28	↓	↑		↑	↓	↑
29	↓	↑		↑	↓	↑
30	↓	↑		↑	↓	↑
31	↓	↑		↑	↓	↑
32	↓	↑		↑	↓	↑
33	↓	↑		↑	↓	↑
34	↓	↑		↑	↓	↑
35	↓	↑		↑	↓	↑
36	↓	↑		↑	↓	↑
37	↓	↑		↑	↓	↑
38	↓	↑		↑	↓	↑
39	↓	↑		↑	↓	↑
40	↓	↑		↑	↓	↑
41	↓	↑		↑	↓	↑
42	↓	↑		↑	↓	↑
43	↓	↑		↑	↓	↑
44	↓	↑		↑	↓	↑
45	↓	↑		↑	↓	↑
46	↓	↑		↑	↓	↑
47	↓	↑		↑	↓	↑
48	↓	↑		↑	↓	↑
49	↓	↑		↑	↓	↑
50	↓	↑		↑	↓	↑
51	↓	↑		↑	↓	↑
52	↓	↑		↑	↓	↑
53	↓	↑		↑	↓	↑
54	↓	↑		↑	↓	↑
55	↓	↑		↑	↓	↑
56	↓	↑		↑	↓	↑
57	↓	↑		↑	↓	↑
58	↓	↑		↑	↓	↑
59	↓	↑		↑	↓	↑
60	↓	↑		↑	↓	↑
61	↓	↑		↑	↓	↑
62	↓	↑		↑	↓	↑
63	↓	↑		↑	↓	↑
64	↓	↑		↑	↓	↑
65	↓	↑		↑	↓	↑
66	↓	↑		↑	↓	↑
67	↓	↑		↑	↓	↑
68	↓	↑		↑	↓	↑
69	↓	↑		↑	↓	↑
70	↓	↑		↑	↓	↑
71	↓	↑		↑	↓	↑
72	↓	↑		↑	↓	↑
73	↓					

[illegible]


[Print this Page for Your Records](#)
[Close Window](#)
**Control/Tracking Number:** 2016-S-4156-SfN

**Activity:** Scientific Abstract

**Current Date/Time:** 5/3/2016 12:57:55 AM

**Explore the exocytotic proteins that interact with Synapsin Ia in a phosphorylation-dependent manner**

**AUTHOR BLOCK:** \*H.-J. YANG<sup>1</sup>, C.-T. WANG<sup>2,3,4,1</sup>;

<sup>1</sup>Genome and Systems Biol. Program, Natl. Taiwan Univ. and Academia Sinica, Taipei, Taiwan; <sup>2</sup>Inst. of Mol. and Cell. Biol., <sup>3</sup>Dept. of Life Sci., <sup>4</sup>Neurobio. and Cognitive Sci. Ctr., Natl. Taiwan Univ., Taipei, Taiwan


**Abstract:**

Synapsins (Syns), a family of evolutionarily conserved phosphoproteins, are widespread in the nervous system and localize to synaptic vesicles (SVs). Syns are encoded by three distinct genes (*syn I*, *syn II*, and *syn III*) and consist of ten homologous proteins by alternative splicing, i.e., Syn Ia-b, IIa-b, and IIIa-f. Among all homologous proteins, Syn Ia is the best studied in regulating the dynamics of SVs by controlling their storage and mobilization in a phosphorylation-dependent manner. These physiological functions of Syn Ia are mainly mediated by interaction with certain presynaptic proteins (such as cytoskeleton) through phosphorylation of Syn Ia. To date, only a few of exocytotic proteins are found to directly interact with Syn Ia in a phosphorylation-dependent manner. In this study, we explore new exocytotic proteins that interact with Syn Ia through phosphorylation of Syn Ia. To begin with, we performed Bioinformatics approaches. First, we conducted systematic database search to find the proteins that can interact with Syn Ia. Second, we performed the sequence-based protein-protein interaction (PPI) prediction with the software MirrorTree. Based on the results from database search and PPI prediction, we selected the candidate proteins that are exocytotic proteins and likely affect SV release. Furthermore, we performed endogenous co-immunoprecipitation for these candidate proteins. We found that the interaction between Syn Ia and Synaptophysin (Syp) was changed after overexpression of the Syn Ia phosphodeficient mutant, suggesting that the Syn Ia-Syp interaction may be regulated by phosphorylation of Syn Ia. Our results suggest that Syp may potentially involve in Syn Ia's regulation of

<http://www.abstracksonline.com/cSubmit/SubmitPrinterFriendlyVersion.asp?ControlKey=%7B098B5F99%2DDF32%2D4AF6%2D8B77%2D4CC8E80B1F46...> 1/3

### Appendix 3. The 46<sup>th</sup> Annual Meeting of the Society for Neuroscience (12-16

November 2016, San Diego, CA, U.S.A.): Abstract



093

**Explore the exocytotic proteins that interact with Synapsin Ia in a phosphorylation-dependent manner**

4156

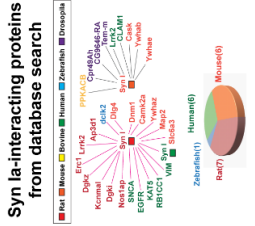
*\*Hui-Ju Yang<sup>1</sup> and Chih-Tien Wang<sup>1,2,3,4</sup>*

<sup>1</sup>Genome and Systems Biology Program, National Taiwan University and Academia Sinica, <sup>2</sup>Institute of Molecular and Cellular Biology, <sup>3</sup>Department of Life Science, <sup>4</sup>Neurobiology and Cognitive Science Center, National Taiwan University, Taipei, Taiwan

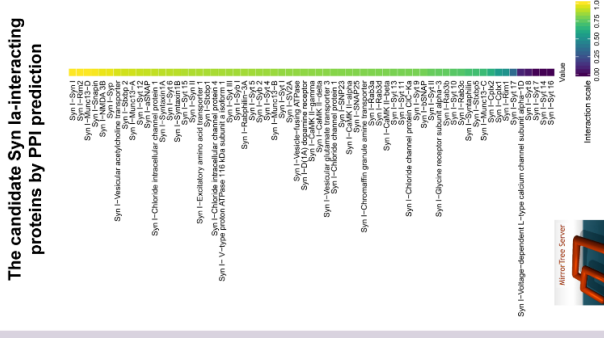
**Introduction**

Synapsins (Syns), a family of evolutionarily conserved phosphoproteins, are widespread in the nervous system and localize to synaptic vesicles (SVs). Syns are encoded by three distinct genes (syn I, syn II, and syn III) and consist of ten homologous proteins by alternative splicing, i.e., Syn Ia-b, IIa-b, and IIIa-f. Among all homologous proteins, Syn Ia is the best studied in regulating the dynamics of SVs by controlling their storage and mobilization in a phosphorylation-dependent manner. These physiological functions of Syn Ia are mainly mediated by interaction with certain presynaptic proteins (such as cytoskeleton) through phosphorylation of Syn Ia. To date, only a few of exocytotic proteins are found to directly interact with Syn Ia in a phosphorylation-dependent manner. In this study, we explore new exocytotic proteins that interact with Syn Ia through phosphorylation of Syn Ia. We found that the interaction between Syn Ia and Synaptophysin (Syp) was changed after overexpression of the Syn Ia phosphodeficient mutant, suggesting that the Syn Ia-Syp interaction may be regulated by phosphorylation of Syn Ia. Our results suggest that Syp may potentially involve in Syn Ia's regulation of vesicle exocytosis in a Syn Ia phosphorylation-dependent manner.

**Syn Ia-interacting proteins from database search**



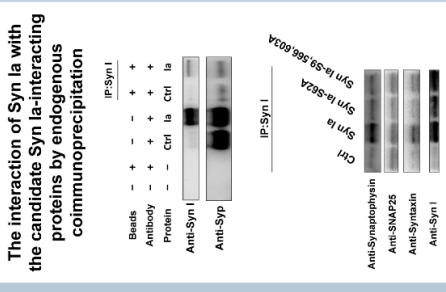
**The candidate Syn Ia-interacting proteins by PPI prediction**



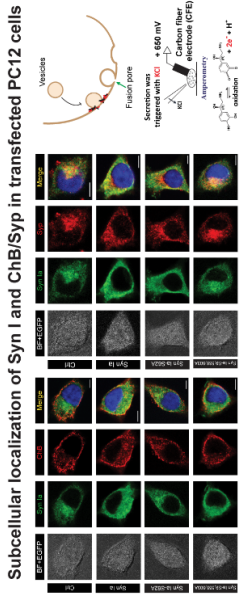
**Acknowledgements**

We thank Drs. Paul Greengard and Meyer B. Jackson for the generous gift of plasmids; Dr. Payne Chang for the unimpaired data software; the staff of Technology Commons, College of Life Science, NTU for help with confocal microscopy; and the staff of the Synaptic Biology and Neurobiology Laboratory for their technical assistance. This work was supported by the NTU startup fund and the Ministry of Science and Technology (MOST-103-2311-B-002-02A-MY3) to CTW.

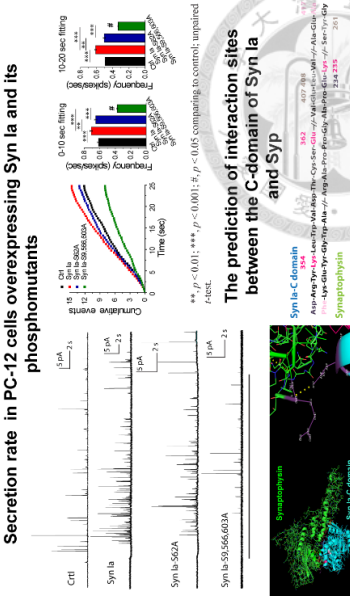
**The interaction of Syn Ia with the candidate Syn Ia-interacting proteins by endogenous coimmunoprecipitation**



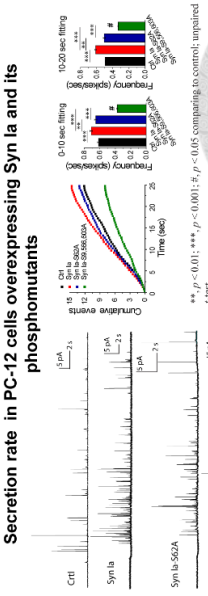
**Subcellular localization of Syn I and ChB/Syp in transfected PC12 cells**




**The prediction of interaction sites between the C-domain of Syn Ia and Syp**



**Secretion rate in PC-12 cells overexpressing Syn Ia and its phosphomutants**



**The prediction of interaction sites between the C-domain of Syn Ia and Syp**



Appendix 4. The 46<sup>th</sup> Annual Meeting of the Society for Neuroscience (12-16 November 2016, San Diego, CA, U.S.A.): Poster

V



[Print this Page for Your Records](#)

[Close Window](#)

**Control/Tracking Number:** 2017-S-11041-SfN

**Activity:** Scientific Abstract

**Current Date/Time:** 5/4/2017 7:15:51 AM

**Investigating the Synapsin Ia's interaction with Syntaxin I in a phosphorylation-dependent manner**

**AUTHOR BLOCK:** \*H.-J. YANG<sup>1</sup>, C.-T. WANG<sup>1,2,3,4</sup>,

<sup>1</sup>Genome and Systems Biol. Program, Natl. Taiwan Univ. and Academia Sinica, Taipei, Taiwan; <sup>2</sup>Inst. of Mol. and Cell. Biol., <sup>3</sup>Dept. of Life Sci., <sup>4</sup>Neurobio. and Cognitive Sci. Ctr., Natl. Taiwan Univ., Taipei, Taiwan

**Abstract:**

Calcium-dependent exocytosis is triggered by the formation of SNARE complex, further inducing vesicle fusion and neurotransmitter release. Synapsin I (Syn I), a particular phosphoprotein localized to synaptic vesicles (SVs), plays an important role in regulating the fusion dynamics of SVs in a phosphorylation-dependent manner. Our previous results from single-vesicle amperometry in PC12 cells showed that Syn Ia also regulates the secretion rate and fusion pore kinetics of norepinephrine-laden dense-core vesicles (DCVs) in a phosphorylation-dependent manner. However, it remains completely unknown what is the molecular mechanism underlying Syn Ia regulation of DCV fusion kinetics. Here, we examined the hypothesis whether the Syn Ia may interact with Syntaxin I (Stx I, a component of fusion pores) in a phosphorylation-dependent manner. First, according to the sequence-based protein-protein interaction (PPI) prediction with the software MirrorTree, we found the score of possible interaction between Syn Ia and Stx I as 0.9. Advanced endogenous co-immunoprecipitation in the presence of high KCl showed that the interaction between Syn Ia and Stx I was regulated by Syn Ia phosphodeficient mutation. In contrast, the interaction between Stx I and v-SNARE was not changed by Syn Ia phosphodeficient mutation. Finally, western analysis showed that the expression levels of these SNARE proteins were not changed by transfecting Syn Ia phosphodeficient mutants. Hence, our results suggested that Syn Ia may interact with Stx I in a phosphorylation-

**Appendix 5. The 47<sup>th</sup> Annual Meeting of the Society for Neuroscience (11-15**

**November 2017, Washington DC, U.S.A.): Abstract**



## 746.13

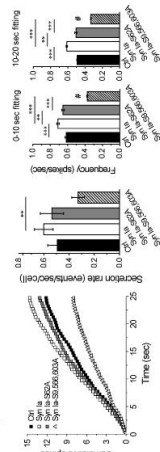
<sup>1</sup>Genome and Systems Biology Program, National Taiwan University and Academia Sinica, <sup>2</sup>Institute of Molecular and Cellular Biology, <sup>3</sup>Department of Life Science, <sup>4</sup>Neurobiology and Cognitive Science Center, National Taiwan University, Taipei, Taiwan

\*Neurobiology and Cognitive Science Center, National Taiwan University, Taipei, Taiwan

C36

Calcium-dependent exocytosis is triggered by the release of SNARE complex, further inducing vesicle fusion and neurotransmitter release. Synapsin I (Syn I), a particular phosphoprotein localized to synaptic vesicles (SVs), plays an important role in regulating the fusion dynamics of SVs in a phosphorylation-dependent manner. Our results suggest that Syn I regulates the fusion rate of vesicle pools of non-labeled vesicles, but not the release rate of vesicle pools of labeled vesicles. The release of the core vesicles (DCVs) in a phosphorylation-dependent manner. However, the molecular mechanism underlying Syn I's regulation of DCV fusion kinetics remains completely unknown. The previous study showed that synaptobrevin (Sbn) constitutes the fusion pore (Him et al., 2004). In this study, we examined that whether Syn I is involved in regulating the fusion pore of DCVs. We found that Syn I is potentially

Figure 1 illustrates the experimental setup and electrophysiological recordings. The schematic shows the isolation of PC12 cells, their transfection with N1, and the subsequent recording of spontaneous exocytosis using a carbon fiber electrode (CFE) in a bath solution containing KCl and ascorbic acid. The CFE is connected to a patch-clamp amplifier and a data acquisition system. The recordings show current responses to the addition of Syn Ia, Syn Ia-502A, and Syn Ia-591-660/63A, with a scale bar of 5 pA and 2 s.



We thank Dr. Chien-Yu Chen for the help with PPI prediction; Dr. Jui-Chin Lu for technical supports in immunoprecipitation and immunoblotting; Drs. Paul Greengard and Meyer B. Jackson for the generous gift of plasmid; Dr. Payne Chang for the amperometry data software; the staff of Technology Commons, College of Life Science, NTU for help with confocal microscopy; and members of the Wang lab for discussion and technical assistance. This work was supported by the NTU (NTU-ERP-105R0805A4) and the Ministry of Science and Technology (MOST96-D02-2311-B-002-007) to C.T.W.

- ## References
1. Wang CT et al. (2000) 1111-1115.
  2. De Camilli P et al. (1998) Biol 6: 433-460.
  3. De Camilli P et al. (1998) 1337-54.
  4. Chiang N, Hsiao YT, CT. (2014) PLoS One.
  5. Han X et al. (2004) 1

**Figure 3.** Quantitative analysis of vesicle fusion and pore opening. **(A)** Fluorescence images of a vesicle fusing with a pore. The top row shows the vesicle (DAPI, red) and the pore (DAPI, blue). The bottom row shows the vesicle (DAPI, red) and the pore (DAPI, blue) after fusion. Scale bar, 5  $\mu$ m. **(B)** Bar graph showing the colocalization (%) of DAPI (red) and DAPI+vesicle (green) after treatment of dopamine for 60 min. The y-axis represents Colocalization (%), ranging from 0 to 100. The x-axis shows three conditions: DAPI, DAPI+vesicle, and DAPI+vesicle+open pore. **(C)** Bar graph showing the spike frequency (spikes/s) for the same three conditions. The y-axis represents Spike frequency (spikes/s), ranging from 0 to 0.4. **(D)** Bar graph showing the PSC duration (ms) for the same three conditions. The y-axis represents PSC duration (ms), ranging from 0 to 25. **(E)** Bar graph showing the PSC open time (ms) for the same three conditions. The y-axis represents PSC open time (ms), ranging from 0 to 25. **(F)** Bar graph showing the PSC amplitude (mV) for the same three conditions. The y-axis represents PSC amplitude (mV), ranging from 0 to 2.5. **(G)** Bar graph showing the PSC peak amplitude (mV) for the same three conditions. The y-axis represents PSC peak amplitude (mV), ranging from 0 to 2.5. **(H)** Bar graph showing the PSC rise time (ms) for the same three conditions. The y-axis represents PSC rise time (ms), ranging from 0 to 25. **(I)** Bar graph showing the PSC decay time (ms) for the same three conditions. The y-axis represents PSC decay time (ms), ranging from 0 to 25. **(J)** Bar graph showing the PSC area (mV·s) for the same three conditions. The y-axis represents PSC area (mV·s), ranging from 0 to 2.5. **(K)** Bar graph showing the PSC area (mV·s) for the same three conditions. The y-axis represents PSC area (mV·s), ranging from 0 to 2.5. **(L)** Bar graph showing the PSC area (mV·s) for the same three conditions. The y-axis represents PSC area (mV·s), ranging from 0 to 2.5. **(M)** Bar graph showing the PSC area (mV·s) for the same three conditions. The y-axis represents PSC area (mV·s), ranging from 0 to 2.5. **(N)** Bar graph showing the PSC area (mV·s) for the same three conditions. The y-axis represents PSC area (mV·s), ranging from 0 to 2.5. **(O)** Bar graph showing the PSC area (mV·s) for the same three conditions. The y-axis represents PSC area (mV·s), ranging from 0 to 2.5. **(P)** Bar graph showing the PSC area (mV·s) for the same three conditions. The y-axis represents PSC area (mV·s), ranging from 0 to 2.5. **(Q)** Bar graph showing the PSC area (mV·s) for the same three conditions. The y-axis represents PSC area (mV·s), ranging from 0 to 2.5. **(R)** Bar graph showing the PSC area (mV·s) for the same three conditions. The y-axis represents PSC area (mV·s), ranging from 0 to 2.5. **(S)** Bar graph showing the PSC area (mV·s) for the same three conditions. The y-axis represents PSC area (mV·s), ranging from 0 to 2.5. **(T)** Bar graph showing the PSC area (mV·s) for the same three conditions. The y-axis represents PSC area (mV·s), ranging from 0 to 2.5. **(U)** Bar graph showing the PSC area (mV·s) for the same three conditions. The y-axis represents PSC area (mV·s), ranging from 0 to 2.5. **(V)** Bar graph showing the PSC area (mV·s) for the same three conditions. The y-axis represents PSC area (mV·s), ranging from 0 to 2.5. **(W)** Bar graph showing the PSC area (mV·s) for the same three conditions. The y-axis represents PSC area (mV·s), ranging from 0 to 2.5. **(X)** Bar graph showing the PSC area (mV·s) for the same three conditions. The y-axis represents PSC area (mV·s), ranging from 0 to 2.5. **(Y)** Bar graph showing the PSC area (mV·s) for the same three conditions. The y-axis represents PSC area (mV·s), ranging from 0 to 2.5. **(Z)** Bar graph showing the PSC area (mV·s) for the same three conditions. The y-axis represents PSC area (mV·s), ranging from 0 to 2.5.

[illegible]

**Proximity ligation assay**

The cells overexpressing Syn *ts*-EGFP were immunostained with primary antibodies (Syn and SN25)

**Western blotting**

**Endogenous co-immunoprecipitation**

Syn Ia plays an important role in regulating the secretion rate and kinetics of fusion pores during DCV exocytosis. This regulation of Syn Ia on DCV exocytosis may act through the interaction with certain exocytotic proteins that localize to DCVs, such as Stx, SNAP25,

**Exploring the mechanism of Synapsin Ia, a synaptic vesicle protein, in regulating the secretion from dense-core vesicles**

Hui-Ju Yang<sup>1</sup>, Chien-Yu Chen<sup>1</sup>, and Chih-Tien Wang<sup>1,2,3,4</sup>.

Genome and Systems Biology Program<sup>1</sup>, National Taiwan University and Academia Sinica, Institute of Molecular and Cellular Biology<sup>2</sup>, Department of Life Science<sup>3</sup>, Neurobiology and Cognitive Science Center<sup>4</sup>, National Taiwan University, Taipei, Taiwan 10617

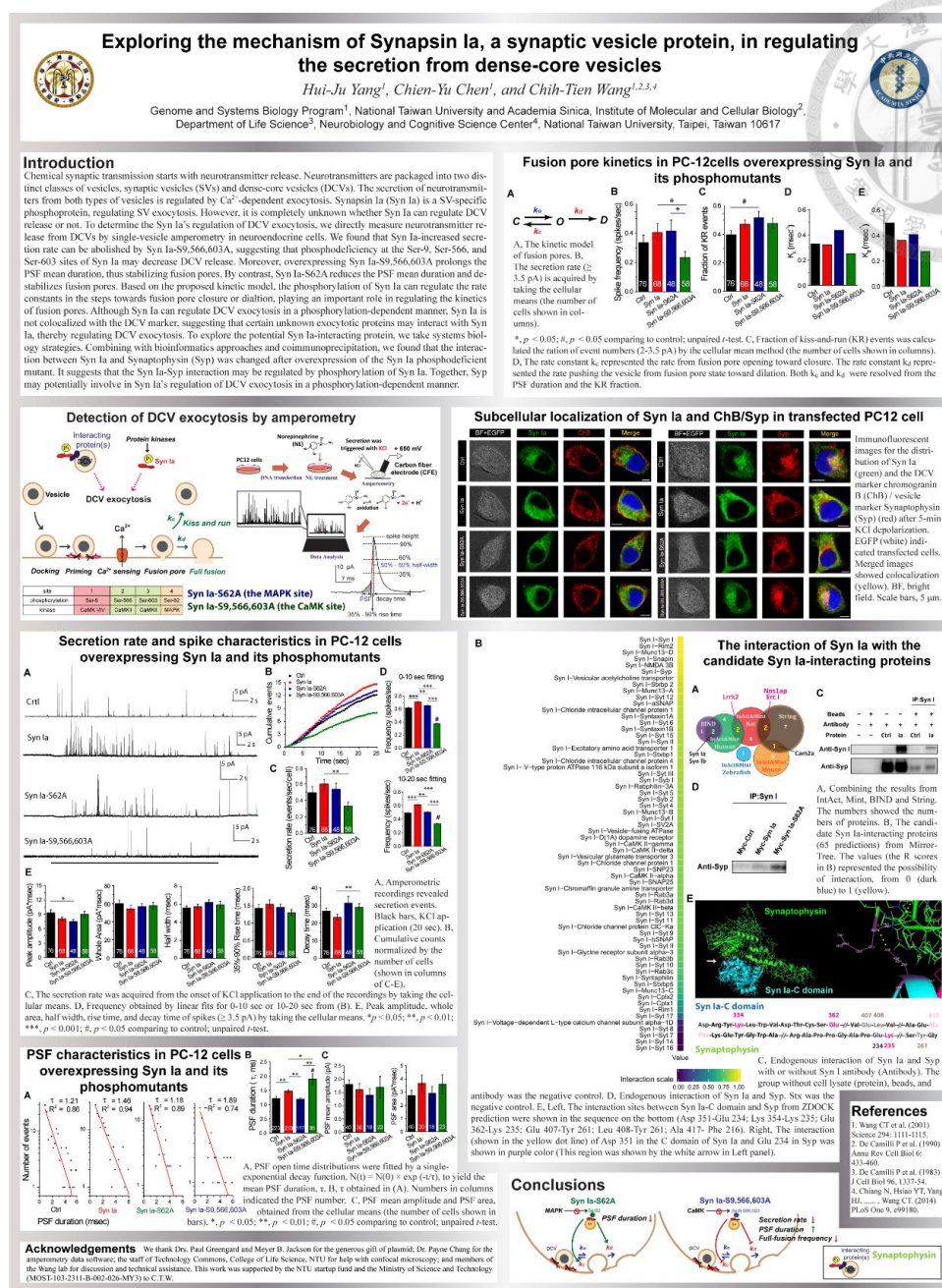


Chemical synaptic transmission starts with neurotransmitter release. Neurotransmitters are packaged into two distinct classes of vesicles, synaptic vesicles (SVs) and dense-core vesicles (DCVs). The secretion of neurotransmitters from both types of vesicles is regulated by  $\text{Ca}^{2+}$ -dependent exocytosis. Synapsin Ia (Syn Ia) is a SV-specific phosphoprotein, regulating SV exocytosis. However, it is completely unknown whether Syn Ia can regulate DCV release or not. To determine the Syn Ia's regulation of DCV exocytosis, we directly measure neurotransmitter release from DCVs by single-vesicle amperometry in neuroendocrine cells. We found that Syn Ia-increased secretion rate can be abolished by Syn Ia-S9,566,603A, suggesting that phosphodeficiency at the Ser-9, Ser-566, and Ser-603 sites of Syn Ia may decrease DCV release. Moreover, overexpressing Syn Ia-S9,566,603A prolongs the PSF mean duration, thus stabilizing fusion pores. By contrast, Syn Ia-S62A reduces the PSF mean duration and destabilizes fusion pores. Based on the proposed kinetic model, the phosphorylation of Syn Ia can regulate the rate constants in the steps towards fusion pore closure or dialtion, playing an important role in regulating the kinetics of fusion pores. Although Syn Ia can regulate DCV exocytosis in a phosphorylation-dependent manner, Syn Ia is not colocalized with the DCV marker, suggesting that certain unknown exocytotic proteins may interact with Syn Ia, thereby regulating DCV exocytosis. To explore the potential Syn Ia-interacting protein, we take systems biology strategies. Combining with bioinformatics approaches and coimmunoprecipitation, we found that the interaction between Syn Ia and Synaptophysin (Syp) was changed after overexpression of the Syn Ia phosphodeficient mutant. It suggested that the Syn Ia-Syp interaction may be regulated by phosphorylation of Syn Ia. Together, Syp may potentially involve in Syn Ia's regulation of DCV exocytosis in a phosphorylation-dependent manner.

**Appendix 7. The Poster Competition of the 2016 GSB Retreat in Genome and**

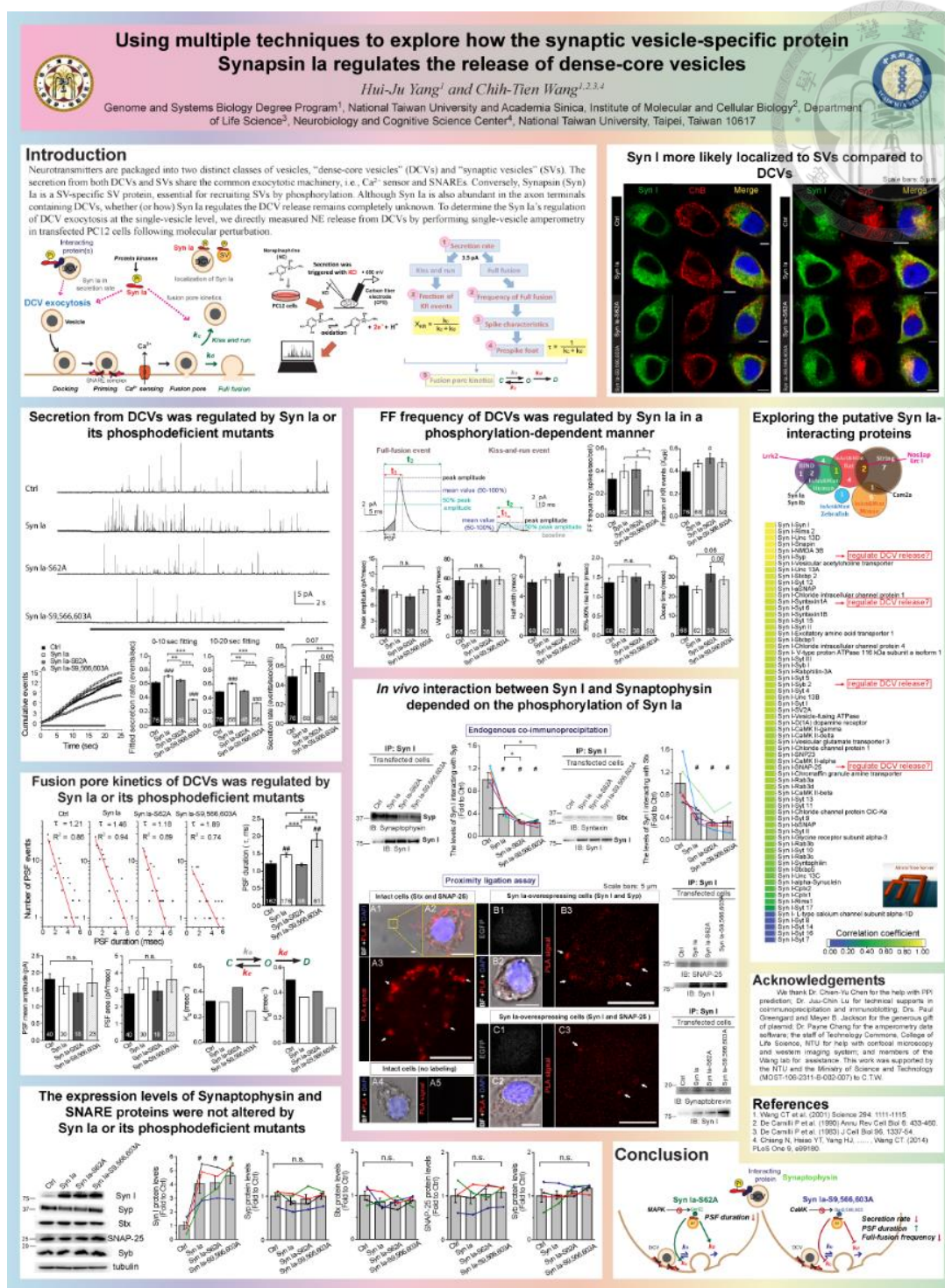
**Systems Biology (GSB) Degree Program at National Taiwan University, Taipei,**

**Taiwan (8/28-29, 2016): Abstract**



# Appendix 8. The Poster Competition of the 2016 GSB Retreat in Genome and Systems Biology (GSB) Degree Program at National Taiwan University, Taipei, Taiwan (8/28-29, 2016): Poster





Appendix 9. The 2019 Poster Competition in Genome and Systems Biology (GSB)

Degree Program at National Taiwan University, Taipei, Taiwan (5/24, 2019):

Poster

X

doi:10.6342/NTU201901181